The Regulation of Brown Adipose Tissue Activation by Multiple Phosphodiesterases

Stephen Michael Kraynik

A dissertation
submitted in partial fulfillment of the
requirements for the degree of

Doctor of Philosophy

University of Washington

2013

Program Authorized to Offer Degree: Pharmacology

University of Washington

Abstract

The Regulation of Brown Adipose Tissue Activation by Multiple Phosphodiesterases

Stephen Michael Kraynik

Chair of the Supervisory Committee:
Professor Joseph A. Beavo
Department of Pharmacology

Brown adipose tissue is a highly thermogenic, energy “wasting” organ that converts glucose and lipids into heat. Many of the critical metabolic and gene transcriptional processes, such as uncoupling protein-1 (UCP1) mRNA expression, lipolysis and glucose uptake are regulated by the β-adrenergic receptor-dependent signaling cascade through the second messenger, adenosine-3’,5’-cyclic monophosphate (cAMP). Cyclic nucleotide phosphodiesterases (PDEs) are enzymes that catalyze the breakdown of cAMP, and thereby regulate the duration and magnitude of this signal. Yet, neither the types of PDEs that are expressed in BAT nor how they regulate the major processes that lead to thermogenesis have been well characterized.

In this dissertation, I present evidence that BAT activity is largely regulated by several different PDEs working in concert. In the basal state, it required a combination of PDE3 and PDE4 inhibitors to fully induce UCP1 mRNA expression and activate lipolysis in brown adipocytes, whereas neither inhibitor had any substantial effect when administered alone. Furthermore, when injected into mice, the combination of PDE3 and PDE4 inhibitors stimulated glucose uptake in BAT under thermoneutral and fasted conditions. This response was further potentiated by the global ablation of PDE8A. On the other hand, when brown adipocytes were co-stimulated with a β-adrenergic agonist, a PDE3 inhibitor could potentiate UCP1 mRNA expression, but not lipolysis; whereas a PDE4 inhibitor could not potentiate UCP1 mRNA expression, but did potentiate lipolysis and cAMP accumulation. This

suggests a differential role for these PDEs when β-adrenergic receptors are activated.

Due to its high metabolic inefficiency, BAT has been implicated as a potential therapeutic target for the treatment of obesity and its various comorbidities. It is thought that increasing the amount and/or the activity of brown fat could lead to increased energy expenditure and a decrease in body weight, a phenomenon that has been demonstrated in rodent models. However, selective pharmacological activation of brown adipose tissue in humans has remained elusive due to a lack of adipocyte-specific adrenergic receptors expressed on its surface. In light of this, new alternative approaches are required to translate this hypothesis to the clinic. Taken together, the results presented here provide a new conceptual basis for the development of therapeutics that activate BAT by selectively targeting a combination of PDEs.

TABLE OF CONTENTS

LIST OF FIGURES

LIST OF TABLES

LIST OF ABBREVIATIONS

18FDG	^{18}Fluoro-deoxyglucose
AC	adenylyl cyclase
ADP	adenosine diphosphate
AKAP	A-kinase anchoring protein
AR	adrenergic receptor or adrenoceptor
ATF-2	activating transcription factor-2
ATGL	adipose triglyceride lipase
ATP	adenosine 5'-triphosphate
cAMP	adenosine 3',5'-cyclic monophosphate
BAT	brown adipose tissue, or brown fat
BMI	body mass index
BMR	basal metabolic rate
BSA	bovine serum albumin
C/EBP-β	CCAAT/enhancer-binding protein-β
CNG	cyclic nucleotide gated channels
cGMP	guanosine 3',5'-cyclic monophosphate
DMEM	Dulbecco's modified eagle medium
DMSO	dimethyl sulfoxide
DTT	dithiothreitol
EC_{50}	concentration of drug for half-maximal (50%) response
EDTA	ethylenediamine-N,N,N',N'-tetraacetic acid
EGTA	ethylene glycol (β-aminoethyl ether)-N,N,N',N'-tetraacetic acid
ELISA	enzyme-linked immunosorbent assay
Epac	exchange protein activated by cAMP
FA	fatty acid
FAD	flavin adenine dinucleotide
FBS	fetal bovine serum
g	gram
g	gravitational force

GLUT	glucose transporter
h	hour
HEPES	4-(2-hydroxyethyl)-1-piperazineethanesulfonic acid
HSL	hormone sensitive lipase
^{3}H	tritium
IBMX	3-isobutyl-1-methylxanthine
IC_{50}	concentration of drug for half-maximal (50%) inhibition
IMS	intermembrane space
Iso	isoproterenol
kDa	kilodalton
K_i	inhibition constant
K_m	Michaelis-Menten constant. The concentration of substrate at which the rate of an enzymatic reaction is at half-maximal velocity.
KO	knockout
min	minute
mL	milliliter
mM	millimolar
MOPS	3-(N-morpholino)propanesulfonic acid
mRNA	messenger RNA
NAD	nicotinamide adenine dinucleotide
nCi	nanocuries
NE	norepinephrine
nM	nanomolar
OMM	outer mitochondrial membrane
PAS	Per, Arnt and Sim proteins
PAT	perilipin, adipose differentiation-related protein
PBS	phosphate buffered saline
PET	positron emission tomography
PGC-1α	PPARγ-cofactivator-1α
PKA	protein kinase-A
PKG	protein kinase-G

pmol	picomoles
PDE	phosphodiesterase
PMSF	phenyl methyl sulfonyl fluoride
PPARγ	peroxisome proliferator-activated receptor-γ
PRDM16	PRD1-BF-1-RIZ1 Homologous Domain Containing Protein-16
Rp-	Rp isomer
s	second
Sp-	Sp isomer
TG	triglycerides
UCP1	uncoupling protein-1, or thermogenin
µL	microliter
µM	micromolar
V_{max}	maximum reaction rate
vol	volume
W	watt
WT	wild type

ACKNOWLEDGEMENTS

First, I thank my mentor, Dr. Joseph A. Beavo, for the opportunity to study under his guidance. I am forever grateful for his dedication to my scientific development and for the freedom to pursue my topic of research in his laboratory. It was a great honor to have been able to spend these years modeling my scientific style after his. I also thank the rest of the Beavo Laboratory members, both past and present, for their help and advice. I especially thank Dr. Thomas Hinds for being both a trusted colleague and "life coach," and whose friendship has become one of my most treasured. I thank my thesis committee for their longstanding encouragement and suggestions. I want to thank Dr. Robert Miyaoka and his staff for their experimental contributions. I also thank all of my previous science teachers over the years for making science so fun and for encouraging my fascination with the subject. In particular, I thank Mr. Jim Vassallo for calling on me once each week to recite the speed of light in front of my 7th grade class. I also thank Dr. Sally Vonderbrink, whose lessons on dimensional analysis and chemical calculations at St. Xavier High School I still use to this day.

I thank my parents, Charles and Patricia Kraynik, for sacrificing so much to put me through good schools, and for encouraging me to be the best that I can be no matter what I choose to do in life. I thank my brother, David Kraynik, for making several long trips to Seattle to spend Thanksgiving with me and for being the best brother I could ever hope to have. I thank my aunt, Victoria Patterson, for filling in for Mom during some of the toughest times over the past 12 years. I also thank my cousin, Scott Patterson, for encouraging me to never give up. I also thank all of my

friends that I have made in Seattle. The fun that we have had, both in celebration and commiseration, as well as the memories that we have forged will stay with me for the rest of my life. I would also like to thank Daniel Pegher for being a daily source of hilarity.

Finally, this dissertation would not have been possible without the constant love, patience, support, and devotion of my lovely wife, Lindsay. I thank her for the extraordinary sacrifices that she has made in her life in order to be part of mine. I am forever in debt to her for everything she has been for me during these years.

DEDICATION

For Lindsay, my wife.

Chapter 1:
Introduction and Statement of Problem

Cyclic-AMP Signaling

Since the first discovery of the second messenger molecule cAMP by Earl Sutherland in the 1950's, it has been widely recognized that this second messenger regulates a host of physiological processes in virtually every cell type studied. Cyclic-AMP is generated from ATP by adenylyl cyclases, some of which are activated at the cellular membrane through G-protein coupled receptors after they are bound with agonist, and at least one of which is regulated by bicarbonate and calcium in the cytosol. 3',5'-cyclic nucleotide phosphodiesterases (PDEs) are ubiquitously expressed enzymes that catalyze the breakdown of intracellular cyclic nucleotide second messengers. These enzymes are critical for the regulation of both the duration of action and the intensity of a given pulse of cyclic nucleotides, thereby controlling one, or often a variety, of molecular signaling events that occur downstream. These signaling events are mediated through direct binding of cAMP to one or more of several effector molecules: protein kinase-A (PKA), cyclic-nucleotide gated ion channels (CNG), and the exchange protein activated by cAMP (Epac) (Fig. 1.1). The resulting effects on the cell include, but are not limited to, changes in gene expression patterns, metabolic processes, and cell growth and differentiation.

Due to the fact that signaling effector molecules can cluster together in different combinations within a given signaling compartment, there is a large degree of complexity to the regulation of cAMP signaling. Further complicating matters, for

a given class of effector molecule, such as a cyclase, kinase, or phosphodiesterase, there can be multiple forms of that effector molecule expressed in a given cell type. More specifically, in mammals there are ten different adenylyl cyclases (nine membrane, one soluble), eleven different PDE families (Fig. 1.2), and several different variants of PKA and Epac. Often, specific combinations of these proteins, PKA, cyclases, and sometimes PDEs, are anchored together via A-kinase-anchoring-proteins (AKAPs), allowing for very tight, spatial control of the cAMP second messenger signal.

PDEs are a class of enzymes whose biochemical properties and physiological function have been thoroughly explored and characterized over the last four decades (Beavo et al., 1982). After their first description in the late 1950s (Sutherland and Rall, 1958), improved radiolabeled nucleotide-based biochemical PDE assays led to the notion that there were likely multiple isotypes of these enzymes. It wasn't until the development of improved protein purification techniques, specific immunoreactive antibodies, and molecular cloning that the size of this enzyme family was fully appreciated. It is widely accepted that there are 11 families of PDEs in mammals, spanning 21 different gene products (Fig. 1.2). Within each gene product, there can be multiple variants expressed due to alternative splicing of the mRNA message or alternative start sites for transcription. Altogether there are estimated to be >100 different PDE enzymes.

The various PDE subtypes within each class often differ in their substrate specificity, mechanism of activation or inhibition, as well as their kinetic properties. For example, the PDE1 family is the only PDE family we know of that is activated by

calcium-calmodulin. The PDE2 and PDE3 families hydrolyze both cAMP and cGMP. Interestingly, PDE2 activity towards cAMP is enhanced by low levels of cGMP, whereas the PDE3 family is inhibited by cGMP. It is thought that this variety allows for diversified regulation of cyclic nucleotide signals in a context specific manner.

Splice variant products of the same PDE transcript often vary in their N-terminal protein-protein interaction domains, which can affect their subcellular localization or binding partners. For instance, the PDE4 family contains 4 different genes (labeled A, B, C, and D), and over 20 different variants each with distinct N-terminal regions (numbered numerically after the letter). In rat cardiomyocytes, PDE4D3 interacts with PKA/AKAP signaling complexes, an interaction that does not seem to occur in vascular smooth muscle cells where it is also expressed. Instead, it is PDE4D8 that seems to interact with PKA/AKAP complexes in that context (Raymond et al., 2009). Furthermore, in cardiomyocytes, it has been shown that different PDE4D splice variants can differentially interact with beta adrenoceptors depending on the activation state of the receptor, and these different interactions can have dramatic consequences for cellular function (De Arcangelis et al., 2009). However, PDE4A has been shown to interact with mitochondria via AKAP149 on the outer membrane of mitochondria in T-lymphocytes (Asirvatham et al., 2004), which may be important for apoptosis (Moon and Lerner, 2003). These types of examples illustrate just how complex PDE regulation of cellular physiology can be under different conditions, even when a given process involves only one PDE gene.

Brown Adipose Tissue

Brown adipose tissue (BAT) is classically understood to be a highly thermogenic organ that turns the energy contained in triglycerides and sugars into heat instead of ATP. In fact, the heat generated by BAT has been calculated to be 300 W/kg of body weight when it is fully activated in mice, which is approximately two orders of magnitude higher than the metabolic rate of most other mammalian tissues (Cannon and Nedergaard, 2004; Rothwell and Stock, 1983). The "wasted" heat energy is then circulated around the body keeping an animal warm in times of cold ambient temperature stress, a process known as non-shivering thermogenesis (NST). This function stands in contrast to white adipose tissue, which stores triglyceride as an energy "reserve" for when an animal may undergo dietary scarcity. Though human newborns contain a prototypical BAT pad in the interscapular region on their backs, humans lose this well-defined pad over the course of their childhood. Therefore, it was long thought that adult humans lacked appreciable amounts of brown adipose outside of patients suffering from adrenal tumors, such as pheochromocytoma, where the increased levels of catecholamines stimulate the generation of brown adipocytes in the fat surrounding the adrenal gland (Iyer et al., 2009). However, it was more recently confirmed that healthy adult humans have brown adipose tissue that can be activated by cold temperatures, though the functional characterization of this newly found BAT is still in its infancy. Is this tissue metabolically significant, wherein it converts circulating nutrients such as glucose and fatty acids (FAs) into heat, and could this ultimately prove beneficial as a weight-loss strategy? Though these questions remain unanswered, the discovery of

metabolically active brown fat in healthy adult humans has renewed a long-dormant interest into answering whether activation of BAT has any future in human therapeutics.

BAT is an organ that has a relatively short scientific history compared with other organs found in mammals. The discovery that the brown adipose tissue organ is thermogenic was only first described 52 years ago in rats (Smith and Hock, 1963). BAT's relation to energy expenditure and its role in metabolic inefficiency was not described until the late 1970s and into the 1980s by the seminal experiments conducted by Rothwell and Stock. Their results indicated that despite an 80% increase in energy intake on a high-fat, high-sucrose diet, rats on this cafeteria diet gained only 27% more than their chow-fed counterparts. These same rats also demonstrated an increased thermogenic capacity when exposed to cold temperatures, as well as increased BAT and sympathetic nervous activities (Rothwell and Stock, 1979), reviewed in (Tam et al., 2012). The effect of high caloric diets on BAT activity, known as "diet-induced thermogenesis," was later attributed to the resultant increase in the expression of the uncoupling protein-1 (UCP1), the mediator of proton conductance in brown fat mitochondria referred to at the time as "thermogenin" (Brooks et al., 1980; Nedergaard et al., 1983; Sundin and Nechad, 1983).

Though the increased circulating FAs can stimulate UCP1 induction (Sadurskis et al., 1995), they also cause an increase in the degree of sympathetic nerve-mediated activation of BAT (Young and Walgren, 1994) and an increase in blood flow to the tissue (Glick et al., 1984). Feeding also stimulates the release of

leptin from white adipocytes, which reduces food intake and stimulates the sympathetic nervous system via central mediation (Commins et al., 2000; Rouru et al., 1999). Mice that have targeted disruption of their BAT exhibit an exacerbated increase in weight gain and leptin resistance (Frederich et al., 1995). It has more recently been shown that either increasing the amount of BAT via transplantation or increasing BAT activity by cold exposure can prevent weight gain and improve insulin resistance on a high fat diet (Stanford et al., 2013), as well as serve as a major mediator of triglyceride clearance from the bloodstream (Bartelt et al., 2011). Though the molecular mechanism of the direct effects of FAs on UCP1 transcription is still unknown, the bigger question is why mammals would have evolved to waste the energy that that they have just consumed? This latter point is the central argument over the importance of brown fat as a regulator of diet-induced thermogenesis and whether or not it is a valid therapeutic target (Kozak, 2010).

Only in the past decade has the existence of active brown fat in adult humans become widely appreciated after cancer screening radiologists first noticed a substantial amount of ^{18}Fluoro-deoxyglucose (18FDG) uptake in the supraclavicular neck region of cancer patients undergoing PET/CT scanning for active tumors (for a more detailed history, refer to (Tam et al., 2012)). The prevalence of 18FDG uptake appeared to negatively correlated with ambient outdoor temperature (Cohade et al., 2003) and could be blocked if the patient was either kept warm (Garcia et al., 2006) or administered a β-adrenergic antagonist, such as propranolol (Tatsumi et al., 2004). Such observations would indeed resemble what has been observed in rodent BAT. Biopsied tissue from the necks of thyroid disease patients stained

positively for UCP1 and displayed a multilocular appearance in 57% of patients (Zingaretti et al., 2009). While Cypess, et al. observed the prevalence of BAT to be around 7.5% after retrospectively analyzing ~2000 PET/CT-scanned patients (Cypess et al., 2009), another study indicated that BAT activity could be stimulated by cold exposure in 23 of 24 male subjects that were otherwise negative for BAT under thermoneutral conditions (van Marken Lichtenbelt et al., 2009). Still, another study reported that of 162 healthy subjects aged 20-73, 41% were BAT positive after 2 h of cold exposure (Yoneshiro et al., 2011a). Though these results seem to vary widely in the overall prevalence of BAT in the adult population, these studies often rely on PET/CT scanning for active brown fat, a technique which has been reported as having anywhere from a 13-16% reproducibility rate regarding multiple scans from the same patient (Cohade et al., 2003; Lee et al., 2010; Rousseau et al., 2006). Recently, it was shown that patients who are not positive for BAT activity in PET scans still have brown fat tissue in the supraclavicular region that is positive for all classical BAT markers, such as UCP1, PGC-1α, PRDM16 and others, both at the mRNA and protein levels (Jespersen et al., 2013). Taken together, these results suggest that detecting the presence of BAT in adult humans largely depends on the context in which it is measured as well as the limitations of the methods used.

Body Weight Regulation and Brown Fat

Despite the wide variability in the reported prevalence of human BAT, there are some very important correlations between BAT activity and body composition parameters. First, observable BAT activity and body mass index (BMI) share an inverse correlation that has been documented by several different PET/CT-based

investigations (Cypess et al., 2009; Saito et al., 2009; van Marken Lichtenbelt et al., 2009). Several studies also reveal that age negatively correlates with the prevalence of BAT, where cold-induced BAT activity is observable in >50% of subjects in their 20s, but <10% in subjects over the age of 50 (Cypess et al., 2009; Tam et al., 2012; Yoneshiro et al., 2011a). It has been shown that increased fat content in older age groups positively correlates only with BAT-negative subjects compared with BAT-positive subjects (Yoneshiro et al., 2011b). Naturally, BMI tends to increase with age, therefore complicating whether the loss of BAT is causal for the development of obesity, or if it is merely coincidental.

Furthermore, a polymorphism, A-3826 A/G, in the UCP1 gene has been shown to correlate with a higher incidence of fat gain and obesity, as well as a decreased ability to lose weight on a low calorie diet (Fumeron et al., 1996; Heilbronn et al., 2000; Oppert et al., 1994). However, these findings are controversial and could be population-specific (Gagnon et al., 1998; Hamann et al., 1998; Urhammer et al., 2000). Nevertheless, if generally true, such studies would corroborate the recent finding that mice lacking UCP1 are more prone to obesity than their wild type counterparts when kept at thermoneutrality (Feldmann et al., 2009). Finally, the same investigations into human BAT prevalence noted that women have a higher prevalence of BAT than men. This has also been seen in rodents, where female rat BAT has higher UCP1 expression, higher thermogenic capacity and increased sensitivity to norepinephrine. Treatment of differentiated brown adipocyte precursors with 17-β-estradiol stimulated the same general phenotypes, whereas testosterone inhibited them (Rodriguez et al., 2002).

The contribution of BAT to whole body energy expenditure in humans is still somewhat controversial for several reasons. First, it was originally hypothesized that 40-50 g of BAT could account for 20% of daily energy expenditure in people (Rothwell and Stock, 1979). This number has been since recalculated given that an animal's metabolic rate per unit of body mass negatively correlates to body size. According to Kleiber's law, the metabolic rate for all organisms is roughly a ¾ power of the animal's mass (Kleiber, 1932). In other words, the larger the animal or tissue, the lower the metabolic rate per unit of body mass. Since the amount of brown adipose tissue in people has been estimated to be approximately 50 g based on 18FDG PET/CT imaging (van Marken Lichtenbelt et al., 2009), activated BAT could account for approximately 5% of basal metabolic rate (BMR) (van Marken Lichtenbelt and Schrauwen, 2011). This number could still represent a large enough proportion to impact body weight, though it is substantially less than previous estimates.

Taken together, the notion that decreasing metabolic efficiency by increasing BAT amount and/or activity may provide a protective role against fat deposition and obesity has gained significant momentum in the last 10 years as a potential therapeutic. This hypothesis still remains to be experimentally verified in humans, as currently there are no pharmacological tools to selectively activate human BAT.

cAMP signaling in Brown Adipose Tissue

The cAMP second messenger signaling cascade regulates most of the major biological hallmarks of activation in BAT, both during the chronic "recruitment" phase of brown adipocyte formation and during the acute "activation" phase of heat

generation in a mature cell. Much of the current research on brown adipose tissue as a therapeutic target has centered on the former, “recruitment,” phase of BAT, whereby transcription factors, such as PRDM16 and PGC-1α, and new hormones, such as irisin, have been recently discovered to be major molecular control switches that lead to the transition of brown adipocyte precursors into a mature brown fat cell (Bostrom et al., 2012). However, cAMP remains as a major regulator of the expression of PPARγ-cofactivator-1α (PGC-1α) and UCP1. This activation by cAMP is not merely transcriptional, but also acutely through the breakdown of triglycerides, whose fatty acid components feed into the activation of UCP1 to generate heat. In this section, I will briefly review the body of knowledge on how cAMP regulates brown adipocyte formation and function, and provide a molecular basis for the importance of uncovering which phosphodiesterases control the pools of cAMP that govern these processes.

Adrenergic receptors in brown adipose tissue

The first hints that cAMP was playing a role in brown adipose tissue function were the observations by Dawkins and Hull in 1964 (Dawkins and Hull, 1964) that norepinephrine (NE) could stimulate heat production in the brown adipose tissue of newborn rabbits, as well as increase oxygen consumption, plasma glycerol and free fatty acid production. They later showed that these effects could be blocked by the injection of propranolol prior to injection of NE, isoproterenol, or exposure to cold (Heim and Hull, 1966), therein strongly suggesting that β-adrenergic receptors are primarily mediating the physiological response to cold in BAT. Later, it was shown that NE stimulated cAMP production in brown adipose tissue, and direct

administration of cAMP or its cell-permeable analog dibutyryl-cAMP stimulated glycerol and fatty acid release and oxygen consumption (Beviz et al., 1968). Interestingly, from the same study came the first report that a nonselective phosphodiesterase inhibitor, theophylline, could similarly stimulate lipolysis and oxygen consumption in BAT as NE.

NE is the physiological agonist for a family of seven transmembrane G-protein coupled receptors called the adrenergic receptors (ARs). This family is comprised of α and β classes, of which there are several different subtypes within each family. In rodents, the β-AR that predominantly mediates the thermogenic effects of norepinephrine is the adipocyte-enriched β_3-adrenergic receptor (β_3-AR) (Arch et al., 1984; Zhao et al., 1997). The β_3-AR primarily couples through the stimulatory small GTP binding protein, G_s, (Granneman and MacKenzie, 1988) to activate adenylyl cyclase, though it has been suggested by some to also couple to G_i (Chaudhry et al., 1994) leading to an inhibition of cAMP production and an activation of the mitogen activated protein kinase pathway (Soeder et al., 1999). These two processes would be diametrically opposed to one another, and the stimulation of cAMP signaling would be naturally tempered. Indeed, brown adipocytes obtained from hamsters that had been treated with pertussis toxin, which inhibits G_i-dependent signaling, exhibited a 250-fold shift to the left in oxygen consumption in response to NE (Svoboda et al., 1996). In addition to β_3-ARs, β_1-ARs are also expressed in mature brown adipocytes, while β_2-ARs are not appreciably expressed in BAT (D'Allaire et al., 1995). The α_{1A}-AR, which couples to G_q and leads to an increase in intracellular calcium (Bronnikov et al., 1999b), is also

expressed in BAT and has been shown to potentiate β_3-AR-mediated thermogenesis in brown adipocytes from Syrian hamsters (Zhao et al., 1997). However, possible α_1-AR-mediated effects on brown adipose tissue in other species have not been well explored.

It is somewhat controversial as to whether β_1-ARs contribute significantly to the overall thermogenic response to cold in mature brown adipocytes, as they are approximately 10-fold less abundant compared with β_3-ARs (D'Allaire et al., 1995). Since β_1-ARs have a higher affinity for NE, some have concluded that these receptors mediate the thermogenic response when NE is low during a mild cold stress (Atgie et al., 1997). An important difference between the two receptors is that β_1-ARs have a susceptibility to desensitization via internalization when NE concentrations are high (Bukowiecki et al., 1978), but β_3-ARs do not (Granneman, 1992). This has led to the hypothesis that at the high concentrations (100nM) of NE estimated to be in the synaptic cleft (Depocas and Behrens, 1978) during maximal stimulation of sympathetic outflow, only the β_3-AR will mediate the thermogenic response. While some have contended that β_1-selective agonists do not appreciably stimulate thermogenesis, others have indeed seen this to be apparent. In fact, the β_1-AR can fully compensate for the loss of β_3-AR in a genetically disrupted mouse (Susulic et al., 1995), whereas the complete loss of all β-ARs led to substantial cold-induced and diet-induced thermogenic dysfunction (Bachman et al., 2002). Still another study claims that as brown adipocyte precursors are stimulated to differentiate by NE, there is a switch in the coupling to G_s from β_1 to β_3 (Bronnikov et

al., 1999a). Regardless, it is clear that β-ARs are the receptors responsible for mediating much of the effects of NE in BAT.

cAMP regulates brown adipocyte "recruitment"

Cyclic-AMP-dependent signaling has been shown to stimulate most known processes leading toward brown adipocyte recruitment. In the simplest of descriptions, brown adipocyte "recruitment" refers to the process of increasing the number of brown adipocytes in the BAT organ after repeated exposure to cold temperatures, thereby increasing the overall thermogenic potential of the tissue in response to sympathetic nervous system stimulation, i.e. the more brown fat tissue, the more heat that can be produced. This allows the animal to adequately keep warm in the cold without shivering. This process includes both the expansion/proliferation of brown adipocyte precursors and the differentiation of these precursors into the brown adipocyte phenotype. In primary cell culture, it has been shown that brown adipocyte precursor proliferation is primarily mediated through NE stimulation of β_1-ARs (Bronnikov et al., 1992; Fredriksson and Nedergaard, 2002; Thonberg et al., 2001). However, even though it is widely accepted that PKA is the predominant regulator of all known cAMP-dependent responses in BAT, since virtually all known processes are sensitive to the PKA-selective antagonist H89 (Cannon and Nedergaard, 2004), there is at least one report that implicates a role for Epac as a driver of differentiation in white adipocyte precursors (Petersen et al., 2008). A role for Epac has yet to be identified in brown adipocytes. Since PKA antagonists were not tested against the effects of cAMP on BAT precursor

proliferation in these early studies, the cAMP-dependent pathway that mediates proliferation has yet to be fully defined.

In culture, once brown adipocyte precursors reach confluence, the cells can then differentiate. PRD1-BF-1-RIZ1 Homologous Domain Containing Protein-16 (PRDM16) was recently identified as the major molecular driver regulating brown adipocyte cell fate, and PRDM16 is essential for cAMP-mediated activation (Seale et al., 2007). The process by which cAMP and PRDM16 together mediate differentiation is rather complex. It has long been known that cAMP stimulates the expression of PGC-1α the transcription factor primarily responsible for the activation of UCP1 gene expression (Puigserver et al., 1998) and mitochondrial biogenesis (Kajimura et al., 2010). PKA activation indirectly stimulates the phosphorylation and activation of p38-mitogen activated protein kinase (p38-MAPK), which then phosphorylates activating transcription factor 2 (ATF-2) that binds to the PGC-1α and UCP1 promoters to increase expression (Cao et al., 2004). It has more recently been shown that increased cAMP leads to the increased expression of another important transcription factor, CCAAT/enhancer-binding protein-β (C/EBP-β) (Rehnmark et al., 1993), which forms a complex with PRDM16 (Karamitri et al., 2009). This complex was shown to increase expression of PGC-1α, and PRDM16 was shown to directly interact with PGC-1α to increase its transcriptional activity at the UCP1 promoter (Seale et al., 2007). Importantly, the loss of either PRDM16 or C/EBP-β results in a near complete loss of brown fat characteristics (Kajimura et al., 2009; Seale et al., 2008). C/EBP-β is also important for the expression of peroxisome proliferator-activated receptor-γ (PPARγ), which then drives

adipogenesis and the accumulation of triglyceride droplets through association with PRDM16 (Kajimura et al., 2010). PKA also directly stimulates the phosphorylation of cAMP response element binding protein (CREB), which then binds to the promoter of UCP1 to enhance its expression (Cao et al., 2004). Altogether, cAMP has both direct and indirect impact on the differentiation of brown adipocytes through the expression and activation of critical transcription factors, leading to cells with multilocular triglyceride droplets, increased mitochondria content and enhanced thermogenic capacity through increased UCP1.

cAMP regulates brown adipose tissue thermogenesis

As a brown adipocyte precursor becomes a fully formed, mature brown adipocyte, it can then carry out its physiological function of generating heat during times of cold or dietary stress. This process, as with brown adipocyte recruitment, is also predominantly regulated by increases in cAMP. Brown adipose tissue is densely innervated by sympathetic nerve endings that are regulated by neurons within the preoptic chiasma/anterior hypothalamic nuclei (POAH) and ventromedial hypothalamus in the brain (for a more detailed review, see (Cannon and Nedergaard, 2004)). Norepinephrine is released from these nerve endings, which then can bind to β-ARs and rapidly stimulate the production of cAMP. Cyclic-AMP then binds to the regulatory subunit on PKA, thereby dissociating the catalytic subunit from the regulatory subunit and activating the kinase to phosphorylate several important downstream targets (Fig. 1.3).

Several of these PKA targets are involved in lipolysis, or the breakdown of triglycerides (triacylglycerol or TGs) into their fatty acid and glycerol components.

Perilipin belongs to a family of proteins called PAT proteins, or "perilipin," adipocyte differentiation-related protein (ADRP), and tail-interacting protein of 47kDa (TIP47)." These proteins coat the spherical lipid droplets within the fat cell, and protect the triglyceride stores from cytosolic lipases. For example, perilipin associates with a constitutively active adipose triglyceride lipase (ATGL) in the basal state, but this lipase cannot access the triglyceride substrate until perilipin is phosphorylated. PKA phosphorylates perilipin at Ser-492, which induces a conformational change that turns perilipin into a scaffold around which lipolytic machinery assembles to access the lipid stores (Bickel et al., 2009). ATGL can then remove the first fatty acid, yielding diacylglycerol as a product (Ducharme and Bickel, 2008). Additionally, PKA phosphorylates hormone sensitive lipase (HSL), which facilitates the translocation of the lipase to the lipid droplet from the cytosol (Brasaemle et al., 2000). Phosphorylated HSL has a higher lipolytic activity towards diacylglycerol and monoacylglycerol than triacylglycerol, and therefore removes the second and third FAs from the original TG molecule (Fig. 1.3).

The released FAs have a two-fold impact on thermogenesis in BAT, whereby they are both metabolized in the mitochondria by β-oxidation and act as an allosteric catalyst for UCP1 activity. B-oxidation leads to an increase in the electron transport chain by which $NADH^+$ and $FADH_2$ generated by fatty acid oxidation are oxidized to NAD^+ and FAD, and the resulting electrons are passed along a series of protein complexes (complex I-IV) in the inner mitochondrial membrane in order to finally reduce oxygen and hydrogen into water. Along the way, the transfer of electrons stimulates these protein complexes to pump hydrogen ions (protons) from the

mitochondrial matrix into the intermembrane space (IMS). This generates a proton gradient. This gradient is normally dissipated by ATP synthase, which uses the energy contained in the gradient to convert adenosine diphosphate (ADP) and free inorganic phosphate into adenosine triphosphate (ATP) (Fig. 1.4). Interestingly, brown adipose tissue exhibits very low ATP synthase activity, due to the lack of expression of subunit c (Houstek et al., 1995). The proton gradient is instead dissipated through UCP1, which is also situated on the inner mitochondrial membrane. This electromotive energy is subsequently lost as heat instead of being utilized to phosphorylate ADP into ATP (Fig. 1.4).

UCP1, formerly known as thermogenin, is a member of the mitochondrial carrier protein transport family. Despite extensive study, the mechanism by which UCP1 dissipates the proton gradient remained controversial for decades. Recently, however, it was shown that UCP1 acts as a symporter for the FA charged carboxyl group and the positively charged proton, where the FA bound in the pore of UCP1 physically shuttles the proton from the IMS to the matrix. However, the FA does not dissociate and remains bound to the pore (Fedorenko et al., 2012) (Fig. 1.4). Therefore, cAMP is critically important for the generation of heat in brown fat through the liberation of fatty acids.

cAMP-dependent glucose uptake

During cold exposure, brown adipose tissue exhibits a substantial increase in glucose uptake that is mediated via the sympathetic nervous system (Shimizu et al., 1993; Shimizu et al., 1998) (Fig. 1.3). Although insulin also stimulates glucose uptake in BAT, this sympathetically stimulated phenomenon has been shown even

in fasted rats and mice, in which blood insulin levels are low (Fueger et al., 2006; Shibata et al., 1989). In fact, BAT is only one of two tissues in mice that can be stimulated by NE to acutely take up glucose (the other being the heart), whereas NE either has no effect or even inhibits glucose uptake in most other tissues (Cooney et al., 1985). This effect could be mimicked by the injection of a β_3-AR agonist in rats (Liu et al., 1998), and it has been shown by numerous groups that NE or β-adrenergic agonists can stimulate glucose uptake in isolated brown adipocytes *ex vivo* (Ebner et al., 1987; Marette and Bukowiecki, 1989). Additionally, this effect could also be mimicked by cAMP analogues and blocked by either adenylyl cyclase or PKA inhibition in cultured brown adipocytes (Chernogubova et al., 2004).

However, the mechanistic details of how adrenergic agonists stimulate glucose uptake remain unclear and perhaps somewhat controversial. While it is well established that insulin stimulates the translocation of glucose transporter-4 (GLUT-4) to the cell surface in all tissues in which it is expressed, including BAT, norepinephrine fails to stimulate GLUT-4 translocation (Dallner et al., 2006), even though GLUT-4 is much more highly expressed in BAT than GLUT-1. Additionally, there are conflicting reports as to how adrenergic signals regulate GLUT-1. It has been shown that NE can increase both GLUT-1 mRNA and cell surface expression in differentiated brown adipocytes from mice by recruitment of PI3K and PKC (Chernogubova et al., 2004; Dallner et al., 2006). However, others have indicated that cAMP does not stimulate expression or translocation of GLUT-1 at all (Shimizu et al., 1998), but rather increases GLUT-1's affinity for glucose in rat brown adipocytes (Shimizu et al., 1994). It should be emphasized that these discrepancies

could simply be due to interspecies variance. Nevertheless, cAMP has a pronounced effect on glucose uptake in brown adipocytes regardless of the species, and this effect is consistently different than that of insulin signaling and GLUT-4 translocation.

It has also been demonstrated that norepinephrine-dependent glucose uptake can partially be attenuated by inhibiting fatty acid oxidation in the mitochondria, suggesting that this uptake is not directly dependent on PKA but rather an indirect result of uncoupling (Marette and Bukowiecki, 1991). This seems logical given the low expression of ATP synthase and the high expression of UCP1, leading to an overall depletion of ATP and the need for alternative ATP generation. Indeed a similar phenomenon has been observed in a rat liver cell line, where fatty acid oxidation inhibition led to an activation of GLUT-1 activity, but not translocation to the cell surface (Shetty et al., 1993). This change in transport activity has been correlated to the activation of AMPK (Barnes et al., 2002). The increased glucose could then provide an additional source of ATP in the cytosol through glycolysis, or could be converted into fatty acids, as fatty acid synthesizing enzymes are also increased during cold exposure (Cannon and Nedergaard, 2004). However, it is unclear as the extent that this is needed, since fatty acids do not dissociate from UCP-1 once they are bound (Fedorenko et al., 2012), and fatty acids in circulation could more than satisfy this need (Cannon and Nedergaard, 2004). Moreover, it is not entirely intuitive why the cell would synthesize fatty acids from glucose only to break them back down again in what would seem an energetically wasteful process.

It may be that the glucose simply provides alternate energy source via production of acetyl CoA.

Clinically, the notion of a major insulin-independent glucose uptake pathway is certainly provocative. The hallmarks of type 2 diabetes are insensitivity to circulating insulin and a resulting lack of control over blood glucose levels. The ability to bypass an insulin-mediated pathway could therefore have a major therapeutic potential, particularly if the energy sources are then converted to heat and not fed into the further storage of triglycerides. A better understanding of the molecular mechanism for cAMP-dependent glucose uptake is required for the future development of therapeutics targeting this process.

Phosphodiesterases in Adipose Tissue

PDEs in white adipose tissue

As described above, cyclic-nucleotide PDEs are enzymes that catalyze the conversion of cyclic nucleotide second messengers into inactive nucleotide monophosphate products (i.e. cAMP -> 5'-AMP, cGMP -> 5'-GMP). These enzymes regulate both the duration of action and the spatial confinement of the cyclic nucleotide signal that has been generated by the activation of a cyclase. Since cAMP is probably the most important second messenger in adipocyte physiology, understanding the regulation of these adipocyte processes by PDEs has been an important topic of study ever since PDEs were first discovered. In fact, one of the first studies on the physiological relevance of PDEs utilized adipocytes as a model system to test the efficacy of what are now known to be nonselective PDE inhibitors, including the most widely used isobutyl-n-methylxanthine (IBMX) (Beavo et al.,

1970b). This study showed that inhibiting PDEs stimulated lipolysis in white adipocytes isolated from rats. Since then, the different PDE subtypes that are expressed in white adipocytes have been thoroughly characterized and explored, particularly PDE3B but also PDE4.

By 1970 it had been shown by several groups that there may be multiple types of PDEs that can be found within a given tissue (Beavo et al., 1970a; Brooker et al., 1968), and it was in that year that white adipocytes were also shown to have two distinct PDE subtypes (Loten and Sneyd, 1970). These two activities were then often referred to in later adipose tissue studies as the "low-K_m" and "high-K_m" PDE enzymes, with the V_{max} of the low-K_m enzyme being substantially increased by pretreating the cells with insulin. We now know that this "low-K_m" PDE is PDE3, more specifically PDE3B, and the "high-K_m" is likely one or more PDE4 subtypes, which do not appreciably vary from one another in their kinetic properties.

Insulin has long been known to physiologically inhibit lipolysis in adipocytes and other tissues, and PDE3B was identified as the major effector molecule that regulates this phenomenon. Briefly, insulin stimulates the activation of protein kinase-B (PKB) via phosphatidylinositol-3-phosphate kinase (PI3K), which then phosphorylates PDE3B (Wijkander et al., 1998). This phosphorylation increases the rate of hydrolysis (V_{max}) of cAMP by PDE3B, thereby lowering cAMP levels and PKA activity and subsequently decreasing the rate of lipolysis. PDE3B can also be phosphorylated and similarly activated by PKA, thereby providing a negative feedback loop in the regulation of cAMP signaling in PDE3B-containing microdomains (Degerman et al., 1990). The global loss of PDE3B in mice results in

a complex phenotype, where overall white fat pad size is decreased, and adipocytes are more responsive to isoproterenol with regards to lipolysis (Choi et al., 2006). However, lipogenesis and fat cell size are increased, and these mice show a diabetic phenotype (Choi et al., 2006), possibly due to the chronic stimulation of lipogenic enzymes such as acetyl co-A carboxylase (ACC) (Omar et al., 2009).

PDE4 has also been implicated in the regulation of lipolysis in white adipocytes under a mild stimulation by isoproterenol or other agents, as a PDE4 inhibitor will also potentiate the lipolytic effects of isoproterenol. However, this effect will all but disappear when insulin is co-administered, after which PDE3B becomes the major regulator of lipolysis (Van Harmelen et al., 1999; Zmuda-Trzebiatowska et al., 2006). A similar finding was observed in the regulation of adenosine monophosphate kinase (AMPK) stimulation by cAMP. In this particular case, it was shown that a PDE3 inhibitor could reverse the antagonistic effects of insulin on isoproterenol-stimulated AMPK phosphorylation, whereas a PDE4 inhibitor could not. Conversely, a PDE4 inhibitor alone could stimulate AMPK phosphorylation in the absence of hormone, but it could not reverse the negative effects of insulin on that process (Omar et al., 2009).

PDE3B has two membrane targeting domains in its N-terminal region that mediate its association with the endoplasmic reticulum and the plasma membrane (Shakur et al., 2000), and it has also been shown to directly interact with caveolin-1 in primary white adipocytes (Nilsson et al., 2006). This targeting to cell membranes may partially explain why PDE3 and PDE4 differentially regulate certain processes depending upon which hormones are present (i.e. insulin). These findings highlight

the complexity with which hormones can regulate adipocyte metabolic activation through PDEs.

As previously mentioned, some of the first studies on PDE inhibitors demonstrated that nonselective PDE inhibitors were sufficient to generate a large increase in lipolysis without co-administration of the various hormones (Beavo et al., 1970b). Therefore, PDE activity is essential in the basal state to keep lipolysis in check, though it remained unclear as to which specific PDE subtypes were mediating this process. It was recently shown that neither a PDE3 nor a PDE4 inhibitor significantly augmented lipolysis in several mouse white adipocyte models when either drug was administered alone in the absence of insulin or adrenergic agonists (Snyder et al., 2005). However, these inhibitors cause a very large increase in lipolysis when they are combined, and the magnitude of this effect was shown to be similar to the effect of IBMX or a maximal dose of isoproterenol (Snyder et al., 2005). This demonstrated that the full IBMX effect on basal lipolysis is accounted for by PDE3 and PDE4, suggesting either that both seem to share the same basal pool of cAMP or that there are parallel pathways that each PDE regulates. It is likely that this basal pool of cAMP is generated due to the relatively high basal activity of β-ARs (Rasmussen et al., 2007), which seem to spontaneously flip back and forth from inactivated to activated conformations even in the absence of agonist (Yao et al., 2009). While many of these structure-function studies were conducted on the β_2-AR, selective inverse agonists to each of the three different β-ARs have been shown to inhibit basal production of cAMP (Hoffmann et al., 2004).

It would seem that both PDE3 and PDE4 activity in white adipocytes act to suppress the basal production of cAMP thereby preventing the stimulation of lipolysis.

PDEs in brown adipose tissue

The physiological regulation of brown adipose tissue by PDEs is a virtually unexplored area of research. The first characterization of PDEs in BAT described the same low-K_m and high-K_m activities that were observed in white adipocytes (Bertin and Portet, 1975), which we now know are PDE3 (Reinhardt et al., 1995) and PDE4, respectively. It was later shown that PDE3B, and not PDE3A, was the particular PDE3 subtype that was expressed in BAT (Nagaoka et al., 1998). The specific activities for these two PDEs were decreased in brown adipocytes from rats that were acclimatized to cold (Bertin and Portet, 1975), indicating some sort of a feedback inhibition in the amount or activity of the enzymes. Yet, neither the significance nor the mechanism of this decrease has been explored. Later, it was shown that PDE2, in addition to PDE3 and PDE4, was expressed in rat BAT and was increased in a genetic model for obesity (Coudray et al., 1999). However, the physiological role of PDE2 in BAT also has not been determined.

Evidence for the physiological effects of PDEs in BAT is equally scarce, since most studies were conducted with non-selective inhibitors as controls to illustrate that a process was cAMP-dependent. For example, it was shown that theophylline, a non-selective PDE inhibitor that pharmacologically resembles caffeine, could stimulate sodium flux in isolated hamster brown adipocytes, a process that could also be stimulated by norepinephrine and the adenylyl cyclase activator, forskolin (Connolly et al., 1986). It was also shown that IBMX could stimulate glucose uptake

in freshly isolated rat brown adipocytes (Marette and Bukowiecki, 1989; Omatsu-Kanbe and Kitasato, 1992). Furthermore, there were several studies conducted by Wang and Lee in the 1980s demonstrated that theophylline and aminophylline, a theophylline derivative, enhance cold tolerance by increasing non-shivering thermogenesis in rodents and man (Lee et al., 1987; Wang and Anholt, 1982). It remains somewhat unclear whether these effects may have more to do with inhibiting A1 adenosine receptors, which are G_i-coupled, both peripherally and centrally (Dulloo et al., 1991; Wang et al., 1989) or by PDE inhibition (Dulloo et al., 1992).

Probably the most comprehensive study into PDE regulation of brown adipocytes came in 1999, when it was showed that increases in intracellular calcium in response to norepinephrine was linked to a decrease in the maximal cAMP levels and UCP-1 mRNA expression in differentiated brown adipocytes *in vitro* due to the activation of PDE activity (Bronnikov et al., 1999b). This negative feedback response was shown to be dependent on the α-adrenergic receptor, and coupled to intracellular calcium increases via G_q and phosphatidyl inositol-3-phosphate (IP_3). This study also showed that this decrease in maximal cAMP could be inhibited by 1 mM 8-methoxymethyl-IBMX (8-MM-IBMX), one of the few inhibitors at the time known to inhibit the PDE1 family, but not by OPC-3911 nor by Ro-20-1724, which are selective inhibitors to PDE3 and PDE4, respectively. However, PDE3 and PDE4 inhibitors enhanced the efficacy of norepinephrine on cAMP accumulation. This shift in baseline indicated that both PDEs are important for at least the initial surge of cAMP generated by β-ARs. The authors did not combine PDE3 and PDE4 inhibitors

together to see if the combined inhibition of these two major PDEs were important for the biphasic regulation of cAMP. This is of particular importance, as they might not have realized at the time this study was done that a concentration of 1 mM 8-MM-IBMX inhibits all PDEs with the same efficacy as IBMX, which they showed inhibits the calcium-dependent inhibition of forskolin-stimulated cAMP in these cells. Regardless, the study was one of the first to characterize the effects of selective PDE inhibition on cAMP accumulation, and the first and only to suggest a role for PDE1 in the tissue (Bronnikov et al., 1999b).

Later it was shown that increases in intracellular calcium in brown preadipocytes were β-AR/cAMP/PKA dependent, as opposed to α-AR dependent in mature brown adipocytes, and this effect was similarly biphasic at higher concentrations of cAMP (Dolgacheva et al., 2003). In this study, it was shown that both PDE3 and PDE4 inhibitors could potentiate the effect of NE alone on Ca^{2+}, with the PDE3 inhibitor resulting in the larger increase of the two. At first glance, this would seem like PDE3 regulates this process while PDE4 is relatively minor. However, when the two inhibitors are combined the calcium response was no greater than the PDE4 inhibitor. It is highly likely, given their biphasic response to cAMP, that the synergistic combination of PDE3 and PDE4 inhibitors may be increasing cAMP such that it inhibits Ca^{2+} accumulation, and is therefore on the downside of the biphasic curve. In light of this possibility, and the nature of biphasic kinetics, it could also be that PDE4 inhibition mediates a much larger increase in cAMP than fully realized. In fact, it was previously shown that PDE4 inhibition has a

much larger effect on NE-induced cAMP accumulation in mature brown adipocytes than a PDE3 inhibitor (Bronnikov et al., 1999b).

Obesity, diabetes, and the roles BAT PDEs may play in future therapeutics

Over the last 30-40 years, obesity has become one of the fastest growing and most prevalent medical problems in the United States. Currently, over one-third of adult Americans are obese (35.7%, CDC), representing a number that has doubled in that span of time (Guyenet and Schwartz, 2012). An additional one-third of adults are considered "overweight." Approximately 15-17% of children are also obese, a number that has tripled since 1980 (Flegal et al., 2010). As a result, obesity has become a leading cause of several other co-morbidities, such as type 2 diabetes, cardiovascular diseases and cancer, leading to a decreased lifespan and a lower quality of life (Baker et al., 2007; Calle et al., 2003; Flegal et al., 2007; Jensen et al., 2012). According to the Center for Disease Control, the estimated medical cost of obesity and obesity-related diseases in 2008 was $147 billion, nearly double than that of the costs just 10 years before (Finkelstein et al., 2009). Obese patients were estimated to have spent over $1,400 per year more than their non-obese counterparts, and the main driver of these costs was attributed to pharmaceuticals.

Despite almost six decades of research into the causal relationship between central/abdominal obesity and these other co-morbidities and adipocyte biology (Vague, 1956), very few non-invasive therapeutic options for the treatment of obesity itself have been developed. So far, the leading strategies have been targeted towards decreasing caloric intake, either physically with bariatric surgery or centrally with drugs whose side effects are notably decreased appetite, or towards increasing

exercise. In addition, there is a substantial challenge faced by clinicians as to patient compliance, and a growing understanding that mammals tend to homeostatically defend a new metabolic set point (Brownell, 2010). A classic demonstration of this is shown by studies in which a subject on a high caloric diet will become resistant to the hormone leptin (Frederich et al., 1995; Williams, 2012), which acts as a satiety signal that is released into circulation by adipose tissue after the ingestion of a meal. In light of these realities, new therapeutic approaches will be required to combat obesity, potentially by directly targeting adipocytes.

As described above, BAT has gained a renewed interest with regards to the development of future therapeutics designed to combat obesity and its co-morbidities. The ability for activated BAT to convert excess energy into heat separates it from virtually all other tissues in the body, particularly WAT, liver and muscle. In which excessive accumulation of triglycerides is thought to be toxic and lead to insulin resistance. However, the pathophysiology of obesity and the other diseases it causes remains inordinately complex and virtually impossible to define in a unified model (for a detailed review, ref. to (Tchernof and Despres, 2013)).

It is the opinion of this author and others that increasing the amount, or more importantly the activity, of BAT could prove therapeutically beneficial. What is most interesting from a therapeutic standpoint is not that BAT converts excess calories into heat, but that it does so in an insulin independent fashion. BAT activation is dependent on a cAMP/PKA-dependent pathway. Given that PDEs bind to and inactivate cAMP, these enzymes represent a very attractive family of pharmacological candidates for the development of future pharmaceuticals that

activate BAT. One can imagine that inhibiting the process by which cAMP is degraded could lead to enhanced UCP1 expression, lipolysis, glucose uptake, fatty acid clearance, and an increase in thermogenesis. Therefore, identifying the major PDE candidates that mediate all of these given processes in BAT is a necessary first step that so far has yet to be determined by the scientific community.

Statement of Problem

The last 50 years of research into brown adipocyte physiology has yielded very little information regarding the roles of PDEs on BAT function. In particular, the subtypes that regulate a given intracellular process, either basally or under adrenergic stimulation, have not been identified or fully characterized. There is evidence that PDE inhibitors in the absence of adrenergic stimulus can stimulate BAT metabolic processes, such as lipolysis and glucose uptake and even differentiation. However, there are significant gaps in knowledge remaining that this dissertation is intended to investigate.

The specific questions addressed were:

1) **What PDE or PDEs regulate the major cAMP-dependent molecular and metabolic processes that encompass brown adipocyte activation?**
2) **Are these processes differentially regulated by PDEs or are they regulated synergistically by multiple PDEs?**
3) **Does PDE8A interact with mitochondria in BAT? If so, to what mitochondrial compartment does it localize?**

Chapter 2 describes the effects of pharmacological inhibition of PDEs on many of the important cAMP-dependent process that are critical for BAT activation, namely UCP1 mRNA expression, cAMP levels, protein phosphorylation, and glucose

uptake. Additionally, chapter 2 highlights the necessity of inhibiting multiple PDEs at the same time in order to observe maximal responses. Chapter 3 discusses preliminary investigations into the nature of PDE8A interactions with the mitochondria, and suggests that PDE8A interacts with the mitochondria exterior. Finally, Chapter 4 discusses the conclusions from these findings as they relate to the future of pharmacological therapies that target BAT.

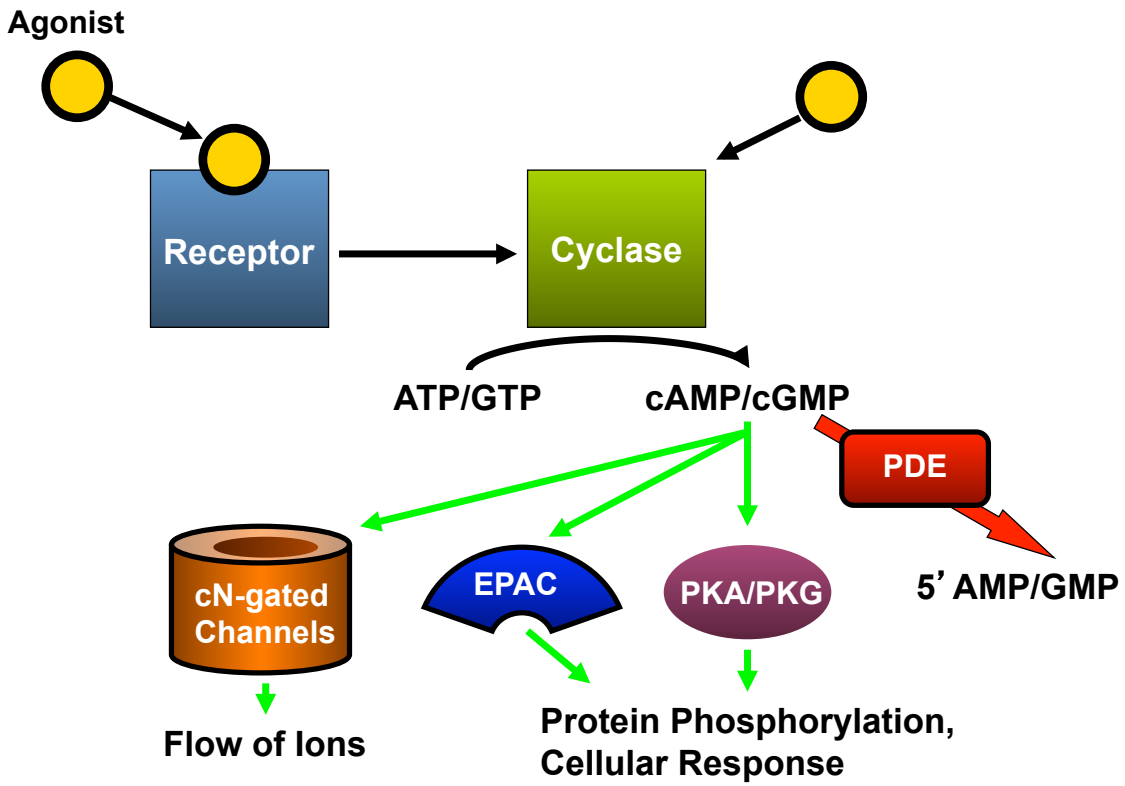

Figure 1.1. Cyclic Nucleotide Signaling.
Agonists either bind to a receptor that is coupled to a cyclase enzyme, or directly bind to the cyclase itself. Activated cyclases convert ATP or GTP into the second messengers cAMP or cGMP, respectively. Cyclic nucleotides can then bind to a number of effector molecules downstream, namely cyclic-nucleotide gated ion channels (cN-gated Channels), exchange protein directly activated by cAMP (EPAC), and protein kinases A or G. Phosphodiesterases convert cyclic nucleotides into inactive 5'-AMP or 5'-GMP.

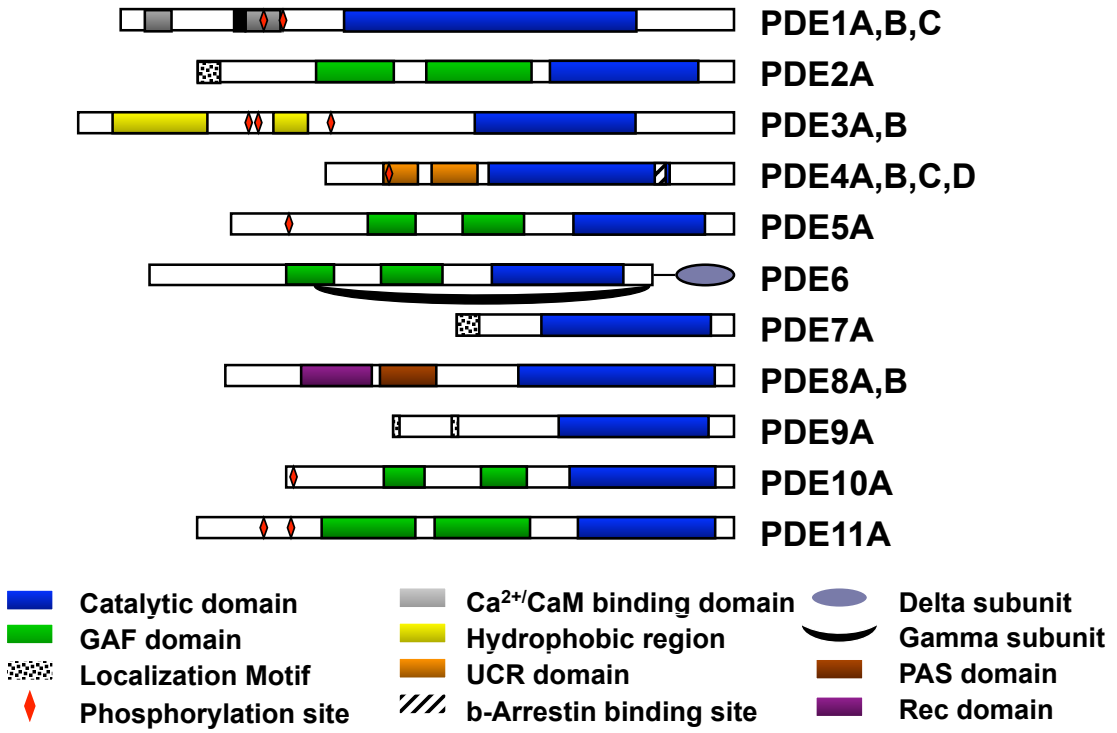

Figure 1.2. Phosphodiesterase Superfamily.
There are 11 PDE subtypes comprised of 22 different genes. PDEs have a C-terminal catalytic domain and an N-terminal domain that is involved in enzyme regulation or localization within the cell.

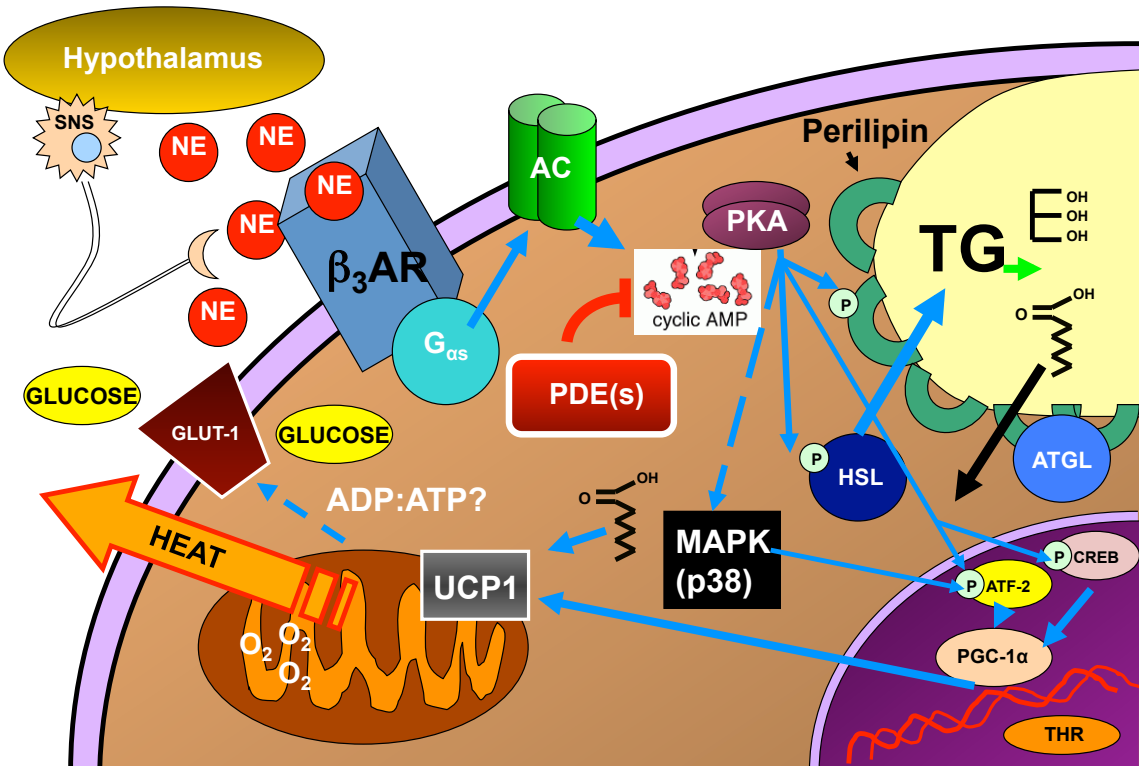

Figure 1.3. Cyclic-AMP Mediates BAT Thermogenesis.
When an animal senses cold, the hypothalamus releases norepinephrine (NE) onto brown adipocytes via the sympathetic nervous system (SNS). NE binds to and activates β_3-adrenergic receptors, which are coupled to the small g-protein Gαs, which activates adenylyl cyclase (AC). AC generates cAMP, which then stimulates protein kinase A (PKA). PKA then phosphorylates lipolytic enzymes perilipin and hormone sensitive lipase (HSL), which allow for triglycerides (TG) to be broken down into fatty acids and glycerol. Adipose triglyceride lipase (ATGL) is constitutively active and gains access to the TG droplet after perilipin phosphorylation. PKA also stimulates UCP1 expression via the phosphorylation of transcription factors ATF2 and CREB. FAs then bind to and activate UCP1 to dissipate the proton gradient generated by the metabolism of FAs and glucose in the mitochondria. This generates heat to be circulated throughout the body. The resultant drop in ATP production due to uncoupling may also stimulate glucose uptake through GLUT-1.

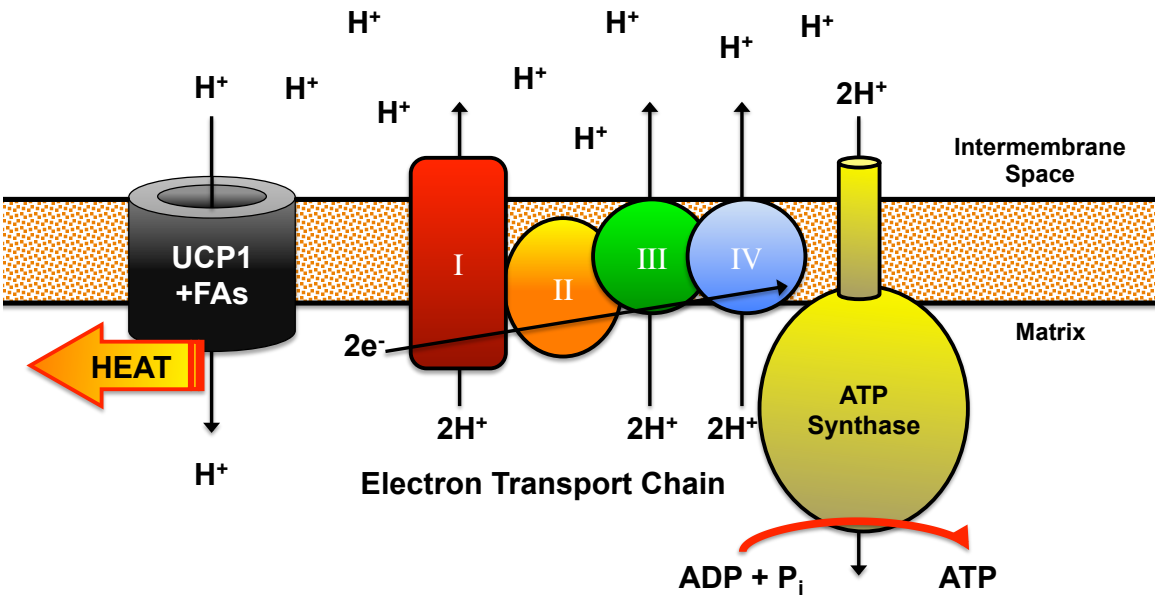

Figure 1.4. The Molecular Basis of Thermogenesis in BAT.
The electron transport chain pumps hydrogen ions (protons) from the mitochondrial matrix to the intermembrane space. This gradient is dissipated either through ATP synthase to generate ATP from ADP and inorganic phosphate (P_i) or through uncoupling protein-1 (UCP1) to generate heat. Fatty acids (FAs) are directly bound inside the pore in UCP1, and these act as a symporters to facilitate the movement of hydrogen ions from the intermembrane space into the matrix.

Chapter 2:
PDE3 and PDE4 isozyme selective inhibitors are both required for synergistic activation of brown adipose tissue

Summary

Brown adipose tissue (BAT) is a highly thermogenic organ that converts lipids and glucose into heat. Many of the metabolic and gene transcriptional hallmarks of BAT activation, namely increased lipolysis, uncoupling protein-1 (UCP1) mRNA, and glucose uptake are regulated by the adrenergic second messenger, adenosine-3',5'-cyclic monophosphate (cAMP). Cyclic nucleotide phosphodiesterases (PDEs) catalyze the breakdown of cAMP, thereby regulating the magnitude and duration of this signaling molecule. In the absence of adrenergic stimulus, we found that it required a combination of a PDE3 and a PDE4 inhibitor to fully induce UCP1 mRNA and lipolysis in brown adipocytes, whereas neither PDE inhibitor alone had any substantial effect under basal conditions. Under submaximal β-adrenoceptor stimulation of brown adipocytes, a PDE3 inhibitor alone could potentiate induction of UCP1 mRNA, while a PDE4 inhibitor alone could augment lipolysis, indicating differential roles for each of these two PDEs. Neither induction of UCP1 nor lipolysis was altered by inhibition of PDE1, PDE2 or PDE8A. Finally, when injected into mice, the combination of PDE3 and PDE4 inhibitors stimulated glucose uptake in BAT under thermoneutral and fasted conditions, a response that was further potentiated by the global ablation of PDE8A. Taken together, these data illustrate that multiple PDEs work in concert to regulate three of the important pathways leading to BAT activation, a finding that may provide an improved conceptual basis for the development of therapies for obesity-related diseases.

Introduction

Brown fat function and its relation to obesity and obesity-related diseases was widely studied in rodents throughout the 1980s and 1990s. However, as described in detail in Chapter 1, a revival of interest in BAT has taken place due to the discovery that adult humans possess functionally active depots of brown adipose tissue (Cypess et al., 2009; van Marken Lichtenbelt et al., 2009; Virtanen et al., 2009). Previously, it was shown that animals on a high fat diet have increased expression of UCP1 protein and increased thermogenesis due to higher sympathetic tone (Rothwell and Stock, 1979). It also is known that animals lacking functional brown adipose tissue, due to ablation of UCP1, gain more weight than their wild type counterparts under thermo-neutral condtions (Feldmann et al., 2009). In rodent models of obesity, administration of β_3-adrenoceptor agonists not only leads to enhanced lipolysis in white adipocytes (Murphy et al., 1993), but also enhanced insulin sensitivity, glucose utilization, and triglyceride (TG) clearance (Bartelt et al., 2011; Liu et al., 1998; Yoshida et al., 1994). These latter effects are partially mediated by an increase in thermogenesis, whereby circulating fatty acids mobilized from white fat stores are converted into heat by activated brown fat (Weyer et al., 1999). Recently, increased fatty acid oxidation by brown fat has been shown in adult human males exposed to cold (Ouellet et al., 2012). It is this glucose- and fatty acid-“clearing” characteristic of brown fat that makes it such an attractive potential target for drug development to treat obesity-related diseases like diabetes.

Differentiated brown adipocytes are activated by norepinephrine, which increases cAMP production and stimulates cAMP-dependent protein kinase (PKA)

(Janssens et al.). Activation of PKA in turn leads to breakdown of TG stores and increased expression and activation of uncoupling protein-1 (UCP1) to generate heat (Fedorenko et al., 2012). Increased cAMP also results in increased glucose uptake and metabolism in several tissue types, including brown adipocytes but not in white adipocytes (Jensen, 2007; Marette and Bukowiecki, 1989; Taylor et al., 1976).

However, to date an effective pharmacological strategy for combating obesity that selectively targets the cAMP-signaling system, particularly via the β_3-adrenoceptor, in human brown adipose tissue has not been developed due to low expression of this receptor in humans (Barbe et al., 1996; Deng et al., 1996; Larsen et al., 2002; Ursino et al., 2009). Moreover, pharmacological strategies that avoid β-receptor activation will likely be required to avoid cardiovascular and other β-receptor-mediated side effects. This is of particular importance, as it has been speculated by several groups that any therapy aimed at increasing the amount of brown fat tissue by differentiation of adipocyte precursors into mature brown adipocytes may not be effective without also providing a means of increasing the activity of the new brown fat tissue (Cannon and Nedergaard, 2009; Gesta et al., 2007; Sell et al., 2004). It is therefore imperative to better understand the mechanisms that regulate the acute activation phases of heat production *in vivo*.

Although the cAMP-dependency of brown fat metabolism has been extensively described, the field has only begun to address the roles played by the negative regulators of cyclic nucleotide signaling, the cyclic nucleotide phosphodiesterases (PDEs), that suppress or modulate each of the thermogenic processes described above. Previous studies have identified the expression of

PDE2, PDE3, and PDE4 in rat brown adipose tissue (Coudray et al., 1999), and at least one study suggested the presence of a PDE1 activity in differentiated brown adipocytes from NMRI mice (Bronnikov et al., 1999b). However, which distinct PDE subtype regulates each of the various cAMP-dependent processes of brown fat activation has yet to be determined. Selective inhibitors to most of the PDE families have been developed and inhibition of PDEs often leads to activation of cAMP-dependent physiological processes, thereby making PDEs attractive pharmacological targets (Bender and Beavo, 2006).

In this study, we have determined which PDE subtypes are important regulators of three major cAMP-dependent pathways of BAT activation, namely UCP1 gene expression, lipolysis, and glucose uptake. We have found that the activity of PDE3 and PDE4 both can regulate basal UCP1 expression, lipolysis and glucose uptake, and that combining inhibitors to these PDEs synergistically stimulates each of these processes in BAT. We also have identified PDE8A as a potential regulator of BAT glucose uptake *in vivo* in conjunction with PDE3 and PDE4. Most importantly, these findings indicate that a single selective PDE inhibitor alone is not sufficient to substantially activate basal BAT function, but rather a combinatorial inhibitor approach may prove more effective.

Materials and Methods

Animals.

Wild type C57/Bl6 mice were purchased from Taconic (Hudson, NY) or the Jackson Laboratory (Bar Harbor, MA). For a description on the generation of the PDE8A knock-out (PDE8A-/-) mouse line refer to (Vasta et al., 2006). For the experiments involving mice reported here, PDE8A-/- and wild type littermate mice between the ages of 10 and 16 weeks were used as controls. The Institutional Animal Care and Use Committee (IACUC) of the University of Washington, in accordance with the National Institutes of Health Guide for Care and Use of Laboratory Animals, approved all procedures.

Real-Time PCR

Mouse interscapular brown adipose tissue was excised, weighed, and disrupted using a rotor-stator tissue homogenizer. RNA was isolated using the RNeasy Lipid Tissue Mini kit (QIAgen, Valencia, CA). RNA was isolated from cells in culture by using either the QIAshredder system and RNeasy Mini kit (QIAgen, Valencia, CA) or the NucleoSpin RNA II kit (Macherey-Nagel). Complementary-DNA (cDNA) was then generated from 0.125-0.5 μg RNA using SuperScript III reverse transcriptase (Invitrogen, Grand Island, NY) and oligo-dT primers modified with a 5'-phosphate. Relative gene expression was determined by performing real-time PCR on a MX3000P QPCR system (Stratagene, La Jolla, CA) and analyzed with Mx-Pro software. Real-time PCR reactions were run with iTaq SYBR Supermix (Bio-Rad Laboratories, Hercules, CA) with the following thermoprofile: 95°C for 15 s, followed

by 60°C for 45 s for 40 cycles. Primer (IDT, Coralville, IA) sequences for the different PDE isoforms are found in Table 2.1. All primer sets were determined to anneal on different exons.

Culturing and Differentiation of Immortalized Brown Adipocyte Precursors

The immortalized brown adipocyte precursor cell line was a generous gift from Dr. Bruce Spiegelman's laboratory (Dana Farber Cancer Institute, Boston, MA). The precursor isolation, immortalization procedure, and growth conditions have been described previously (Uldry et al., 2006). In brief, cells were routinely seeded at 25,000 cells/cm^2 (day 0) in culture medium, comprised of high glucose Dulbecco's Modified Eagle's Medium (HyClone, Thermo Scientific, Waltham, MA) supplemented with 10% fetal bovine serum (FBS)(HyClone, Thermo Scientific, Waltham, MA) and 50 U / 50 μg penicillin/streptomycin in 500 mL (Gibco, Life Technologies, Grand Island, NY). The following day (day 1), the medium was changed to induction medium, which was culture medium supplemented with 20 nM insulin, 1 nM triiodo-thyronine (T3)(Sigma, St. Louis, MO), 0.5 μM dexamethasone (Sigma, St. Louis, MO), 0.5 mM isobutyl-1-methylxanthine (IBMX)(Sigma, St. Louis, MO), and 0.125 mM indomethacin (Sigma, St. Louis, MO). On day 3, the media were changed to culture medium supplemented with 20 nM insulin and 1 nM T3, and subsequently changed every day thereafter. By day 6, 95% of cells exhibited a fully differentiated phenotype with a large accumulation of multilocular fat droplets. All experiments were conducted on day 6 unless otherwise stated.

PDE Activity Assay

Differentiated brown adipocytes were washed 3 times with PBS, then lysed by briefly sonicating in ice cold 50 mM Tris, pH 7.4, 2 mM EDTA, 1 mM DTT, 1 mM sodium orthovanadate, 200 nM phenylmethylsulfonyl fluoride, and 1X protease inhibitor cocktail III (Calbiochem, EMD Millipore, Darmstadt, Germany). PDE activity was measured as described previously (Hansen and Beavo, 1982; Soderling et al., 1998). In brief, the activity assay was carried out in 40 mM MOPS, pH 7.5, 15 mM magnesium acetate, 2 mM EGTA, and 0.2 mg/ml bovine serum albumin (BSA)(Sigma, St. Louis, MO) supplemented with ~100,000 cpm ^{3}H-cAMP or ^{3}H-cGMP (Perkin-Elmer, Waltham, MA) in a final volume of 0.25 ml. The total substrate and inhibitor concentrations are indicated in the figure legends. The reaction time and amount of lysate were maintained so that less than 30% of the substrate was hydrolyzed.

Preparation of Freshly Isolated Primary Brown Adipocytes

Primary brown adipocytes were isolated using a modified Rodbell method (Matthias et al., 2000; Rodbell, 1964). Routinely, the interscapular fat pads from 3-5 C57/Bl6 mice were pooled, and initially placed in a 20 ml plastic scintillation vial (Research Products International, Mount Prospect, IL) containing filter-sterilized Krebs-Ringer HEPES Isolation Buffer (20 mM HEPES, 118.5 mM NaCl, 25.3 mM $NaHCO_3$, 1.2 mM NaH_2PO_4, 1.2 mM $MgSO_4$, 10 mM D-glucose, 10 mM D-fructose, 4% bovine serum albumin, pH 7.4) warmed to 37°C and equilibrated with 95% O_2-5% CO_2 bubbling through a diffuser. Whole tissue was pre-incubated in 3 ml Isolation Buffer

supplemented with 2.0 mg/ml Collagenase (Sigma C6885, St. Louis, MO) shaking in a Dubnoff shaking water bath (Thermo Scientific, Waltham, MA) for 7 min shaking at 90 cycles/min. Every 2 min, the tissue was removed and gently vortexed for 10 s. At the end of the 7 min, the tissue was removed and rinsed with Isolation Buffer. The tissue was then finely minced with surgical blades (Bard Parker, no. 371110) in a scissor fashion and placed back into a plastic scintillation vial containing 4 ml fresh Isolation Buffer containing collagenase. The mixture was gassed with 95%/5% O_2/CO_2 for 2 min bubbling through a 25 gauge syringe needle. The vial was then placed in a Dubnoff incubator shaker for 40 min shaking at 120 cycles/min, and gently vortexed every 5 min for 10 s. The tissue fragments were then homogenized further by triturating gently with a plastic pasture pipette. The mixture was then filtered through a 70 μm nylon filter (BD Falcon 352350, San Jose, CA), and the filtrate was diluted with Isolation Buffer to 12 ml. Usually it was necessary to gently press the remaining tiny tissue fragments through the filter with a gloved finger. The collected cells were centrifuged at 70 x *g*, and the infranatant below the floating brown adipocytes was removed through a tube with a peristaltic pump. The cells were then washed twice more by flotation with 6 ml of 37°C Isolation Buffer that contained 4% Fatty Acid-Free BSA (Sigma, St. Louis, MO) and gassed with 95%/5% O_2/CO_2, centrifuging after each wash at 70 x *g*. Finally, the cells were resuspended in 1ml FA-Free Isolation Buffer and counted on a hemacytometer. Cells containing multilocular fat droplets were identified as brown adipocytes. The yield usually ranged from $0.5x10^6$ to $2x10^6$ adipocytes per 3-5 fat pads.

Glycerol Release Assay

Freshly isolated brown adipocytes were diluted to a final concentration of 75,000 cells/ml into 200uL FA-Free Isolation Buffer containing pharmacological agents in 1.5 mL centrifuge tubes. The tubes were placed in heating blocks in a Dubnoff shaking water bath at 37°C, and shaken at 90 cycles/min. The reaction was terminated by freezing the tubes in liquid nitrogen. Tubes were thawed in ice water and centrifuged at 16,000 x *g* at 4°C for 5 min. The infranatant was removed and the glycerol content was measured using the reagents listed in the Free Glycerol Determination Kit (Sigma, St. Louis, MO). The contents of the Free Glycerol Reagent are as follows: 20 mM Tris, pH 7.0, 3.75 mM $MgCl_2$, 0.188 mM 4-aminoantipyrine (4-AAP), 2.11 mM N-ethyl-N-(3-sulfopropyl)-anisidine sodium salt (sodium ESPA), 1.25 U/mL glycerol kinase (GK), 2.5 U/mL glycerol phosphate oxidase (GPO), 2.5 U/mL horseradish peroxidase type IV (HPO), 0.75 mM ATP, and 0.05% sodium azide. The GK, GPO, and HPO were reconstituted in 20mM Tris, pH 7.4, and stored in aliquots at -20°C. ATP was dissolved in water (100 mM) and stored in aliquots at -80°C. 4-AAP was dissolved in water at 1000X and stored at -20°C. Sodium ESPA was added to the reagent mixture immediately before use, and the reagent mixture was made freshly the day of the experiment. Leftover reagent was stored at 4°C and protected from light with aluminum foil. Background lipolysis in a given experiment was defined as glycerol released in the presence of 1 μM propranolol (Sigma, St. Louis, MO), and was subtracted from the total.

Determination of cAMP concentration by EIA

Brown adipocyte precursors were grown and differentiated in 12-well plates, preincubated with PDE inhibitors in DMEM for 30 min, then isoproterenol in DMEM for 5 min. The medium was removed, and the reaction stopped with ice cold 99% ethanol-1% hydrochloric acid. The ethanol acid containing the cAMP was pipetted into Eppendorf tubes and dried down in a speed vac (Savant, Thermo Scientific, Waltham, MA). The samples were then resuspended to 200 μL and cAMP was measured according to the manual for the cAMP EIA Kit (American Qualex Molecular, San Clemente, CA). The cell monolayer was then resuspended in water and protein content was assessed by BCA assay (Pierce, Rockford, IL).

Western Blotting

Differentiated brown adipocytes were lysed in 50 mM Tris pH 8.0, 0.5% Triton-X100, 150 mM NaCl, 1 mM EDTA, 1 mM DTT, 1 mM sodium orthovanadate, 1 mM sodium fluoride, 200 nM phenylmethylsulfonyl fluoride (PMSF), and 1X protease inhibitor cocktail III (Calbiochem, EMD Millipore, Darmstadt, Germany), and denatured in sample buffer (125 mM Tris, 20% glycerol, 2% sodium-dodecyl sulfate (SDS), 2% 2-mercaptoethanol) by boiling for 5 min. The samples were then separated by 10% SDS-PAGE at 0.75 mm thickness, and transferred to PVDF membranes for 1h at 60V. Membranes were blocked overnight shaking on an orbital shaker at 4°C in 5% BSA in Tris-buffered saline containing 0.05% Tween-20 (TBST). Membranes were probed for phospho-CREB Ser-133 [1:1000 (vol/vol)] (Cell Signaling 9198S, Danvers, MA) or GAPDH [1:20,000 (vol/vol)] (Fitzgerald Industries, Acton, MA)

overnight shaking on an orbital shaker at 4°C in 5% BSA in TBST. Membranes were then washed three times for 10 min with TBST at room temperature, rinsing with TBST between washes, then probed with secondary antibody conjugated to horseradish peroxidase (goat anti-rabbit 1:5000 (vol/vol), goat anti-mouse 1:20,000(vol/vol)) (Bio-Rad Laboratories, Hercules, CA) in 5% BSA in TBST at room temperature for 1h. The washing steps were repeated as before, and membranes were developed with SuperSignal West Pico Chemiluminescent Substrate (Thermo Scientific, Waltham, MA). Immunoreactivity was imaged using a Bio-Rad Molecular Imager ChemiDoc XRS+ with Image Lab Software, and band intensity was quantified using ImageJ. For the detection of PDE8A in whole mouse BAT, tissue was harvested from wild type and PDE8A-/- mice and homogenized as described in (Nolan et al., 2004). The homogenates were centrifuged at 10,000 *g* for 15 min, and the protein content of the infranatant was determined. Samples were denatured as described above. 30μg protein were separated by SDS-PAGE, transferred to PVDF for 3 h at 60V, and membranes were blocked in 5% milk in TBST for 1 h at room temperature. Membranes were probed for PDE8A [1:1200 (vol/vol)] (PDE8-121AP, FabGennix International, Frisco, TX) or UCP1 [1:1000 (vol/vol)] (C-17, Santa Cruz Biotechnology, Santa Cruz, CA) in 5% milk in TBST overnight at 4°C. Membranes were washed 3 times for 10 min with TBST, and then probed with secondary antibody conjugated to horseradish peroxidase (goat anti-rabbit 1:3000 (vol/vol) (Bio-Rad Laboratories, Hercules, CA), or rabbit anti-goat 1:3000 (Jackson Immunoresearch Laboratories, West Grove, PA)) for 1 h at room temperature. The membranes were washed and developed as described above. Immunoreactivity

was imaged using autoradiography film (Genesee Scientific, San Diego, CA).

18F-flurodeoxyglucose (FDG) and PET scanning.

The mice were fasted overnight prior to the day of imaging. On the day of imaging, the mice were housed in portable containers that were warmed by placing them on heating pads between 30°-35°C(Deltaphase Isothermal Pad, Braintree Scientific, Braintree MA). Thirty min prior to administration of FDG mice received an intraperitoneal injection of a single PDE inhibitor, a combination of PDE inhibitors or vehicle control. The injected mouse was then placed in a heated chamber. The chamber was warmed using heating pads and maintained at a temperature between 30-35°C. The mouse was awake in the chamber and allowed to move freely. After 30 min the mouse was anesthetized with isoflurane and administered 200-300 µCi of FDG via retro-orbital injection. The amount of FDG administered (in µCi) was approximately 10 times the weight of the mouse in grams. The mouse was placed in a warmed induction chamber and kept lightly sedated using 1-2% isoflurane anesthesia. After a 40 min uptake period the mouse was placed on the small animal PET scanner, Inveon Dedicated PET system (Siemens, Munich, Germany) and imaged for 20 min. During the PET imaging, the mouse was kept warm by a small heating pad on the table and maintained while anaesthetized with 2-3% isoflurane. A transmission scan was also collected for attenuation correction. Following imaging, the mouse was euthanized and tissue harvested. The data were reconstructed using software provided by the vendor. The three-dimensional ordered subsets expectation maximization - maximum a posterior (3D OSEM-MAP)

method was used to reconstruct the images. A smoothing parameter to achieve 1.5 mm image resolution was used. The images were analyzed using Siemens's ASIPRO analysis software (Siemens, Munich, Germany). The system was calibrated to report image voxel values in radioactivity concentration (i.e., nCi/g). Regions of interest were drawn encompassing the two brown adipose tissue lobes in a coronal plane of the mouse as shown in Figure 2.14. The maximum pixel values from the two regions of interest were averaged and used to determine the standardized uptake value (SUV) for FDG. The SUV is a semi-quantitative metric used to express glucose uptake in tissue. It is calculated using the following formula:

$$SUV = \frac{c(t)}{injected\_activity / body\_weight}$$

c(t) was defined as the maximum activity concentration. Injected activity (nCi) was corrected to the start of scanning. Body weight of the mouse was measured in grams. When using comparative SUV as an uptake metric it was important that all imaging be done at the same time after injection, in this case 40 min (Mankoff, Muzi et al. 2003).

Drugs

SCH51866 (Schering-Plough/Merck, Whitehouse Station, NJ) is a selective PDE1 inhibitor that does not distinguish between PDE1 isoforms and was a gift from the manufacturer (structure published in (Vemulapalli et al., 1996)). BAY 60-7550 (Cayman Chemicals, Ann Arbor, MI) is a PDE2 selective inhibitor. Cilostamide (Tocris, Bristol, UK) is a selective PDE3 inhibitor that does not distinguish between

PDE3A and PDE3B. Rolipram (Enzo Life Sciences, New York, NY) is a selective PDE4 inhibitor that does not distinguish between PDE4 isoforms. PF-04957325 (Pfizer, New York, NY) is a selective PDE8 inhibitor that will inhibit PDE8A and PDE8B with similar affinities and was a gift from the manufacturer (structure published in (Vang et al., 2010)). IBMX (Sigma, St. Louis, MO) is a non-selective PDE inhibitor that will inhibit most PDEs except PDE8s. H-89 (Tocris, Bristol, UK) is a protein kinase inhibitor with substantial selectivity for PKA. PDE and PKA inhibitors were dissolved in dimethyl-sulfoxide (DMSO)(Sigma, St. Louis, MO) and stored at -20°C. Rp-8-Bromoadenosine-3',5'-cyclic monophosphorothioate (Rp-8-Br-cAMPS) (BioLog, Bremen, Germany) is a competitive inhibitor to the cAMP binding site on the regulatory subunit of PKA and was dissolved in water. 8-(4-Chlorophenylthio)-2'-O-methyladenosine-3',5'-cyclic monophosphate (8-pCPT-2-O-Me-cAMP) (BioLog, Bremen, Germany) is an Epac agonist and was dissolved in water. 8-Bromoguanosine 3′,5′-cyclic monophosphate (8-Br-cGMP) is a protein kinase-G (PKG) agonist and was dissolved in water. Isoproterenol (Sigma, St. Louis, MO) was dissolved at 10 mM in 1 M ascorbic acid immediately before use in gene induction experiments. For lipolysis experiments, isoproterenol was dissolved in water immediately before use. For glucose uptake experiments, isoproterenol was dissolved in phosphate-buffered saline immediately before injection into mice.

Results

Phosphodiesterase expression in mouse brown adipocyte models

We first assessed the PDE mRNA expression profile in mouse interscapular brown fat tissue, freshly isolated primary brown adipocytes, and brown adipocytes differentiated from a brown adipocyte precursor cell line *in vitro*. Quantitative qRT-PCR analysis revealed that the mRNAs for PDE1A, 2A, 3B, 4B, 4D and 8A were the predominant ones expressed in whole brown fat tissue (Fig. 2.1A), primary brown adipocytes isolated from BAT tissue via collagenase digestion (Fig. 2.1B), and immortalized brown adipocyte precursors on day 6 after differentiation (Fig. 2.1C). Since it was thought that PDE8A expression is limited to a small number of tissues (Soderling et al., 1998), expression of PDE8A in mouse BAT was unexpected. We further verified the presence of PDE8A protein by Western blot analysis (Fig. 2.2), and also found that both PDE8A RNA and protein was absent in the BAT of PDE8A-/- mice. (Fig. 2.1A, Fig.2.2). Additionally, we did not detect any major compensatory changes in the expression of other PDEs in the BAT from PDE8A-/- mice compared to wild type littermates (Fig. 2.1A). These data indicate that the pattern of PDE expression from whole BAT tissue is largely representative of that found in isolated brown adipocytes, and that these patterns are similar amongst all models of BAT utilized.

Enzyme activity assays confirmed the functional presence of the major PDEs identified by the mRNA profile in immortalized brown adipocytes. The PDE1 family is stimulated by calcium-calmodulin, and PDE1A has an ~70-fold higher selectivity for cGMP versus cAMP at low substrate levels. We therefore confirmed the

presence of PDE1 activity by measuring cGMP hydrolysis in the presence and absence of calcium and calmodulin in the whole BAT extract. This hydrolytic activity was increased 2.7-fold by calcium and was fully inhibited by 100 nM SCH51866, a relatively selective PDE1 inhibitor (IC_{50} for PDE1A = 10 nM (Dunkern and Hatzelmann, 2007)) (Fig. 2.3A).

PDE2 is a dual-substrate PDE, as it hydrolyzes cAMP and cGMP with approximately equal specificity. However, its cAMP-hydrolyzing activity is stimulated by cGMP. Therefore, in order to assay for PDE2 activity, we measured the hydrolysis of cAMP in the presence and absence of 1 μM cGMP. We included 10 μM cilostamide and 10 μM rolipram to these reactions to eliminate background PDE3 and PDE4 activity and to eliminate potential complications in the interpretation of the data since PDE3s can be inhibited by cGMP. Under these conditions the addition of 1 μM cGMP, increased hydrolytic activity towards cAMP 2.8-fold. This increased activity was completely inhibited by the addition of 50 nM of the PDE2 inhibitor, BAY 60-5770, a 10-fold excess over the reported IC_{50} for PDE2 (Bender and Beavo, 2006) (Fig. 2.3B).

PDE3 and PDE4 activities were detected by measuring the hydrolysis of 1 μM cAMP in the presence and absence of 200 nM cilostamide (PDE3 inhibitor) or 10 μM rolipram (PDE4 inhibitor), respectively. These inhibitor concentrations are 10-fold higher than their reported IC_{50} values for PDE3 and PDE4 (Bender and Beavo, 2006). Cilostamide inhibited total cAMP-hydrolyzing activity approximately 60%, while rolipram inhibited total activity approximately 40%. When combined together, approximately 88% of the total cAMP PDE activity was inhibited (Fig. 2.3C).

Finally, since the PDE8 family is insensitive to IBMX and has a K_m for cAMP below 100 nM, PDE8 activity was detected by assay of cAMP hydrolytic activity at 0.012 μM substrate in the presence of 100 μM IBMX and the presence or absence of 10 nM PF-04957235. PF-04957235 decreased the IBMX-insensitive activity by 46% (*$p<0.05$) illustrating the presence of PDE8 activity in these extracts (Fig. 2.3D).

PDE3 and PDE4 regulate basal UCP1 and PGC-1α mRNA expression

Since it is widely accepted that cAMP stimulates expression of UCP1 mRNA (Cannon and Nedergaard, 2004), we next tested which cAMP-dependent PDE or PDEs regulate the pool(s) of cAMP that control induction of UCP1 gene transcription in differentiated brown adipocytes. For these studies, an immortalized brown adipocyte precursor cell line was differentiated into mature brown fat cells *in vitro*. The differentiated adipocytes were then pre-treated with selective inhibitors to PDE1 (SCH51866), PDE2 (BAY 60-7550), PDE3 (cilostamide), PDE4 (rolipram), or PDE8 (PF-04957235), either individually or in combination. Somewhat unexpectedly, when administered individually, none of the PDE inhibitors increased the basal expression of UCP1 mRNA. However, when administered together, 10 μM cilostamide and 10 μM rolipram resulted in an approximately 40-fold increase in basal UCP1 mRNA expression, similar to that seen with a high dose of isoproterenol (10 μM) (Figure 2.4A) or IBMX (200 μM) (Fig. 2.5A). This latter observation strongly suggests that inhibition of PDE3 and PDE4 together is sufficient to explain the stimulatory effect of the non-selective PDE inhibitor, IBMX, on induction of UCP1. The same magnitude of potentiation was observed when the concentration of

cilostamide was reduced to 300 nM (Fig. 2.5B). Additionally, we detected a 2.7-fold increase of UCP1 mRNA in the interscapular brown fat of fasted, warmed mice that were injected with the combination of cilostamide and rolipram (*$p<0.05$), where an injection of either drug alone had no significant effect compared to an injection of vehicle (Fig. 2.5D). A similar pattern of stimulation was also observed in immortalized brown adipocytes for basal expression of PGC-1α mRNA (Fig. 2.6), a transcription factor also regulated by cAMP that is important for UCP1 gene induction during BAT activation. The PDE8-selective inhibitor, PF-04957325 (200 nM), did not stimulate UCP1 mRNA expression when administered either alone or in combination with IBMX, cilostamide or rolipram (Fig. 2.5C, Fig. 2.4B). Similarly, PDE1 or PDE2 inhibitors administered either alone or in combination with PDE3 and PDE4 inhibitors did not stimulate expression of UCP1 mRNA, nor did they augment the effect of combined PDE3 and PDE4 inhibition (Fig. 2.4C). Finally, PDE3 and PDE4 inhibitors administered individually did not stimulate basal cAMP accumulation, but when administered together they increased cAMP 9.6-fold (Fig. 2.7). Together, these results suggest that the combined inhibition of PDE3 and PDE4 removes an important physiological suppressive effect of these two PDEs on basal cAMP signaling and BAT activation in the absence of β-adrenoceptor agonists.

PDE3B controls β-adrenoceptor stimulation of UCP1 mRNA expression

Our finding that both PDE3 and PDE4 together control basal UCP1 expression prompted us to determine whether or not inhibition of the same combination of PDEs regulates the increase in induction of UCP1 mRNA caused by

β-adrenoceptor agonists. Typically, inhibition of the PDE or PDEs that regulate a given process will shift the dose-response curve of agonists for that process to the left or up and to the left. Since β-adrenoceptor activation is known to stimulate expression of UCP1 mRNA, we hypothesized that a PDE inhibitor or combination of inhibitors would potentiate a low dose of isoproterenol based on the dose-response relationship shown in Supplemental Figure 2A. For these experiments, cells were pretreated with individual inhibitors to PDE1, PDE2, PDE3, PDE4 and PDE8, followed by 1 nM isoproterenol. We found that only pretreatment with the PDE3 inhibitor, cilostamide, dose-dependently potentiated the expression of UCP1 mRNA in response to this low dose of isoproterenol (***$p<0.001$ at 10 μM cilostamide). In contrast, a PDE4 inhibitor, rolipram, had no effect on isoproterenol-induced UCP1 expression (Fig. 2.5A). Interestingly, cAMP accumulation did not follow the same pattern of potentiation (Fig. 2.7). At 1 nM isoproterenol, neither cilostamide nor rolipram potentiated global cAMP accumulation, even though UCP1 mRNA was substantially increased under these conditions. PDE1, PDE2, and PDE8 inhibitors also did not potentiate induction of UCP1 by isoproterenol (Fig. 2.8, Fig. 2.5C).

Effects of PDE3 and PDE4 inhibition are PKA-dependent

Two major pathways for cAMP-mediated mechanisms for control of transcription have been described: the exchange protein activated by cAMP (Epac) pathway and the cAMP-dependent protein kinase (PKA) pathway. We therefore wanted to test by which of these molecular pathway(s) PDE inhibition caused stimulation of UCP1 mRNA expression. We pretreated differentiated brown

adipocytes with PDE3 and PDE4 inhibitors along with increasing doses of H-89, a known PKA inhibitor. Cilostamide and rolipram alone had minor effects on PKA-substrate phosphorylation and CREB phosphorylation (1.8- and 2.5-fold, respectively). However, when combined, they produced a 9.6-fold stimulation of CREB phosphorylation compared to the control. H-89 was able to fully reduce expression of UCP1 mRNA and CREB-phosphorylation at a dose of 25μM (Fig. 2.9A-C). Similarly, while 1 nM isoproterenol alone increased CREB-phosphorylation 3.6 fold (**$p<0.01$), combining isoproterenol with cilostamide further increased CREB-phosphorylation to 5.9-fold (***$p<0.001$). The difference between isoproterenol alone and isoproterenol with cilostamide was statistically significant ($^{\#}p<0.05$). Furthermore, H-89 (10 μM) was sufficient to inhibit the stimulatory effect of cilostamide on isoproterenol-stimulated UCP1 induction and on CREB-phosphorylation (Fig. 2.9D-E). We also saw a significant inhibition of UCP1 induction when cells were pretreated with a more selective PKA inhibitor (1mM Rp-8-Br-cAMPS) that binds to a different site on PKA than H-89 (Figure 2.10). A selective agonist for Epac, 8-pCPT-2-O-Me-cAMP, did not stimulate UCP1 mRNA (data not shown). Since it has been shown that H-89 can inhibit protein kinase-G (PKG) (K_i=0.5 μM) with a K_i that is only 10-fold higher than the K_i for PKA (K_i=0.05μM) *in vitro* (Hidaka and Kobayashi, 1992), we also tested whether 8-Br-cGMP, an agonist to cGMP-dependent protein kinase (PKG), could stimulate accumulation of UCP1 mRNA; we observed no appreciable change upon application of this PKG agonist (data not shown). Together these data strongly suggest that the

stimulatory effect of combined PDE3 and PDE4 inhibition on UCP1 mRNA accumulation is largely through the canonical PKA-dependent signaling pathway.

PDE3 and PDE4 in combination regulate lipolysis in primary brown adipocytes

Noradrenergic regulation of BAT function also requires stimulation of lipolysis to provide both the energy for establishing the mitochondrial proton gradient and also the allosteric activation of UCP1 by free fatty acids. Therefore, we were interested in determining which PDEs were important for cAMP-dependent regulation of lipolysis in brown fat. Freshly isolated primary brown adipocytes were pretreated with 10 μM cilostamide, 10 μM rolipram, or both, and then treated with vehicle or isoproterenol for 1 h. Lipolysis was measured as glycerol released into the media. We found that cilostamide alone did not significantly alter basal lipolysis or lipolysis stimulated by 10 nM isoproterenol. Conversely, rolipram alone did significantly potentiate both basal and isoproterenol-stimulated glycerol release by 7.8-fold and 2.8-fold, respectively, over the vehicle control (Fig. 2.11A). This suggested that PDE4, but not PDE3, was a primary regulator of the pool of cAMP that regulates lipolysis in primary brown adipocytes. However, when both inhibitors were combined there was an even larger 30 to 40-fold increase in lipolysis that is of the same magnitude as that seen with the non-selective PDE inhibitor isobutyl-n-methylxanthine (IBMX) (Fig. 2.11A). Interestingly, despite substantial expression of PDE8A in brown fat, the PDE8 inhibitor did not augment lipolysis in primary brown adipocytes, either alone or in combination with IBMX, cilostamide and/or rolipram

(Fig. 2.11B, Fig. 2.12). Taken together these data indicate synergistic roles for PDE3 and PDE4, but not for PDE8A, as regulators of lipolysis in brown adipocytes.

Inhibition of PDE3 and PDE4 stimulate *in vivo* glucose uptake in BAT.

Glucose uptake in brown adipocytes can be regulated by cAMP-dependent signaling (Marette and Bukowiecki, 1989). We therefore hypothesized that selective inhibition of the appropriate PDE(s) would potentiate glucose uptake in BAT. To test this we treated fasted, warmed, wild type and PDE8A-/- littermates with 3mg/kg cilostamide, 3mg/kg rolipram, a combination of both, or the vehicle control, followed by an injection of 18F-fluorodeoxyglucose (FDG). FDG can be taken up via glucose transporters and phosphorylated by hexokinase. However, it cannot be further metabolized, thus it is trapped in any cells that take it up. The mice were then imaged using a positron emission tomography scanner (PET). Basal glucose accumulation by brown adipose tissue from wild type and PDE8A-/- mice was very low (Fig. 2.13A,B). Moreover, neither PDE inhibitor alone induced a significant increase in BAT glucose uptake activity compared with the vehicle control in the wild type mice. On the other hand, cilostamide treatment alone produced a small, but significant, increase in glucose uptake compared with the vehicle control in the PDE8A-/- mice (2.7-fold, $*p<0.05$), although the maximum glucose uptake in response to cilostamide was not significantly different between the two genotypes (Fig. 2.13C). We then tested the effect of a combination of PDE3 and PDE4 inhibitors on glucose uptake in BAT. Treatment with a combination of both cilostamide and rolipram resulted in a large increase in BAT FDG uptake in both the

wild type and PDE8A-/- mice. Surprisingly, the maximum response to both PDE inhibitors in the PDE8A-/- mice was consistently 1.8-fold higher than what was observed in the wild type littermate controls (**$p<0.01$). Conversely, when injected with isoproterenol, there was no difference in BAT FDG uptake between wild type and PDE8A-/- mice. Taken together, these data suggest that each these three PDEs can suppress basal cAMP-dependent glucose uptake in BAT and that all three PDEs need to be inhibited to allow full stimulation in the absence of agonist. However, under conditions of β-adrenoceptor stimulation, this attenuation of glucose uptake by the PDEs can be overridden, presumably by the high adenylyl cyclase activity resulting from adrenergic stimulation.

Discussion

While many brown fat directed studies have focused on brown adipocyte differentiation or the recruitment of adipocyte precursors into more brown-like adipocytes, it also has been shown that simply having more brown fat is insufficient to influence whole animal metabolism if the tissue remains in a non-activated state (Sell et al., 2004). Therefore selective pharmacological stimulation of this non-stimulated state of brown adipose tissue could provide an effective new treatment paradigm for obesity and obesity-related diseases in humans. In early studies, non-selective PDE inhibitors were shown to potentiate the thermogenic response of cold-exposed rats (Wang and Anholt, 1982). However, non-selective inhibitors of PDEs, such as theophylline, have a very narrow therapeutic index and substantial toxicity (Beavo et al., 2007). Studies with non-selective PDE inhibitors also cannot identify which specific PDEs are most important to BAT thermogenesis. The experiments described in this manuscript were designed to test the hypothesis that inhibition of the specific PDEs that regulate BAT activation might provide a conceptual basis for the design of new PDE related therapies for the treatment of obesity-related diseases.

In this study we addressed the question of which subtype(s) of PDE regulate lipolysis, glucose uptake, and mRNA expression of UCP1. We identified PDE3 and PDE4 (likely PDE3B and PDE4B/D) as the major regulators of these three BAT processes both *in vitro* and *in vivo* (Figs. 2.3, 2.5, 2.11, and 2.13). Under basal conditions the effects of the individual PDE3 and PDE4 inhibitors were synergistic in nature, in that individual inhibitors to PDE3 or PDE4 had little or no effect on their

own, but when combined would produce a large, synergistic response. In fact, the same magnitude of potentiation on UCP1 expression was observed over a wide range of cilostamide doses, suggesting a truly synergistic relationship between rolipram and cilostamide (Fig. 2.5B). The only conditions where a single selective PDE3 or PDE4 inhibitor was sufficient to potentiate UCP1 induction or lipolysis, respectively, were those in which an adrenoceptor agonist was also present (Figs. 2.5, 2.11). Finally, we also observed that PDE8A may play a role in the regulation of basal BAT glucose uptake, but this global knockout effect was only observed when PDE3 and PDE4 were also inhibited (Fig. 2.13).

We also found that PDE1, PDE2, or PDE8 inhibitors had virtually no effect on UCP1 mRNA either alone or in any combination with either PDE3 or PDE4 inhibitors (Fig. 2.4B, Fig. 2.5C), despite the fact that we can detect PDE1, PDE2, and PDE8 mRNAs as well as enzyme activities (Fig 2.1, 2.3A, 2.3B) in extracts from these differentiated brown adipocytes. Therefore, inhibition of both PDE3 and PDE4 together is necessary to fully activate basal UCP1 induction and lipolysis, and is sufficient to fully account for the IBMX response. We did observe what appears to be a greater, though not statistically significant, effect of IBMX on cAMP levels compared to the cilostamide-rolipram combination at 10 nM isoproterenol. This may suggest that PDE1 and PDE2 may have some role under high cAMP levels, which is consistent with what has been shown previously in several other tissue types (Bronnikov et al., 1999b) (Beavo et al., 2007). Therefore, different PDEs can regulate different processes in BAT, but not all PDEs regulate all processes.

We next investigated which phosphodiesterase subtypes regulate adrenoceptor-mediated lipolysis and induction of UCP1 mRNA transcription. We found that PDE3 inhibition potentiated induction of UCP1 mRNA in response to 1 nM isoproterenol, whereas PDE1, PDE2, PDE4, and PDE8 inhibition did not (Figure 2.5A, right panel, Fig. 2.4C). This observation suggests that PDE3, but not PDE4, regulates a local pool of cAMP that is generated by the stimulation of β-adrenoceptors and leads to full induction of UCP1 mRNA. As we did not observe changes in global cAMP accumulation at any of the various concentrations of isoproterenol and PDE inhibitors (Fig. 2.7) it is likely that the cAMP EIA method is not sensitive enough to detect small, local changes in cAMP concentration. However, under similar conditions we were able to observe a potentiating effect on the PKA phosphorylation of CREB (Figure 2.9B,C) when isoproterenol and cilostamide were combined. This supports the model set forth by many investigators of compartmentalized cAMP signaling being critically regulated by specific PDEs, in this case PDE3. In accordance with this finding, we observed PDE4 inhibition potentiated lipolysis in primary brown adipocytes in response to 10 nM isoproterenol, whereas PDE3B and PDE8A inhibition did not (Fig. 2.11). Therefore, in contrast to a major role for PDE3 regulation of UCP1 induction in differentiated brown adipocytes, PDE4 seems to be the major regulator of lipolysis in brown adipocytes under adrenergic stimulation. These results suggest that PDE3 and PDE4 are, at least partially, in distinct compartments that are important for receptor-mediated signals, but not necessarily for basal adenylyl cyclase tone.

The similarities that we observed across two different brown adipocyte models with respect to PDE3 and PDE4 dual inhibition resulting in a stimulation of multiple BAT processes prompted us to test the significance of the paradigm *in vivo.* It has been shown that glucose uptake in brown adipocytes is a cAMP-dependent phenomenon, and that IBMX can stimulate glucose uptake in isolated brown adipocytes (Marette and Bukowiecki, 1989). However, no study to date has determined which PDE subtype(s) regulate(s) this effect. If the PDE inhibitors stimulated basal BAT glucose uptake in the same pattern as they did for UCP1 and lipolysis, then we expected that injections of PDE3 or PDE4 inhibitors alone to have little, if any, effect on glucose uptake, but to have a substantial synergistic effect on glucose uptake when co-injected. Indeed, this is exactly what we observed (Fig. 2.13A,B), indicating that PDE3 and PDE4, possibly working together, regulate/suppress basal glucose uptake into the BAT of wild type mice *in vivo*.

The pathway(s) and mechanism(s) by which cAMP stimulates glucose uptake in BAT are controversial. It has been suggested that there may be an indirect response of the cell to the increased ATP demand due to the uncoupling process stimulated by lipolysis in rat brown adipocytes (Marette and Bukowiecki 1991). Since PDE3 and PDE4 inhibition stimulates lipolysis to the same order of magnitude as IBMX in freshly isolated primary adipocytes, our data suggest that the injection of these isozyme selective inhibitors into mice might synergistically stimulate glucose uptake possibly via free fatty acid stimulation of UCP1. Furthermore, one study indicated that there was an increase in glucose transporters to the surface of primary isolated mouse brown adipocytes stimulated by cAMP-elevating agents (including

IBMX) (Omatsu-Kanbe and Kitasato, 1992) while another study indicated that the cAMP effect was largely on the affinity of GLUT-1 receptors, and not on translocation, in differentiated adipocyte precursors isolated from the stromal fraction of mouse BAT (Shimizu et al., 1998). Despite the lack of a potentiating effect of the PDE8-selective inhibitor on either UCP1 mRNA expression or lipolysis (Fig. 2.5, 2.11), we found that glucose uptake in response to PDE3-PDE4 dual inhibition was 1.8-fold higher in BAT from PDE8A-/- mice than BAT from their wild type littermates (Fig. 2.13A,B), whereas isoproterenol had no differential effect between the two genotypes (Fig. 2.13C). These results suggests that there may be at least two cAMP-dependent pathways that converge on glucose uptake, one mediated by lipolysis and uncoupling via PDE3 and PDE4, and a second mediated more chronically by the global ablation of PDE8A. Further studies are needed to elucidate this mechanism, as the global knockout of PDE8A potentially could indirectly affect brown fat activation via some other cell type.

cAMP-dependent glucose uptake is a major point of distinction between BAT and WAT, and therapeutically targeting BAT's insulin-independent glucose uptake might prove beneficial in an insulin resistant condition. This is further suggested by the observation that activated human BAT can take up and metabolize circulating fatty acids and glucose (Ouellet et al., 2012), and that obese humans can exhibit reduced thermogenesis and low responsiveness to noradrenaline (Jung et al., 1979). Additionally, given that human fat tissues of any type express a negligible number β_3-adrenoceptors, selective activation of the tissue with β_3-adrenoceptor

agonist approaches have failed in clinical trials. Therefore, alternative approaches that bypass receptor-mediated activation may be useful in the future.

A synergistic relationship between PDE3 and PDE4 has been described previously in other tissues, such as rat vascular smooth muscle cells (Palmer et al., 1998) and even in the regulation of lipolysis in white adipocyte models from mice (Snyder et al., 2005). Additionally, dual PDE3/PDE4 inhibitors have been tested clinically for the treatment of chronic obstructive pulmonary disease with limited success. However, these drugs were fairly well tolerated in early phase clinical trials with low incidence of side effects that are traditionally associated with effective doses of PDE4 inhibitors alone (Banner and Press, 2009). To our knowledge, the effects of these dual inhibitors on brown adipose tissue function have not been determined.

In summary, understanding the regulation of the basal state of cAMP/PKA in BAT may prove critically important in the design of future therapies for disease states. In this case, it appears that there are multiple BAT PDEs that suppress tissue activation in the absence of agonists that drive cAMP production. Removing this inhibition with the correct combination of PDE inhibitors is sufficient to fully activate these processes. It is now well known that identifying small molecules that target only subsets of PDEs is possible from a medicinal chemistry point of view, and examples of single molecules that selectively inhibit both PDE3 and PDE4 have been described (reviewed in (Bender and Beavo, 2006)). However, it remains to be seen if such an approach, perhaps involving a single molecule that inhibits multiple PDEs, might be efficacious in a clinical setting.

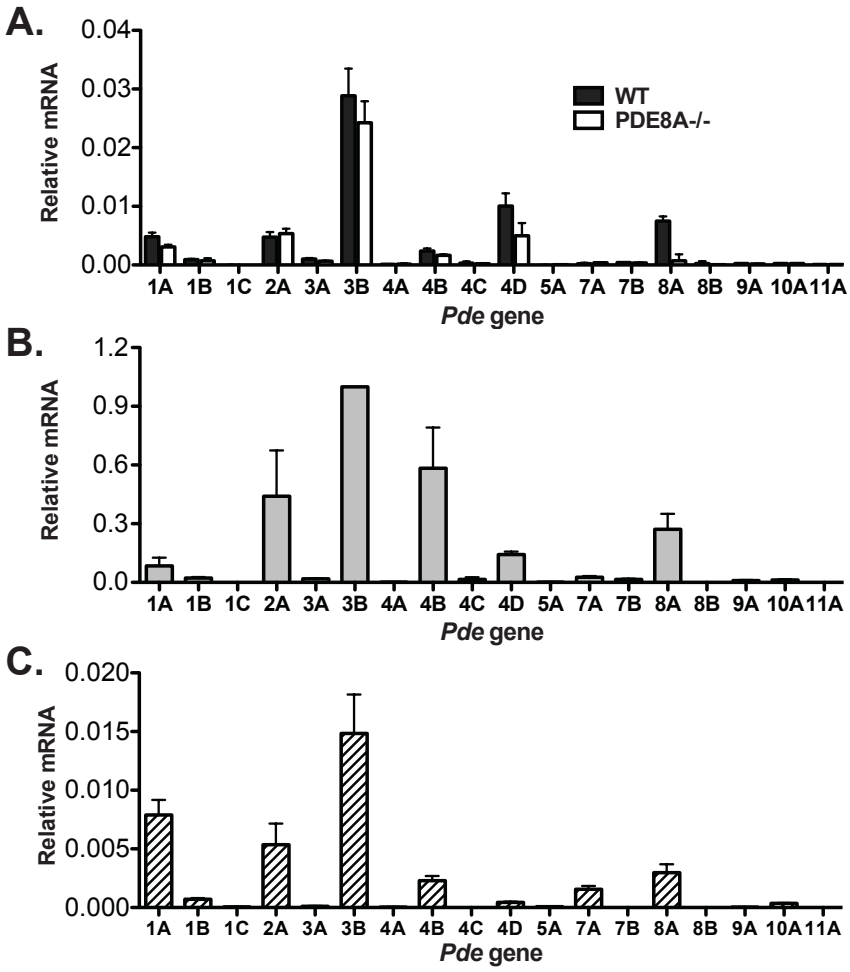

Figure 2.1. PDE mRNA expression profile in multiple models of BAT is similar. [A] RNA was extracted from whole mouse interscapular brown adipose tissue from wild type and PDE8A-/- littermates, then analyzed by RT-PCR as described in materials and methods. Mean values ± S.E.M. are expressed relative to GAPDH mRNA (n=3). The PDE gene name is abbreviated as a number and letter. [B] Isolated primary mouse brown adipocytes were pooled from 3-5 mice and analyzed by RT-PCR as described in materials and methods. Mean values ± S.E.M. are expressed normalized to PDE3B mRNA (n=3). [C] RNA from immortalized brown adipocyte precursor cells on day 6 of differentiation was isolated and analyzed by RT-PCR as described in materials and methods. Mean values ± S.E.M. are expressed relative to 18S mRNA (n=5-6).

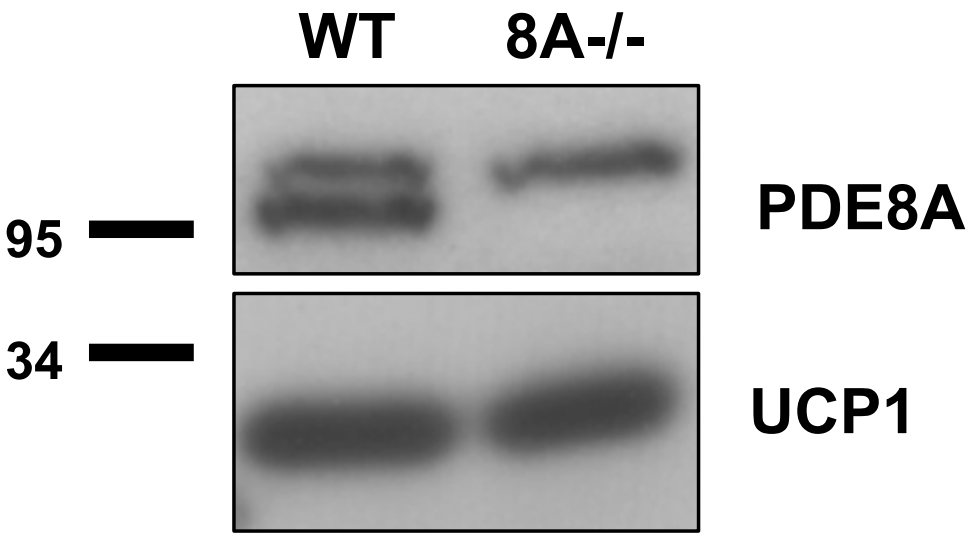

Figure 2.2. PDE8A protein is present in mouse brown adipose tissue.
Mouse brown adipose tissue was excised and homogenized as described in Materials and Methods. 30 μg of protein were loaded onto SDS-PAGE, transferred onto PVDF and blotted for PDE8A and UCP1. An immunoreactive band towards a PDE8A antibody at 95 kDa is present in the wild type but absent in the PDE8A-/- (n=5).

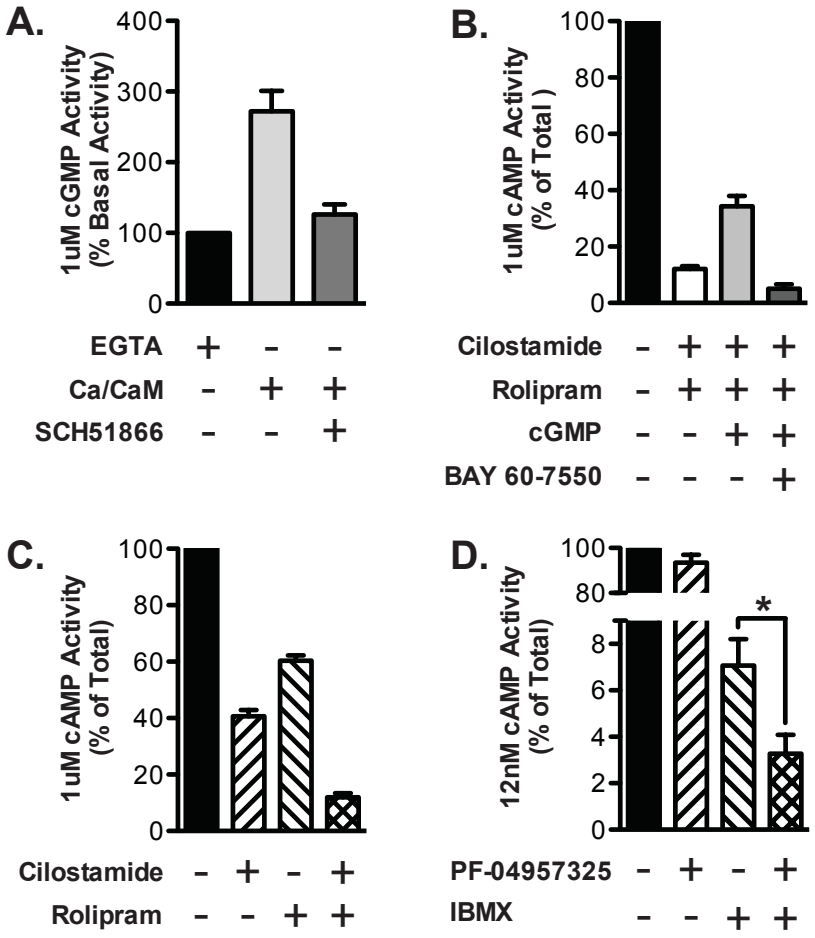

Figure 2.3. PDE enzymatic activities were confirmed in differentiated immortalized brown adipocytes.
[A] PDE1 activity was detected by the addition of calcium/calmodulin to whole extract using 1μM cGMP as substrate. The increase in activity was inhibited with 100 nM SCH51866 (n=3-8). [B] PDE2 activity was detected by stimulating cAMP-hydrolyzing activity with cGMP. PDE3 and PDE4 were first inhibited with cilostamide and rolipram. cAMP-hydrolysis using 1 μM substrate was then stimulated by 1 μM cGMP. The increased activity was inhibited by the addition of 50 nM BAY 60-7550. (n=3-4). [C] PDE3 activity was detected by the addition of 10 μM cilostamide using 1 μM cAMP as substrate. PDE4 activity was detected by the addition of 10 μM rolipram using 1 μM cAMP as substrate (n=3-4). [D] PDE8 activity was defined as PDE activity that is insensitive to 100 μM IBMX and is inhibited by 10 nM PF-04957325 with 12 nM cAMP substrate (n=3-6). Data are presented as mean % of total cyclic-nucleotide hydrolysis ± S.E.M., and statistical analysis in [D] was performed by paired Students t-test: *$p<0.05$ between IBMX alone and IBMX+PF.

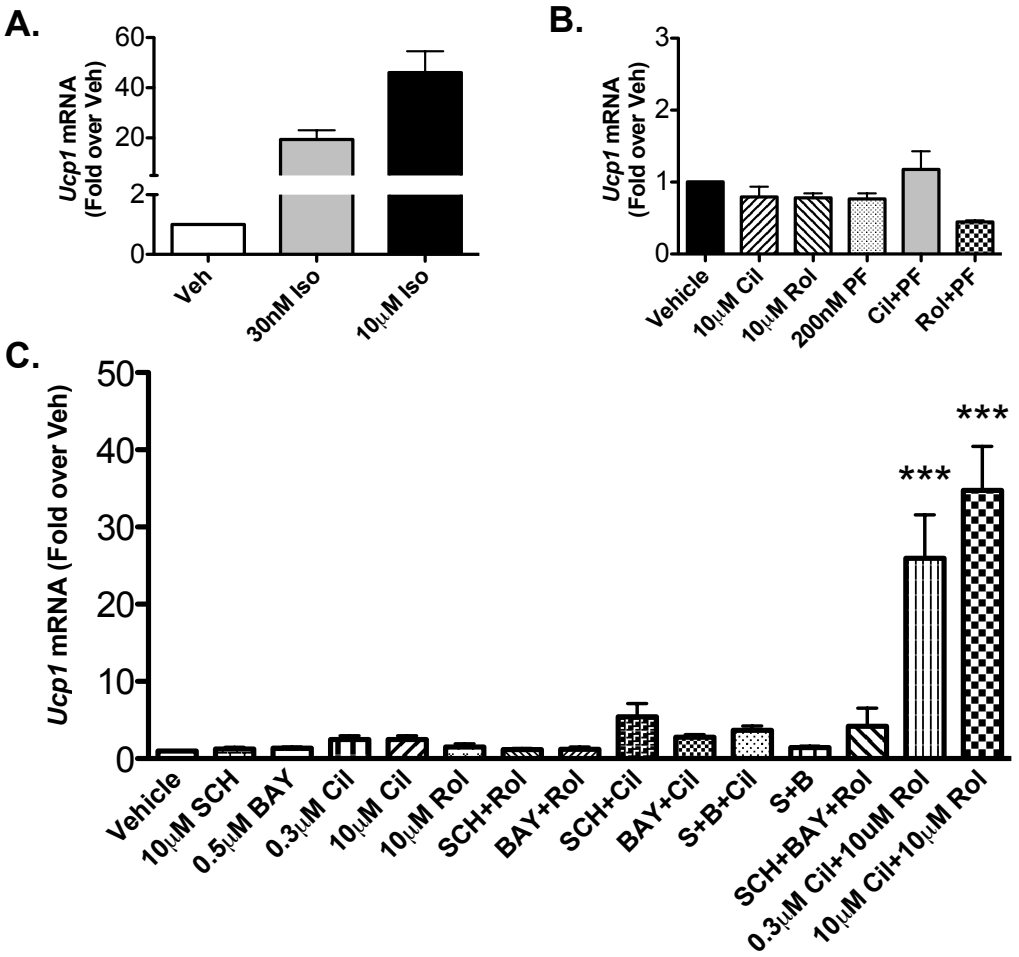

Figure 2.4. The effects of isoproterenol and PDE inhibitor combinations on UCP1 mRNA expression in differentiated brown adipocytes.
[A] Differentiated brown adipocyte precursors were stimulated with increasing doses of isoproterenol for 4 hours (n=5). [B] Differentiated brown adipocyte precursors were treated with 10 μM cilostamide, 10 μM and/or 200 nM PF-04957325 as described in materials and methods (n=3). [C] Differentiated brown adipocyte precursors were treated with SCH51866, BAY 60-7550, cilostamide, and/or rolipram at the indicated doses as described in materials and methods (n=3-8). RNA was isolated and UCP1 mRNA was quantified relative to 18S mRNA using RT-PCR as described in Materials and Methods. Data are presented as mean fold over vehicle control ± S.E.M., and statistical analyses were performed by One-way ANOVA with Dunnet post hoc test: ***, $p<0.001$ versus vehicle control in each group.

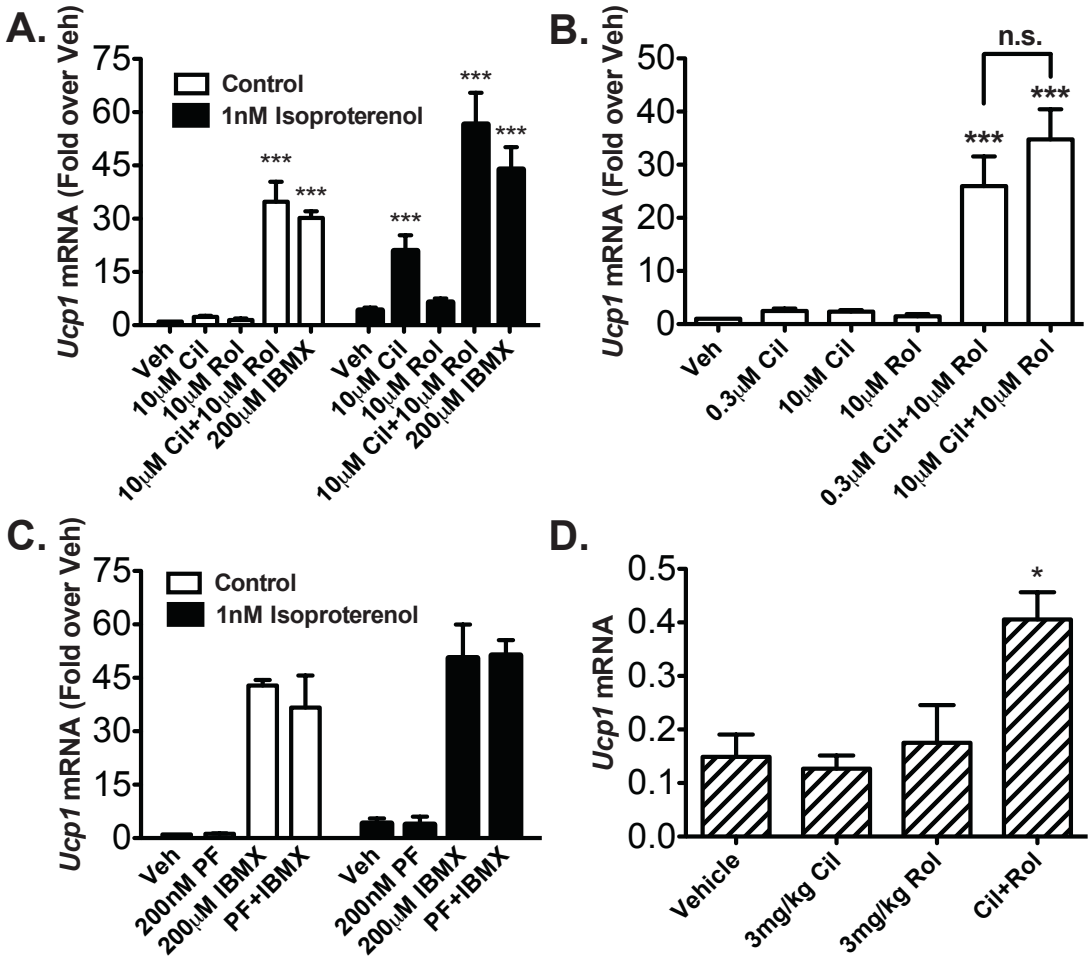

Figure 2.5. PDE3 and PDE4 inhibitors increase Ucp1 mRNA expression in differentiated brown adipocytes.
UCP1 mRNA expression was measured in differentiated brown adipocytes that were: [A] pre-treated with 10 μM cilostamide, 10 μM rolipram, both, or 200μM IBMX for 30 min, then stimulated by vehicle or 1 nM Isoproterenol for 4 h (n=3-13), [B] treated with 300 nM cilostamide or 10 μM cilostamide with or without 10 μM rolipram (n=3-8), and [C] pre-treated with either 200 nM PF-04957325, 200 μM IBMX, or both for 30 min, then stimulated by vehicle or 1 nM isoproterenol for 4 h (n=3). UCP1 mRNA was quantified relative to 18S mRNA using RT-PCR as described in Materials and Methods. [D] UCP1 mRNA expression was measured from the RNA extracted out of the interscapular BAT pads harvested from mice undergoing PET scanning after the procedure was terminated (see Materials and Methods). UCP1 mRNA was quantified relative to GAPDH mRNA using RT-PCR as described in Materials and Methods. Data are presented as mean fold over vehicle control ± S.E.M., and statistical analyses were performed by One-way ANOVA with Dunnet post hoc test: ***p<0.001; *p<0.05 versus vehicle in each group.

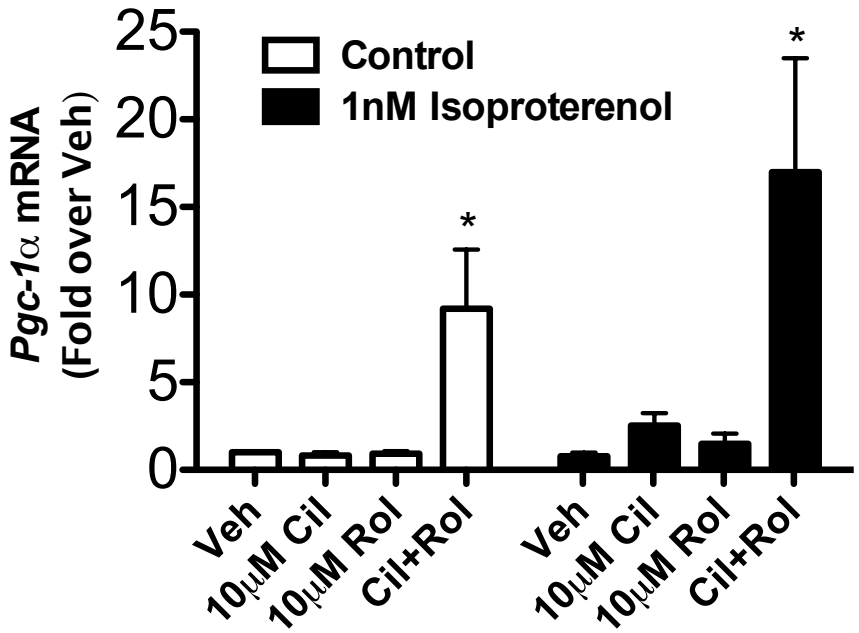

Figure 2.6. PDE3 and PDE4 inhibitors increase PGC-1α mRNA expression in differentiated brown adipocytes.

PGC-1α mRNA expression was measured in differentiated brown adipocytes that were pretreated with PDE inhibitors for 30 min, then stimulated by vehicle or 1 nM isoproterenol for 2 h. RNA was isolated and UCP1 mRNA was quantified relative to 18S mRNA using RT-PCR as described in Materials and Methods. Data are presented as mean fold over vehicle control ± S.E.M. (n=3), and statistical analyses were performed by One-way ANOVA with Dunnet post hoc test: *$p<0.05$ versus vehicle in each group.

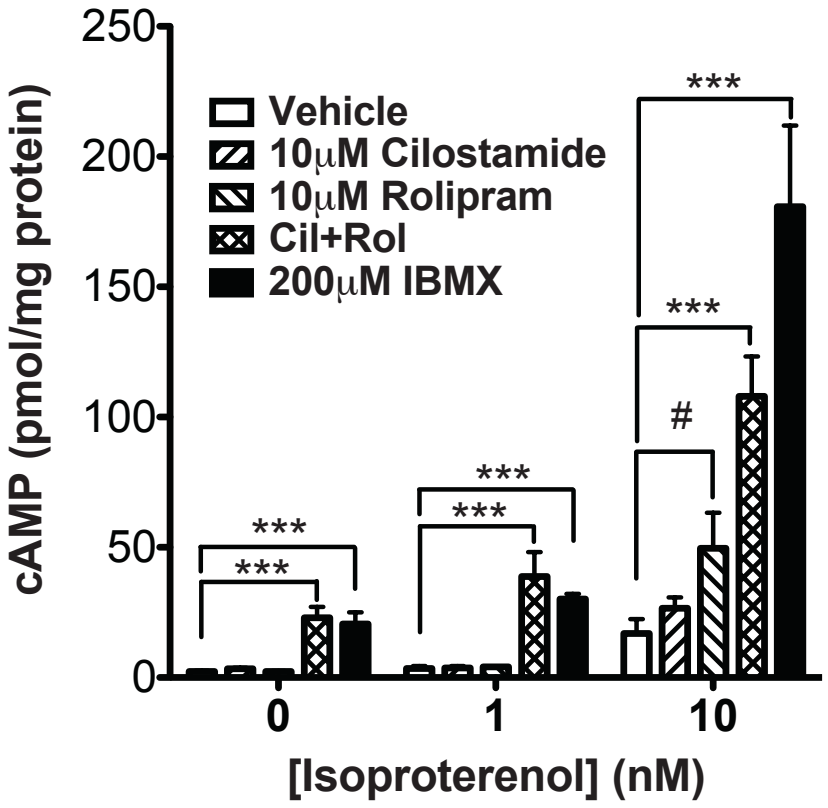

Figure 2.7. PDE3 and PDE4 inhibitors stimulate cAMP accumulation in differentiated brown adipocytes.
Differentiated brown adipocytes were pre-treated with PDE inhibitors for 30 min, and then stimulated with vehicle, 1 nM or 10 nM isoproterenol for 5 min. cAMP was measured as described in Methods. Data are presented as mean ± S.E.M. (n=3-5), and statistical analyses were performed by One-way ANOVA with Dunnett post hoc: ***$p<0.001$ versus vehicle control in each group, and by Two-way ANOVA with Bonferonni post hoc: $^{\#}p<0.05$ versus vehicle control.

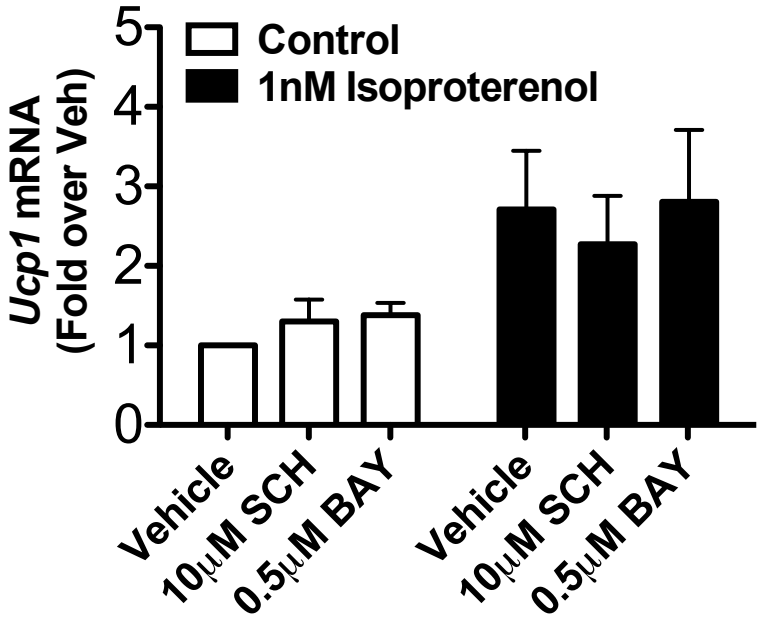

Figure 2.8. PDE1 or PDE2 inhibitors did not potentiate isoproterenol-stimulated UCP1 mRNA induction.
Differentiated brown adipocyte precursors were pretreated with 10 μM SCH51866 or 0.5 μM BAY 60-7550 for 30 min, then stimulated with 1 nM Isoproterenol for 4 h. RNA was isolated and UCP1 mRNA was quantified relative to 18S mRNA as a reference using RT-PCR as described in materials and methods. Data are presented as mean fold over vehicle control ± S.E.M (n=3).

Figure 2.9. Potentiating effect of PDE inhibitors on Ucp1 mRNA and CREB-phosphorylation is PKA-dependent.
[A] UCP1 mRNA expression was measured in differentiated brown adipocytes that were pretreated with H-89 for 1 h, then 10 μM cilostamide + 10 μM rolipram for 4.5 h. RNA was isolated and UCP1 mRNA was quantified relative to 18S mRNA using RT-PCR as described in Materials and Methods. Values were then normalized to the cilostamide + rolipram treatment in the absence of H-89 control. [B] CREB-phosphorylation after 40 min of stimulation by 10 μM cilostamide + 10 μM rolipram in differentiated brown adipocytes. [C] Quantification of Western blot in [B]. [D] UCP1 mRNA expression in differentiated brown adipocytes that were pre-treated with H-89 at the indicated doses for 1 h, followed by 10 μM cilostamide added 30 min prior to addition of 1 nM isoproterenol. RNA was isolated and UCP1 mRNA was quantified relative to 18S mRNA using RT-PCR as described in Materials and Methods. Values were then normalized to the cilostamide + isoproterenol treatment in the absence of H-89 control. [E] CREB-phosphorylation after 10 min of isoproterenol stimulation after a 30 min preincubation with 10 μM cilostamide in differentiated brown adipocytes. [F] Quantification of Western blot in [E]. Data are presented as mean ± S.E.M. (n=3-7), and statistical analyses were performed by One-way ANOVA with Dunnett post hoc: ***$p<0.001$; **$p<0.01$ versus vehicle control in each group; $^{\#}p<0.05$; $^{\#\#\#}p<0.001$ versus 1 nM isoproterenol plus 10 μM cilostamide without H-89.

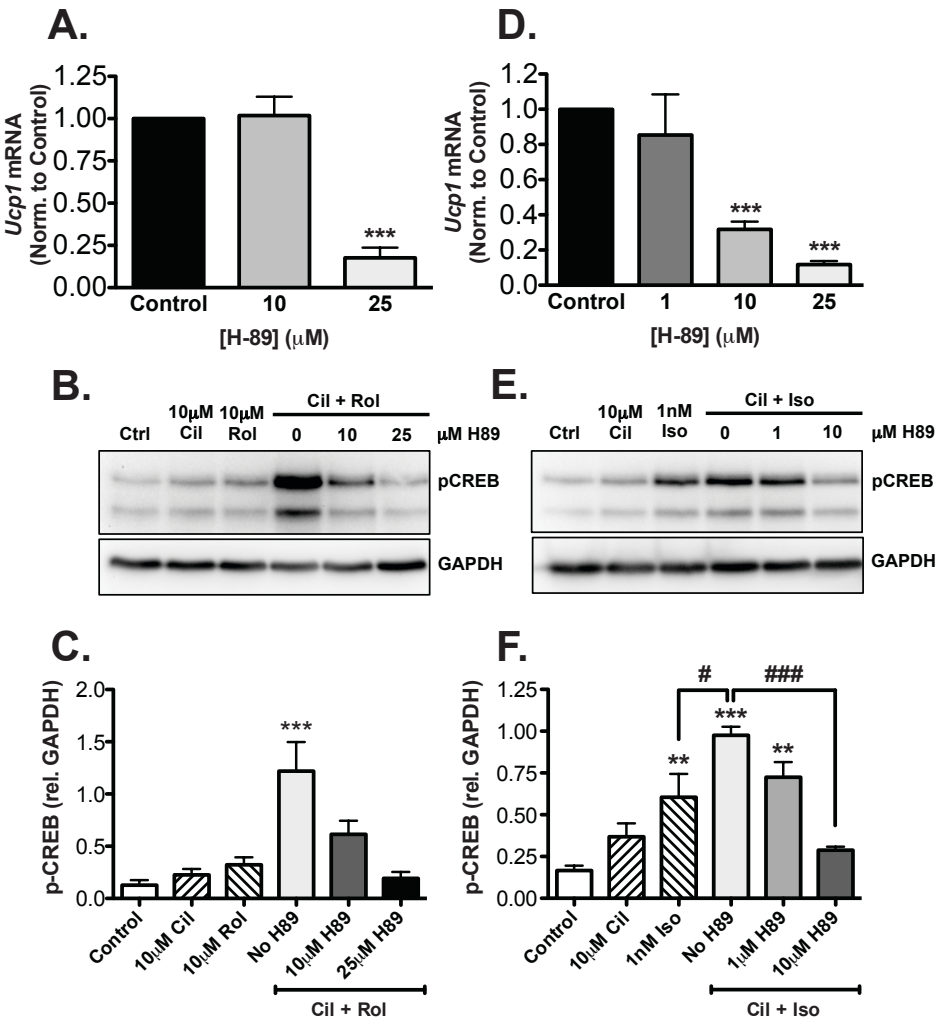
A.
Ucp1 mRNA (Norm. to Control)
1.25
1.00
0.75
0.50
0.25
0.00
***
Control
10
25
[H-89] (μM)
D.
Ucp1 mRNA (Norm. to Control)
1.2
1.0
0.8
0.6
0.4
0.2
0.0
***
***
Control
1
10
25
[H-89] (μM)
B.
Ctrl
10μM Cil
10μM Rol
Cil + Rol
0
10
25
μM H89
pCREB
GAPDH
E.
Ctrl
10μM Cil
1nM Iso
Cil + Iso
0
1
10
μM H89
pCREB
GAPDH
C.
p-CREB (rel. GAPDH)
2.0
1.5
1.0
0.5
0.0
***
Control
10μM Cil
10μM Rol
No H89
10μM H89
25μM H89
Cil + Rol
F.
p-CREB (rel. GAPDH)
1.25
1.00
0.75
0.50
0.25
0.00
#
###
**
***
**
Control
10μM Cil
1nM Iso
No H89
1μM H89
10μM H89
Cil + Iso

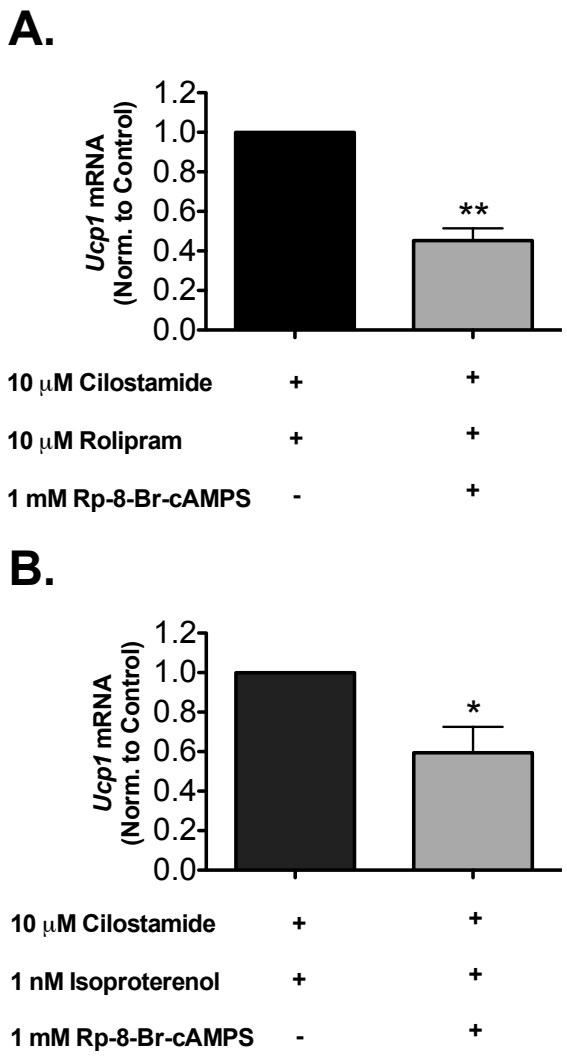

Figure 2.10. The selective PKA antagonist, Rp-8-Br-cAMPS inhibited Ucp1 mRNA induction by PDE inhibitors.
Differentiated brown adipocyte precursors were pretreated with vehicle or 1 mM Rp-8-Br-cAMPS for 60 min, followed by [A] 10 μM cilostamide and 10 μM rolipram or [B] 10 μM cilostamide alone for 30 minutes, and finally stimulated with vehicle or 1 nM Isoproterenol for 4 h (n=4). RNA was isolated and UCP1 mRNA was quantified relative to 18S mRNA as a reference using RT-PCR as described in materials and methods. Data are presented as mean fold over vehicle control ± S.E.M., and statistical analyses were performed by paired Student's t-test: **p<0.01, *p<0.05 versus control.

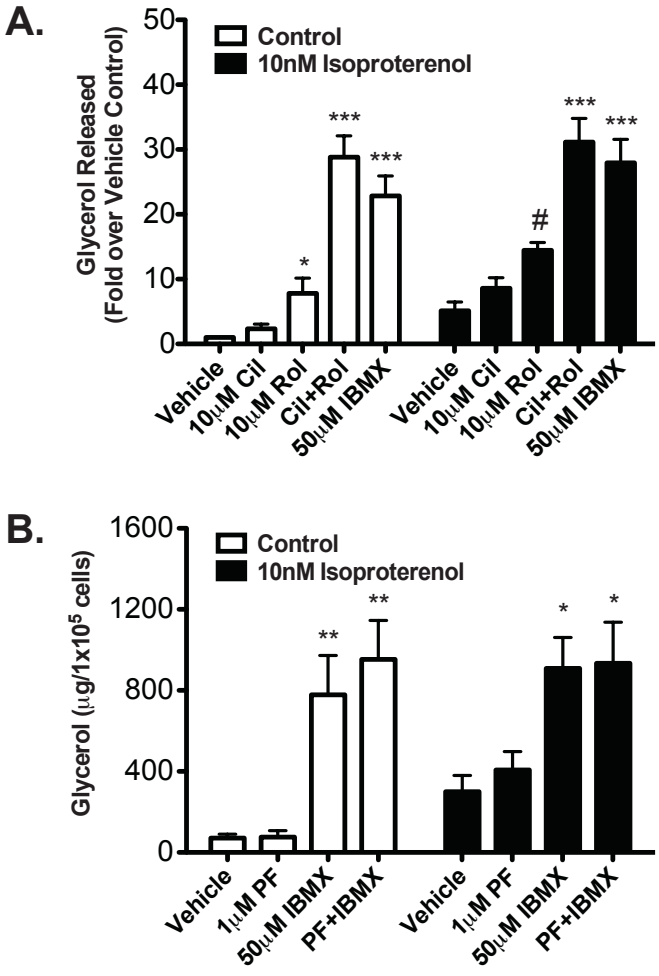

Figure 2.11. PDE3 and PDE4 inhibitors, but not the PDE8 inhibitor, increased glycerol production from isolated primary mouse brown adipocytes.
Primary brown adipocytes were isolated from mouse interscapular brown fat pads as described in materials and methods. [A] Primary brown adipocytes were pre-treated with 10 μM cilostamide, 10 μM rolipram, both or 50 μM IBMX for 20 min, and then stimulated with vehicle or 10 nM isoproterenol for 1 h. [B] Primary brown adipocytes were pre-treated with 1 μM PF-04957325 and/or 50 μM IBMX for 20 min, and then stimulated with vehicle or 10 nM isoproterenol for 1 h. Glycerol was measured as described in Materials and Methods. Data are expressed as mean mg glycerol/10^5 cells ± S.E.M. (n=3-5), and statistical analyses were performed by One-way ANOVA; ***p<0.001 for Cil+Rol and IBMX versus vehicle control in each group, *p<0.05 for Cil or Rol versus vehicle, and a two-tailed t-test $^{\#}$p<0.05 for PDE inhibitors versus vehicle in the presence of 10 nM isoproterenol.

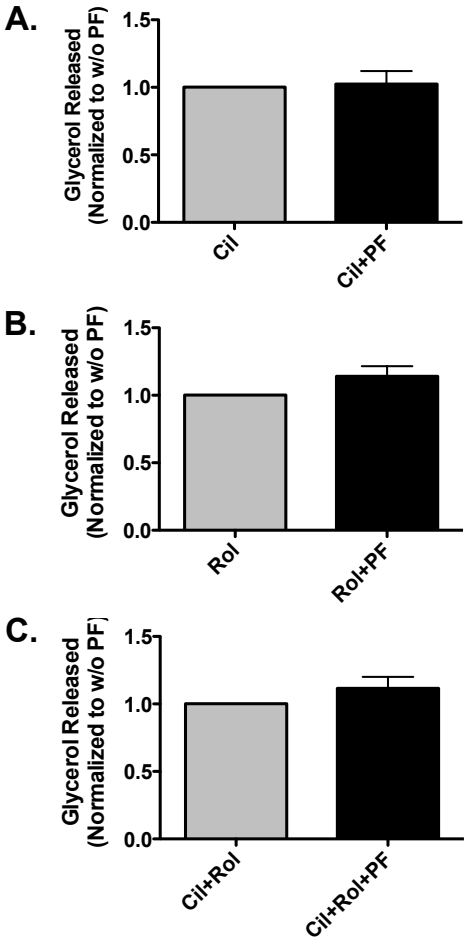

Figure 2.12. PF-04957325 did not potentiate glycerol release when combined with cilostamide, rolipram or both in primary mouse brown adipocytes. Primary mouse brown adipocytes were treated for 80 minutes with: [A] 10 μM cilostamide +/- 200nM PF, [B] 10 μM rolipram +/- 200nM PF, or [C] both 10 μM cilostamide and 10μM rolipram +/- 200nM PF while shaking for 90 cycles/min at 37°C (n=3). Glycerol was measured as described in Materials and Methods. Data are normalized to the amount of glycerol released by PDE inhibitors in the absence of PF, and presented as mean ± S.E.M.

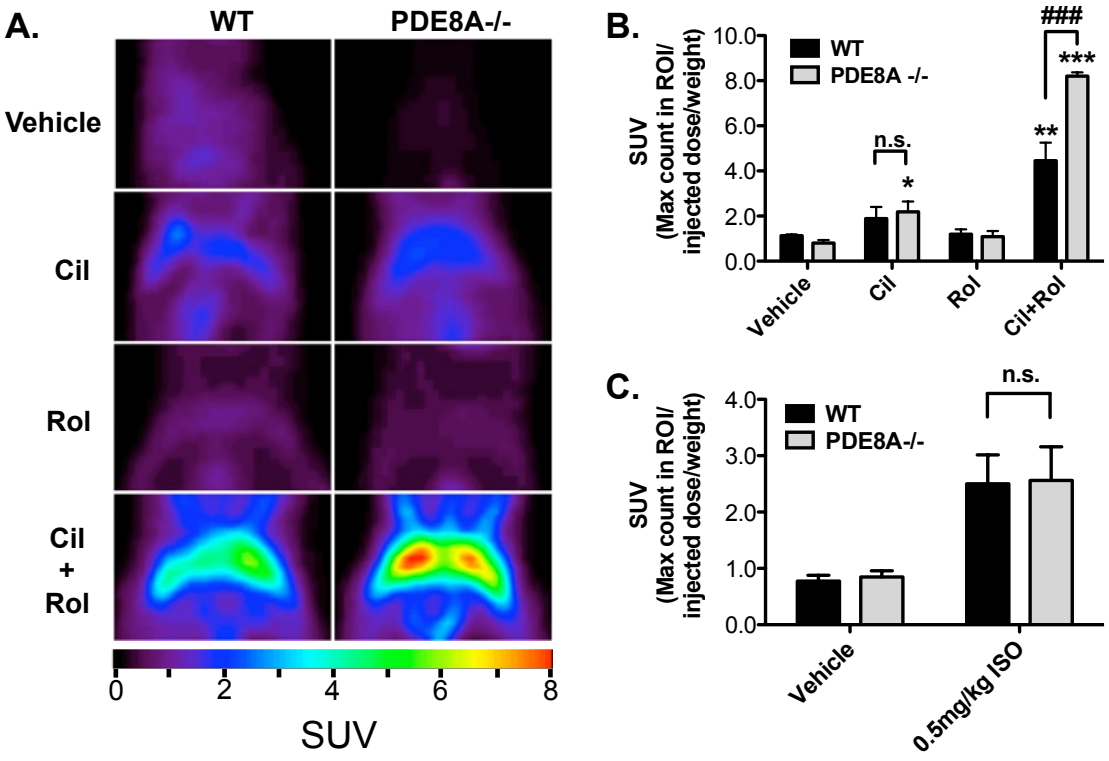

Figure 2.13. PDE3 and PDE4 inhibitors stimulate 18F-Fluorodeoxyglucose (FDG) uptake in the interscapular BAT in vivo.
[A] Wild type and PDE8A-/- littermate mice were injected with 3mg/kg of cilostamide, rolipram, or both. FDG was injected retro-orbitally and mice were imaged using positron emission tomography as described in Materials and Methods. [B] Quantification of BAT region of interest (ROI) expressed as Standard Uptake Value (SUV)=Max count in ROI/Injected Dose/Weight. [C] Wild type and PDE8A-/- littermates were injected with 0.5 mg/kg isoproterenol or vehicle, and FDG uptake was quantified similarly. Data are presented as mean SUV ± S.E.M (n=3-4), and statistical analyses were performed by One-way ANOVA with Dunnett post hoc: **p<0.01 versus vehicle control in each group, and by Two-way ANOVA with Bonferonni post hoc: $^{###}$p<0.001 wild type versus PDE8A-/- treated with cilostamide and rolipram.

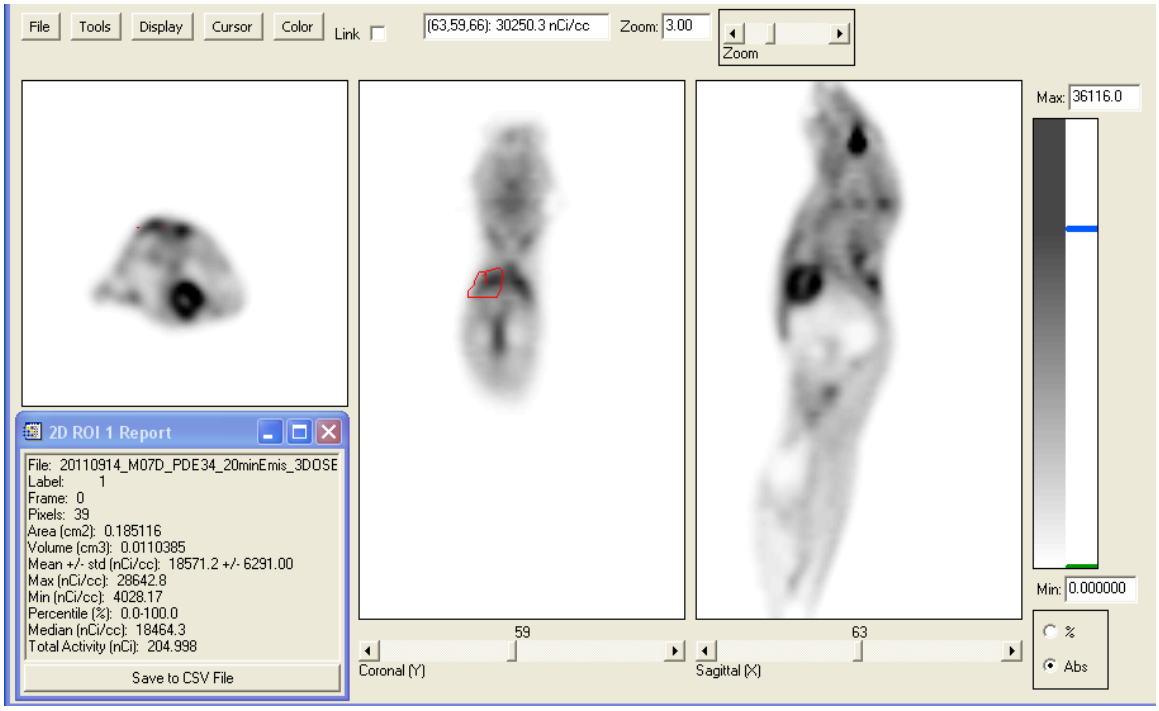

Figure 2.14. FDG uptake was quantified using Siemen's ASPIRO analysis software.
Shown is a screen capture image of a typical ASPIRO analysis of a mouse injected with FDG. A region of interest was drawn around the left (red trace) and right halves of the interscapular brown adipose tissue in a coronal plane that represented the center of BAT glucose uptake. The maximum activity concentrations [Max (nCi/cc)] between the two regions were averaged and used to calculate the SUV for each animal as described in Materials and Methods.

Table 2.1. Primer Sequences for RT-PCR

Primer Name	Sequence 5' -> 3'
PDE1A forward:	GGGCATTTTCAGCAAATTAAA
PDE1A reverse:	CAGCTGCATGGAGTATCAGG
PDE1B forward:	CCAGCAAGTGAAGACTATGAAGA
PDE1B reverse:	CTGATGTCAGCAGCATGAAG
PDE1C forward:	TTGAGATGGTAATGGCCACA
PDE1C reverse:	ATAAGGCTTTCGGCTTCTCA
PDE2A forward:	GGCTGCAATATCTTTGACCA
PDE2A reverse:	GTGGTGTGCCAGGTCTGTAG
PDE3A forward:	CGACTCCGATTCTGACAGTG
PDE3A reverse:	ATATTCCCAGACAGGCATCC
PDE3B forward:	ACGGAAACCAAAGCAGATTC
PDE3B reverse:	GCAGCCATAACTCATATCTGGA
PDE4A forward:	CAAGCGCCAGAAGCAGAG
PDE4A reverse:	CATAGTCTTCAGGTCAGCCAGA
PDE4B forward:	AATGTGGCTGGGTACTCACA
PDE4B reverse:	AAGGTGTCAGATGAGATTTTAAACG
PDE4C forward:	ATGGGGACTTGATGTGTTCA
PDE4C reverse:	TCTTGAGGAGGTCTCGTTCC
PDE4D forward:	CGTTTTCCGAATAGCAGAGC
PDE4D reverse:	TTTTAAACGTTTTTAACAAATCTCG
PDE5A forward:	AAATCAATTCAGTTTTGAAGATCC
PDE5A reverse:	TGTTGAATAGGCCAGGGTTT
PDE6A forward:	CCAGGAGTGGACCCAGTACA
PDE6A reverse:	GGTTTGGTGATGGCTGAGAG
PDE6B forward:	TGAAGATAAGAAGAGTTGGGTTG
PDE6B reverse:	AGCAGACAGGTCACATGCAG
PDE6C forward:	CGAGCAGATGCAAAGTGAAG
PDE6C reverse:	CAGACAGGTCACAGGCAGTC
PDE7A forward:	AAAGGTGACTTACACCTTGACGA
PDE7A reverse:	CCAGTTCCGACATGGGTTAC
PDE7B forward:	AAAGCTCACCTCCACAATAAAGA
PDE7B reverse:	GGATTGCAAATGTCAGCACA
PDE8A forward:	GACAGAAACACCTGCAGCA
PDE8A reverse:	GTTAGGCAGGTCAACGAAG
PDE8B forward:	GTGACTCCGGGGACAACTCT
PDE8B reverse:	TGCCCCGAGAAGATATTGAT
PDE9A forward:	AATTTTGACTGCAGCAACGAG
PDE9A reverse:	ACCTCCATGGGACGGACT
PDE10A forward:	TACCAGACAGGGTCGCTGA
PDE10A reverse:	TGGCCATAGTTTGGTCACAG
PDE11A forward:	CGAGCTTGTCAGGAAAGGAG
PDE11A reverse:	ACGGCTCCAAGGTCACAG
UCP1 forward:	CGATGTCCATGTACACCAAGGA
UCP1 reverse:	TCGCAGAAAAGAAGCCACAA
PGC1α forward:	GCTTTGAAGTTTTTGGTGAAA
PGC1α reverse:	ACGGTAGGTGATGAAACCATAGC
18S forward:	GTAACCCGTTGAACCCCATT
18S reverse:	CCATCCAATCGGTAGTAGCG

Chapter 3:
PDE8A Associates with Mitochondria in BAT

Summary

Cyclic-AMP plays an important role in mitochondrial function. PKA-dependent phosphorylation has been shown to be important for the regulation of mitochondrial fission, steroidogenesis and oxidative phosphorylation. Several PDEs have also been implicated in modulating the cAMP signal that can stimulate both pro- and anti-apoptotic responses as well as the oxidative stress. Brown adipocytes get their colorful name from the dense mitochondria content contained within them, which is important for the generation of heat by uncoupling during BAT activation. Other studies in the Beavo laboratory have indicated that PDE8A localizes to mitochondria in other cell types that contain a lot of mitochondria. Presented here are preliminary results verifying that PDE8A localizes with the mitochondria from BAT. Furthermore, the nature of the interaction was characterized using limited proteolysis of isolated mitochondria fractions, and the results indicate that PDE8A probably localizes to the mitochondria exterior. These studies provide the basis for further studies characterizing this interaction and the effects it has on mitochondrial function.

Introduction

Cyclic-AMP signaling complexes both inside and outside the mitochondria play important roles in mitochondria dynamics and responsiveness to reactive oxygen species. Outside of the mitochondria, PKA dependent phosphorylation is particularly important for the stability of the machinery that mediate mitochondria fission and fusion processes, which is vitally important for mitochondria efficiency and the mediation of apoptosis. One of these PKA substrates is dynamin related protein 1 (Drp1), which is a GTPase that is required for cellular apoptosis and mediates the fragmentation of mitochondria under pro-apoptotic stimuli (Frank et al., 2001). PKA phosphorylation of Drp1 inhibits its GTPase activity leading to its ubiquitination and degradation, promoting mitochondrial fusion (Chang and Blackstone, 2007; Cribbs and Strack, 2007), a process that has been shown to be critically important for the efficiency of ATP synthesis during starvation (Gomes et al., 2011), as well as cell survival during myocardial infarction (Kim et al., 2011). Through anchoring to AKAP1 on the outer mitochondrial membrane (OMM), PKA can phosphorylate Bcl-2 family members to inhibit apoptosis, but can also phosphorylate inhibitor of apoptosis (IAP) to promote apoptosis (Carlucci et al., 2008), thus indicating a complex regulation of cell survival. In steroid-producing cells, PKA is very important in regulating the phosphorylation and activation of the steroidogenic acute regulatory protein (StAR), which is involved in the transport of cholesterol into the mitochondria for steroid synthesis (Stocco, 2001). Inside of the mitochondria, PKA can be stimulated in the mitochondrial matrix by a cAMP pool generated by the soluble adenylyl cyclase. This has been shown to regulate

oxidative phosphorylation (Acin-Perez et al., 2009b), possibly by direct phosphorylation of a number of electron transport chain proteins (Papa et al., 1999).

Since cAMP and PKA are known to play multiple roles in mitochondrial function, PDEs may also play an important role in regulating these processes. It has been shown that PDE4A can interact with AKAP1 in human T-lymphocytes (Asirvatham et al., 2004), and PDE4 inhibition induced an apoptotic response in human chronic lymphocytic leukemia cells (Moon and Lerner, 2003). Inhibition of cardiomyocytes with IBMX seems to be cardioprotective during ischemic insult via a PKA/PKG-dependent inhibition of membrane potential collapse through the mitochondria permeability transition pore (Chanoit et al., 2011). Although, the specific PDE subtypes that mediate this process have not been identified.

There have been several published reports suggesting that PDEs may regulate mitochondria function. In an early study, it was shown that the nonselective PDE inhibitor, dipyridamole, induced an “uncoupled-like” state in isolated heart mitochondria (Sordahl and Schwartz, 1967). Dipyridamole can inhibit a number of PDEs, notably PDE2, PDE3, PDE5, and is one of the few PDE inhibitors that can inhibit the PDE8 family with a reasonable affinity (IC_{50} = 4-23 μM (Fisher et al., 1998; Gamanuma et al., 2003; Soderling et al., 1998). Recently, it was shown that a particular splice variant of PDE2A has a mitochondrial localization sequence that results in PDE2A being imported into the mitochondrial matrix (Acin-Perez et al., 2011). This study also showed that a PDE2A inhibitor could stimulate oxygen consumption in isolated mouse brain mitochondria, whereas a PDE4 inhibitor could not. This suggests that PDE2A may play an important role in oxidative

phosphorylation and ATP production. In fact, PDE2A has been shown to regulate adrenal aldosterone production in the zona glomerulosa cells of the adrenal gland (MacFarland et al., 1991). However, a direct correlation between mitochondrial PDE2A and steroid production has not yet been established. Still, it is clear that different PDEs can regulate mitochondria function in several different tissue types, indicating a potentially important regulatory step in cell physiology and energy utilization.

The Beavo laboratory has recently published several studies demonstrating that PDE8A regulates testosterone production in mouse Leydig cells (Vasta et al., 2006) (Shimizu-Albergine et al., 2012), and also that PDE8A co-localizes with mitochondria as visualized by immunocytochemistry (Shimizu-Albergine et al., 2012). Given the dense mitochondria content in BAT, and given that PDE8A is found in tissues that also contain high concentrations of mitochondria (Soderling et al., 1998), I hypothesized that PDE8A localizes to mitochondria in BAT. Using isolated BAT mitochondria, I attempted to verify the presence of PDE8A in mitochondria fractions and to characterize the nature of the interaction between PDE8A and the organelle. In order to test whether PDE8A localizes to the inside or outside of the mitochondria, I subjected the mitochondria to limited proteolysis in the absence or presence of detergent, and then analyzed the sample using Western blot analysis to probe whether or not the protein was degraded in a given condition. The results clearly indicate that PDE8A is enriched in the crude mitochondria preparation of BAT. Limited proteolysis, though not conclusive, indicated that PDE8A is probably localized to the exterior membrane of the mitochondria. However, it

remains to be seen exactly how this interaction occurs, i.e. whether PDE8A is localized on the cytosolic face of the OMM, in the intermembrane space (IMS) or somehow loosely tethered to protein complexes that associate with the OMM but are perhaps protected by other contaminating membranes. This data could serve as preliminary results for a study probing the physiological mechanism of PDE8A function in BAT, as our recently published results showed that a global ablation of PDE8A results in enhanced glucose uptake in BAT when PDE3 and PDE4 are also inhibited (Kraynik et al., 2013).

Materials and Methods

Isolation of mouse mitochondria by differential centrifugation

Adult C57/Bl6 mice were sacrificed via CO_2 asphyxiation, and the interscapular BAT pads, and/or testes, were excised and trimmed of any remaining white adipose and connective tissues. The tissue was then homogenized in 1 mL ice cold lysis buffer, 10mM HEPES, pH 7.4, 250 mM sucrose, 5 mM EDTA, 1X Protease Inhibitor Cocktail III, (Calbiochem, EMD Millipore, Darmstadt, Germany) in a glass Dounce homogenizer with a Teflon pestle on ice with approximately 30-40 strokes. A small amount of the homogenate was saved for Western blot, and the rest was transferred to a 1.5 mL centrifuge tube and centrifuged at 500 *g* for 10 min at 4°C. The cytosolic fraction was removed with a 1mL syringe fitted with a 25-gauge needle and transferred to a new 1.5 mL centrifuge tube after first removing the needle from the end of the syringe. The remaining pellet was resuspended in lysis buffer and saved for Western blot as P1. The cytosolic fraction was centrifuged again at 500 *g* for 10 min at 4°C, removing the cytosolic fraction once again. The remaining pellet was resuspended in lysis buffer and saved for Western blot as P2. The cytosolic fraction was then centrifuged at 12 200 *g* for 10 min and then removed after saving a small amount for Western blot. The remaining pellet was then resuspended in lysis buffer that contained 3% Ficol and layered over a 6% Ficol lysis solution, and then centrifuged at 10 400 *g* for 30 min. The resulting pellet was defined as the crude mitochondria fraction. For protease digestion, the mitochondria pellet was washed twice with lysis buffer without protease inhibitors and resuspended in 200 µL lysis buffer without protease inhibitors.

Isolation of BAT mitochondria by gradient centrifugation

BAT was homogenized in 2 mL ice cold lysis buffer, 10mM HEPES, pH 7.4, 250 mM sucrose, 5 mM EDTA, 1X Protease Inhibitor Cocktail III, (Calbiochem, EMD Millipore, Darmstadt, Germany) in a glass Dounce homogenizer with a Teflon pestle on ice with approximately 30-40 strokes. The homogenate (Hom.) was diluted to 10 mL in ice-cold lysis buffer and transferred to a 15 mL glass centrifuge tube, saving 500 µL for Western blot analysis. The homogenate was centrifuged at 500 *g* in 4°C for 10 min. The supernatant was transferred to a 30 mL glass centrifuge tube, and the pellet was resuspended in 2 mL ice cold lysis buffer, re-homogenized as described above, diluted to 10 mL with ice cold lysis buffer (500 µL saved for Western as P1) and centrifuged at 500 *g* in 4°C for 10 min. The two supernatants were combined and centrifuged at 10 000 *g* in 4°C for 20 min. The supernatant was discarded. The pellet was resuspended in 3.6 mL 25% Nycodenz in lysis buffer (300 µL was split into 2 fractions: [1] saved as is for PDE activity, and [2] 50 µL was diluted into 88.88 µL lysis buffer for a volume-controlled analysis on a Western blot as crude mitochondria, CM) and layered within a gradient as follows: 1.6 ml of 40%, 1.6 ml of 34%, 2.3 ml of 30%, 3.3 ml of resuspended mitochondria, 2.3 ml of 23%, and 0.7 ml of 20% Nycodenz (Accurate Chemical & Scientific Corporation, Westbury, NY). The tube was then centrifuged at 23 600 *g* in a Beckman SW Ti40 rotor at 4°C for 120 min. Fractions were defined as the band of material at the following interfaces: Fraction A was between 20-23%, Fraction B was between 23-25%, and Fraction C was between 25-30%. Fractions were collected with a glass Pasture pipette and transferred to 15 mL glass centrifuge tubes, diluted to 10 mL

with lysis buffer and centrifuged at 10 000 *g* in 4°C for 20 min. The supernatant was removed and the pellets resuspended in 100 µL lysis buffer. 50 µL of the fraction was diluted with sample buffer and boiled for Western blot, and the remaining material was assayed for PDE activity.

Western blot analysis of BAT mitochondria isolation fractions

For a detailed description of the Western blot techniques used, please refer to Chapter 2 of this dissertation. Primary antibody dilutions unique to this particular chapter are as follows: PDE8A [1:1200 (vol/vol)] (PDE8-121AP, FabGennix International, Frisco, TX), UCP1 [1:1000 (vol/vol)] (C-17, Santa Cruz Biotechnology, Santa Cruz, CA), voltage dependent anion channel, VDAC, [1:1000 (vol/vol)] (VDAC1/Porin, Abcam, Cambridge, MA), superoxide dismutase, SOD, [1:1000 (vol/vol)] (SOD-2 FL-222, Santa Cruz Biotechnology, Santa Cruz, CA), cytochrome C, Cyt C, [1:1000 (vol/vol)] (BD Biosciences, San Jose, CA), protein disulfide isomerase, PDI, (Stressgen, Ann Arbor, MI), β-actin, [1:10 000 (vol/vol)] (A5441, Sigma, St. Louis, MO) in 5% milk in TBST. Secondary antibodies were conjugated to horseradish peroxidase and were diluted as follows: goat anti-rabbit [≤1:1000 (vol/vol)] (Bio-Rad Laboratories, Hercules, CA), rabbit anti-goat [1:3000 (vol/vol)] (Jackson Immunoresearch Laboratories, West Grove, PA), or rabbit anti-mouse [≤1:5000 (vol/vol)] (Bio-Rad Laboratories, Hercules, CA).

PDE Assay

For a detailed description of the PDE Assay, please refer to the Materials and Methods section in Chapter 2 of this dissertation. The assay duration, substrate

concentration, and inhibitor concentrations are given in the figure legends. For more information on the PDE inhibitors used, refer to the Materials and Methods section, subheading “Drugs,” in Chapter 2 of this dissertation.

Proteinase-K activity assay

A 116 ng/µL solution of bovine hemoglobin (Sigma, St. Louis, MO) was prepared in 20 mM TES, pH 7.5, 100 mM KCl, 1 mM $CaCl_2$ (reaction buffer). A 20 mg/mL proteinase-K stock (Invitrogen) was prepared in 10 mM Tris, pH 7.4, 20 mM $CaCl_2$, 50% glycerol (stored at -20°C). Proteinase-K was then diluted by a factor of 100 to generate a 20X working solution. 0.43 mL of hemoglobin was diluted with 45 µL reaction buffer, followed by 25 µL 20X proteinase-K working solution or reaction buffer as a control. This was done for a reaction at room temperature and at 37°C. Immediately after proteinase-K was added, 2x 50 µL aliquots were removed and added to new centrifuge tubes containing 2 µL of 25 mM PMSF in isopropanol on ice for 10 min to stop the reaction (time 0) and to incubate for 60 minutes as a negative control. 50 µL aliquots were removed and stopped with freshly made PMSF in the same fashion at 10 and 60 minutes. After 10 min on ice, the stopped reactions were diluted with sample buffer, boiled for 10 min. Samples were then separated by 10% SDS-PAGE, after which the gels were stained with 0.2% (w/v) Coomassie blue (Brilliant Blue G-250, Bio-Rad) (in 7.5% acetic acid (vol/vol) and 40% methanol (vol/vol)) and de-stained in 7.5% acetic acid, 5% methanol.

Protease digestion of mitochondria

Isolated BAT mitochondria were resuspended in 250 µL lysis buffer without protease inhibitors, except for Fig. 3.8 in which the mitochondria were resuspended in 20mM TES, pH 7.5, 100mM KCl, 1mM $CaCl_2$ in order to re-swell the mitochondria. 35 µL mitochondria were transferred to a 1.5 mL centrifuge tube, followed by the addition of 10 µL Triton X-100 or NP-40 that resulted in a final concentration of 0.2 – 1% (vol/vol) as indicated in the figure legend. Next, 5 µL of trypsin (0.25% w/v final) or proteinase-K (0.1 - 10 µg/mL final) were added to the reaction tube and the tubes were incubated on ice or at 37°C. Reactions were stopped with 2 µL 100 mM PMSF dissolved in isopropanol. Samples were diluted in sample buffer, boiled and protein digestion was analyzed by Western blot.

Results

PDE8A localizes to BAT mitochondria

In order to test the hypothesis that PDE8A localizes to mitochondria in BAT, I first isolated mitochondria and assayed both for the presence of PDE8A protein by Western blot and by enzyme activity. A band corresponding to PDE8A is easily visualized in BAT tissue homogenates from wild type mice, which is completely absent in BAT tissue homogenates from PDE8A knockout mice (Fig. 3.1). After subjecting the homogenates to low- and high-speed centrifugations, the resulting cytosolic fraction, as indicated by the presence of β-actin, had a negligible amount of PDE8A remaining. A substantial portion of the protein content in the high-speed pellet appeared to be the voltage dependent anion channel (VDAC), a mitochondria outer membrane marker. This fraction also appeared to be enriched for the band corresponding to PDE8A (Fig. 3.1). In a similar experiment, the high-speed pellet was assayed for PDE enzymatic activity. At the time of this experiment, the PDE8-selective inhibitor, PF-04957325, was not yet available. Since PDE8A is relatively insensitive to the classical non-selective PDE inhibitor IBMX, and since PDE8A has a K_m for cAMP below 100 nM, PDE8A activity was defined as PDE activity that remains in the presence of IBMX at 12 nM cAMP substrate concentration. Approximately half of the total PDE activity measured in BAT mitochondria appeared to be insensitive to IBMX. In contrast, all of the PDE activity measured in mitochondria isolated from PDE8A knockout BAT pads was inhibited by IBMX (Fig. 3.2). Since PDE8A had recently been shown to be present in mouse Leydig cells (Vasta, 2006), I also isolated mitochondria from wild type and PDE8A knockout

testes. Similarly, a large portion of the PDE activity in wild type testes mitochondria was insensitive to IBMX, whereas all of the PDE activity in knockout mitochondria was inhibited by IBMX. It was later published that PDE8A co-localized with mitochondria markers (Shimizu-Albergine, 2012) (Fig. 3.2). Together, these data indicate that PDE8A is enriched in the crude mitochondria (CM) of BAT.

PDE8A activity is found in a purified fraction of mitochondria

I attempted to determine the recovery yield of mitochondria during the differential centrifugation method by probing the homogenate, cytosolic, and low-speed pellet fractions for mitochondria markers, VDAC and SOD, and PDE8A. To my surprise, large portions of the mitochondria seem to come down in the low-speed pellet P1 fraction when the fractions are normalized to the original homogenization volume (Fig. 3.3A). I also detected a large amount of endoplasmic reticulum in the low-speed P1 and CM fractions, as indicated by the presence of protein disulfide isomerase (PDI) (Fig. 3.3B). It has been previously shown that CM preparations can contain other cellular membranes, such as the cytoplasmic membrane and endoplasmic reticulum (Acin-Perez et al., 2009a).

Due to these contaminations, it is therefore difficult to determine exactly where PDE8A is associated within the CM fraction. Therefore, I then attempted to separate the mitochondria away from other cellular organelles and membranes by gradient centrifugation. There were three visible layers of material, labeled Fractions A, B and C. According to the mitochondrial marker, VDAC, the vast majority of the BAT mitochondria were found in Fraction A (Fig. 3.4A). Since there was limited recovery of material in these fractions, it was necessary to assess the presence of

PDE8A by measuring PDE enzymatic activity in the presence and absence of IBMX and PF-04957325, both alone and in combination, in both wild type and PDE8A mitochondria fractionations. In the wild type CM fraction, approximately 75% of the total PDE activity was sensitive to IBMX, and 25% of the total activity was sensitive to PF-04957325 (Fig. 3.4B, dark blue). When combined, total PDE activity was almost completely abolished. In contrast, virtually all of the PDE activity in the CM fraction from PDE8A knockout BAT was abolished by IBMX, and there was no inhibition by PF-04957325 (Fig. 3.4B, red). This is similar to our previous observations in CM fractions (Fig. 3.2). In Fraction A, which contained most of the VDAC-positive material, we saw a similar pattern of PDE inhibitor sensitivities where PF-04957325 inhibited some portion of the total activity in the wild type (Fig. 3.4B, light blue) but none in the PDE8A knockout (Fig. 3.4B, pink). A similar pattern of inhibitor sensitivities was observed in fractions B and C, as well, except for what appeared to be PF-sensitive activities in the PDE8A knockout. The amount of PDE activity relative to the amount of protein recovered for Fractions A, B and C was approximately 100-1000 fold less than the CM fraction (data not shown), which may have been the result of the harsh isolation conditions. Taken together, these results indicate the presence of PDE8A in a more enriched fraction of mitochondria.

PDE8A associates with mitochondria exterior

In order to determine the nature of the PDE8A-mitochondria interaction, I subjected mitochondria fractions to limited proteolysis in the presence and absence of Triton X-100 detergent. In an early experiment, I found that PDE8A was sensitive to two different sources of trypsin in the absence of any detergent, as shown by a

decrease in band intensity for PDE8A in the presence of detergent compared with the 40 min time point without detergent (Fig. 3.5). The pattern of digestion between the two brands of trypsin was different, with the Worthington trypsin being very active in the early time points and the Gibco trypsin staying fairly active over the duration of the assay. In the presence of Triton-X100, PDE8A was rapidly digested by the Worthington trypsin, but more slowly digested by the Gibco trypsin (Fig. 3.5). It is important to note that the overall signal intensity was lower in the presence of trypsin, making a comparison between the two detergent conditions difficult. Additionally, the mitochondria markers VDAC and SOD were completely insensitive to trypsin digestion.

Since VDAC was shown to be completely resistant to trypsin (Salinas et al., 2006), but sensitive to proteinase-K (Chandra et al., 2004), I next used proteinase-K in the digests of CM preparations. The band corresponding to PDE8A was readily digested by proteinase-K (0.1 and 10 µg/mL) even in the absence of Triton X-100 (Fig. 3.6) at 4°C. However, the VDAC and SOD still seemed to demonstrate insensitivity to proteolysis, which led me to test whether the conditions were adequate for full proteolytic activity. The product information indicates that proteinase-K works best in the presence of calcium and at higher temperatures. In order to troubleshoot these conditions, I designed a proteolytic activity assay using bovine hemoglobin as a substrate. I found that even under high calcium conditions, it required 60 minutes for proteinase K to fully digest hemoglobin at 37°C, whereas hemoglobin was virtually unchanged at room temperature (Fig. 3.7).

These results prompted me to modify the mitochondria digestion assay for longer time points at a higher temperature, as well as increase the calcium concentration. Furthermore, when mitochondria are isolated, it is often the case that the membranes are fully collapsed. It is therefore often necessary to resuspend mitochondria in 100 mM potassium in order to re-swell the mitochondria (Cannon and Nedergaard, 2001). I found that even under these conditions, VDAC is still relatively insensitive to digestion by proteinase K, even requiring detergent and at least 30 minutes at 37°C (Fig. 3.8). This was a similar pattern to the ER marker PDI. On the other hand, UCP1, which resides in the IMM, was partially proteolyzed by 10 minutes of proteinase-K exposure, and completely digested by 30 minutes, in the absence of any detergent (Fig. 3.8). In the presence of detergent, however, UCP1 was completely digested by only 10 minutes of proteinase-K.

Since VDAC appeared to be a non-ideal candidate for the digestion of OMM membrane proteins, I decided to expand the search for a marker that is digested under conditions where IMM membranes are untouched. It has been shown that c-Raf kinase is associated with the outside of mitochondria through an association with VDAC (Le Mellay et al., 2002), and it has been recently shown to interact with PDE8A (Brown et al., 2013). I therefore also probed for c-Raf in this particular assay as a second OMM marker. Indeed, c-Raf is almost immediately digested after the addition of proteinase-K to the CM fraction in the absence of detergent at a time point when UCP1 had yet to be digested.

Together, these results indicate that PDE8A is readily digested by protease under conditions similar to where the OMM protein c-Raf is also digested, but where

IMM proteins, such as UCP1, are not digested. These results strongly suggest that PDE8A is localized to the OMM in some way, however it remains to be seen exactly how this interaction occurs.

Discussion

PDE8A is enriched in mitochondria from BAT and it is readily digested by two different proteases, trypsin and proteinase K. However, it is inconclusive whether it is inside or outside the mitochondria from these experiments. Under a given set of conditions, PDE8A is rather protected from proteolysis by trypsin or Proteinase K, but readily degraded by proteolysis when detergent is present. However, without a well-established control for the degradation of inner or outer mitochondria markers due to their relative insensitivity to proteases, making a definitive statement for where PDE8A actually resides is difficult. For example, VDAC is inherently insensitive to proteolysis because it serves as a junction between mitochondria and endoplasmic reticulum membranes that cannot be removed by washes (Rizzuto et al., 2012; Salinas et al., 2006). Therefore, despite this protein being outside the mitochondria, it is not accessible by protease until detergent is present to dissolve the membranes. On the other hand, superoxide dismutase, a matrix mitochondria marker, is insensitive to proteolysis by virtually all proteases (Li et al., 2010). These subtle details were not immediately known at the time that these experiments were done, but they do retroactively explain the observations that these proteins were insensitive to proteolysis. However, C-Raf kinase, an enzyme that appears to interact with mitochondria through VDAC (Le Mellay et al., 2002), was readily digested by proteases in a similar fashion to what was observed for PDE8A.

Additionally, UCP1, which resides in the mitochondria inner membrane, is also digested by high concentrations of proteinase K. This is interpreted to mean that proteinase K may disrupt membranes by digesting OMM proteins, thereby

allowing the protease access to inner mitochondria proteins under certain conditions. These results indicate that these mitochondria are fairly fragile under these particular conditions, and that the conditions within which these digestion assays were carried out were not fully optimized.

Importantly, under similar conditions where UCP1 is protected, PDE8A seems readily degraded. This would imply that PDE8A is loosely tethered to the outside of mitochondria, but potentially protected in some fashion by contaminating membranes as is VDAC. This is also supported by the finding that the endoplasmic reticulum marker, PDI, which is present in these mitochondria preparations, is completely insensitive to proteolysis in the absence of detergent. A second potential conclusion is that PDE8A is in the intermembrane space (IMS). Further digestion experiments probing for protein markers such as cytochrome C may serve to validate or refute this hypothesis. However, there are only a handful of reports indicating cAMP signaling effectors present in this particular compartment. For example, the optic atropy protein 1 (OPA1) resides in the IMS, but has also been implicated as an AKAP in adipocytes that is important for lipolysis (Belenguer and Pellegrini, 2013; Pidoux et al., 2011).

Altogether, these data indicate a body of preliminary evidence characterizing how PDE8A may interact with BAT mitochondria, though it does not identify how this interaction occurs (e.g. through the N-terminal PAS, Per-Arnt-Sim, domain). So far, BAT is the only tissue by which these limited proteolysis experiments have been probed. Part of this is because BAT is a tissue where PDE8A is abundantly expressed and very easily observed on a Western blot. Additionally, PDE8A is not

proteolytically cleaved upon tissue homogenization in BAT as we have found with liver, which could potentially disrupt native protein-protein interactions that are important in characterizing this loose interaction. Finally, this study lays the groundwork for future experiments in terms of the methods of mitochondria isolation and protease assay characteristics that are in need of further refinement, as well as establish a signaling domain in which PDE8A function could potentially be explored. Such domains include, but are not limited to, the fission and fusion of mitochondria, cell survival/death, and the utilization of nutrients, all of which have a strong PKA-dependent regulation.

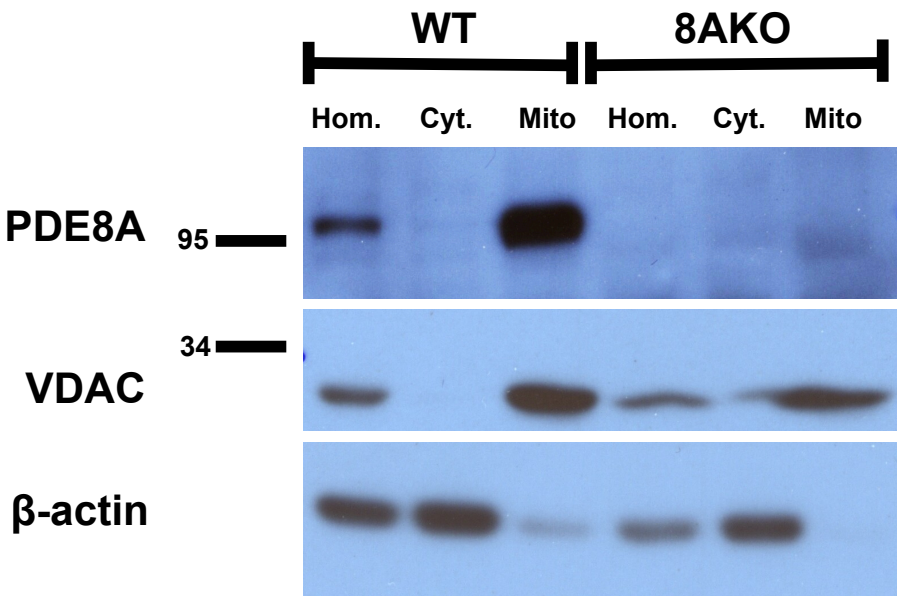

Figure 3.1. PDE8A protein is enriched in crude mitochondria isolated from mouse BAT.
Crude mitochondria were isolated via differential centrifugation from homogenized wild type (WT) and PDE8A knockout (8AKO) BAT as described in Materials and Methods. 35 µg of protein from total homogenate (Hom.), cytosolic (Cyt.) and mitochondria fractions (Mito.) was separated by SDS-PAGE, and blotted onto PVDF. PDE8A, VDAC and β-actin protein were then analyzed via Western blot. Shown is a representative blot (n=5).

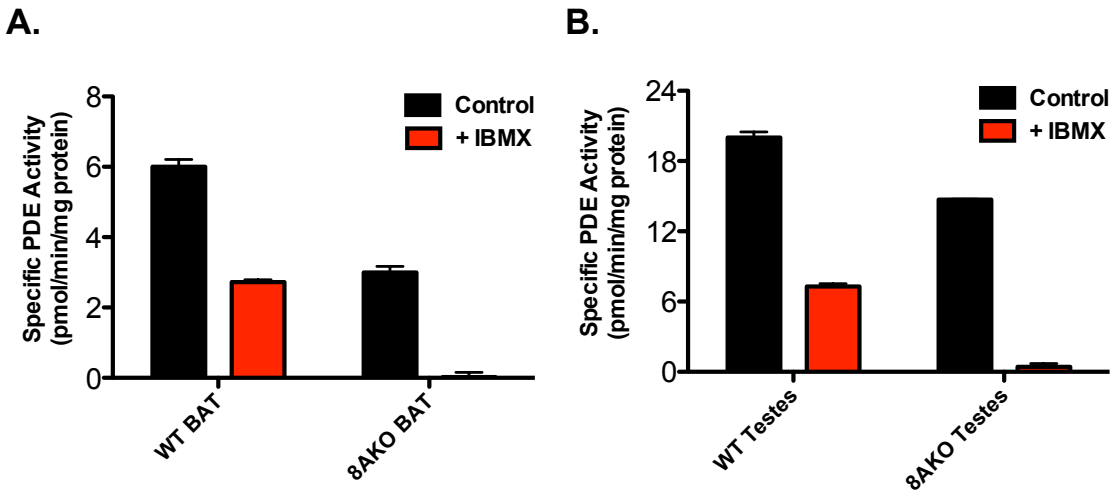

Figure 3.2. IBMX-insensitive PDE activity is present in crude mitochondria isolated from mouse BAT and testes.
Crude mitochondria were isolated via differential centrifugation from homogenized BAT [A] and testes [B] as described in Materials and Methods. The mitochondria were then assayed for PDE activity in the presence of 12 nM cAMP substrate with and without 100 μM IBMX for 15 min. The IBMX-insensitive portion of total PDE activity observed in mitochondria from wild type mice is completely gone in PDE8A knockout mice (8AKO) (n=1). Data are presented as mean specific PDE activity (pmol/min/mg protein) with error bars representing the range of duplicates in a single experiment.

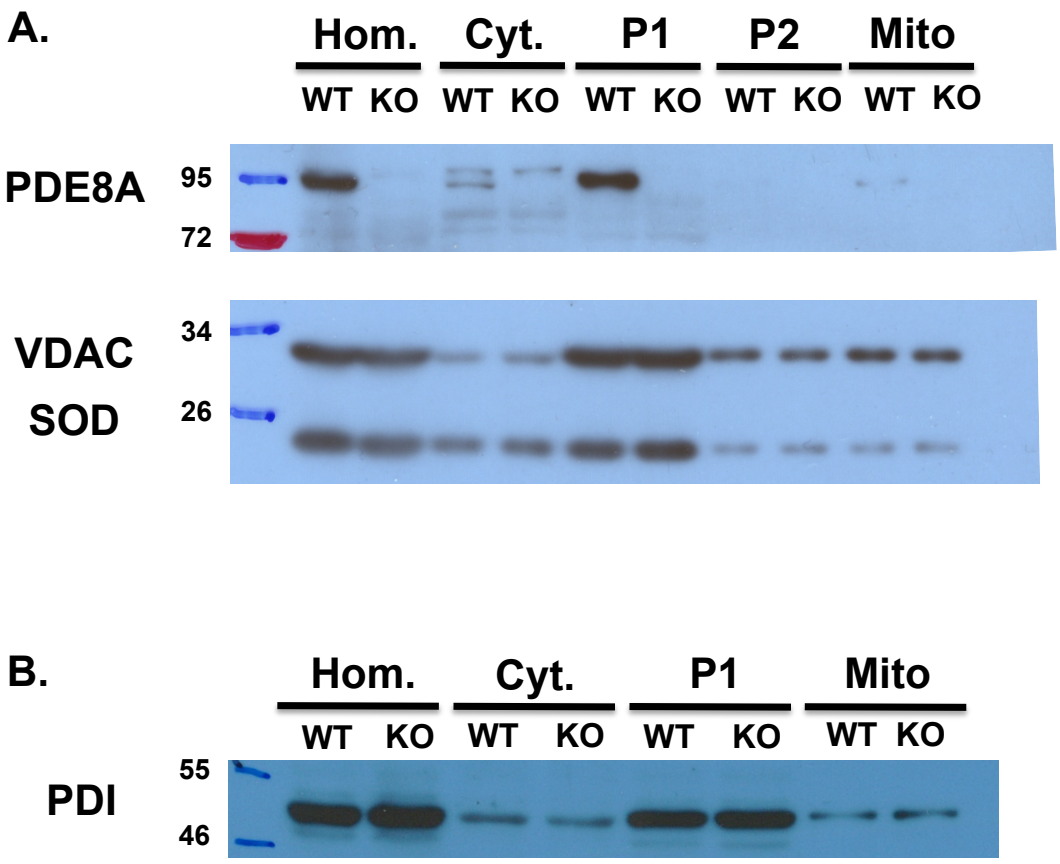

Figure 3.3. BAT mitochondria markers are enriched in the low-speed pellet. Crude mitochondria were isolated from BAT as described in Materials and Methods. Both of the 500 *g* pellets (P1 and P2) and the mitochondria pellet (Mito) were resuspended in the same volume used to homogenize the BAT pad, and an equal volume of protein extract from each fraction was separated by SDS-PAGE, transferred to PVDF and probed for [A] PDE8A, the OMM protein VDAC, the mitochondria matrix protein superoxide dismutase (SOD) (n=2), and [B] the endoplasmic reticulum PDI via Western blot (n=1).

A.

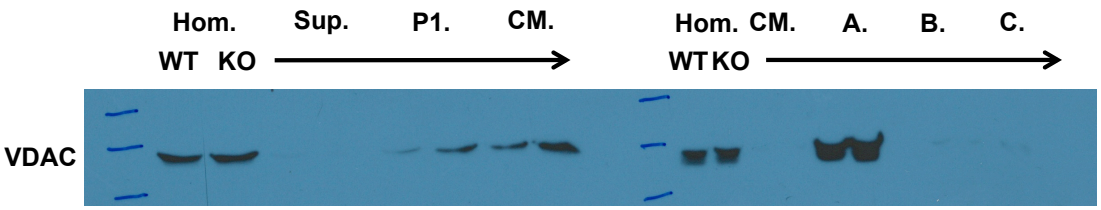

B.

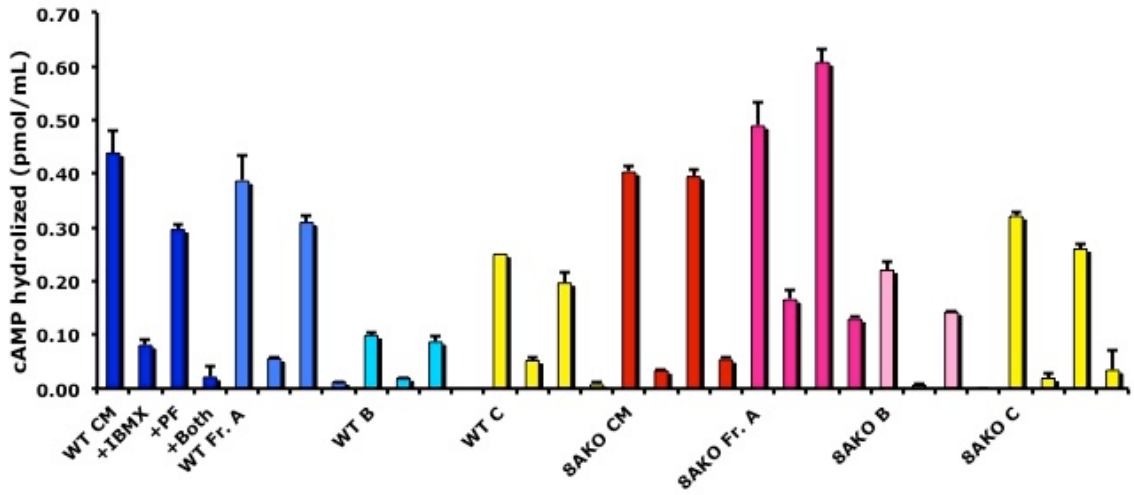

Figure 3.4. IBMX- and PF-04957325-sensitive PDE activities in gradient centrifugation fractions isolated from mouse BAT.
Membrane sub-fractions were isolated from wild type (WT) and PDE8A knockout (8AKO) BAT via gradient centrifugation as described in Materials and Methods. Membrane fractions are labeled as crude mitochondria (CM, blue or red), the mitochondrial fraction A (Fr. A, light blue or magenta), fraction B (B, cyan or pink), fraction C (C, yellow). [A] Western blot for VDAC as a measure for mitochondrial recovery. The left half of the presented blot represents crude fractions that were diluted up to the homogenate volume. The right half represent the gradient fractions. Fractions A, B and C were approximately $1x10^6$-fold more concentrated than the crude mitochondria samples in the right half of the presented blot. [B] PDE activity was measured in each of the gradient fractions and defined as pmol cAMP hydrolyzed over 45 min with, 50 μM IBMX, 200 nM PF-04957325 or both. Due to the scarcity of recovered fractional material, the data was normalized to the volume of the fraction assayed.

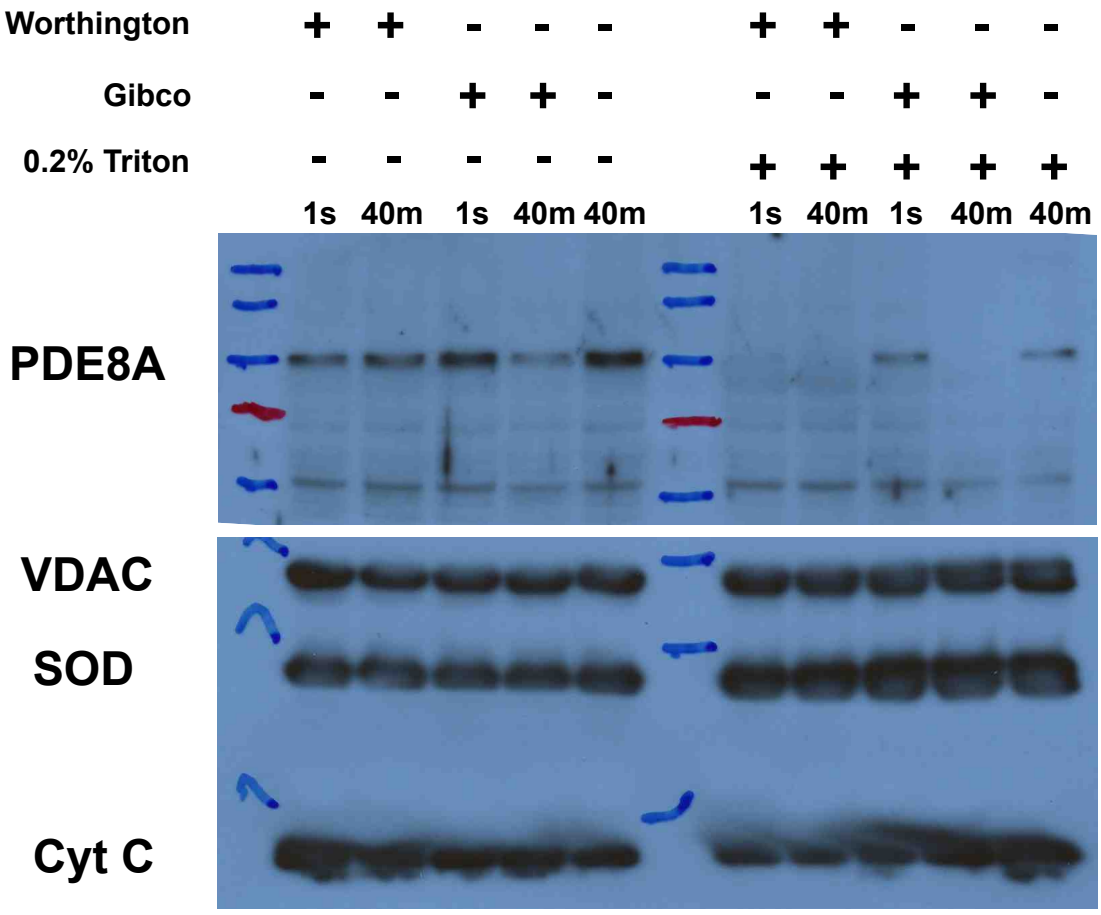

Figure 3.5. Mitochondrial PDE8A is readily degraded by trypsin.
Crude mitochondria were isolated from mouse BAT, divided into equal aliquots, and exposed to 0.25% trypsin from either Worthington or Gibco +/- 0.2% Triton X-100 for 40 minutes as described in Materials and Methods. Reactions were stopped with soybean trypsin inhibitor, diluted in sample buffer and boiled. Samples were then separated by SDS-PAGE and probed for PDE8A, VDAC, SOD, and cytochrome c (Cyt C) (n=1).

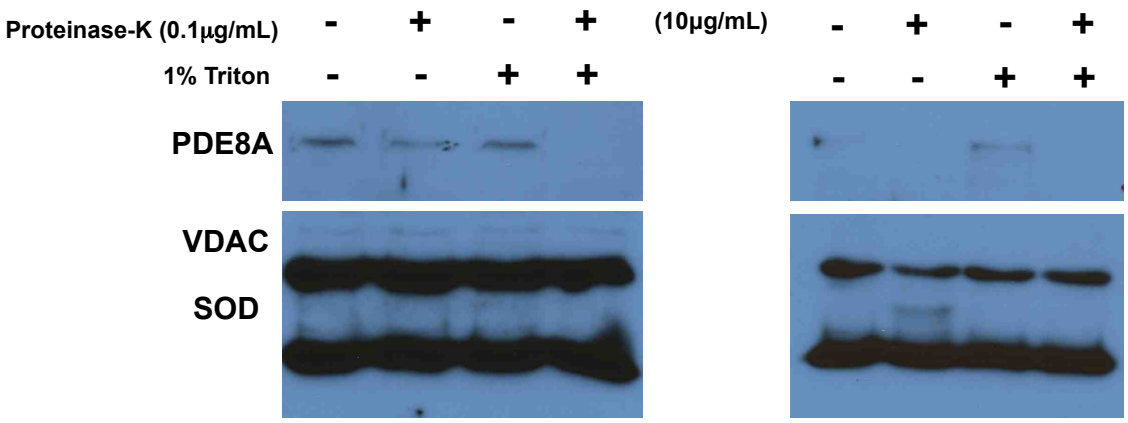

Figure 3.6. Mitochondrial PDE8A is readily degraded by proteinase-K. Crude mitochondria were isolated from mouse BAT, divided into equal aliquots, and exposed to 0.1 µg/mL (left) or 10 µg/mL proteinase-K (right) +/- 1% Triton X-100 at 4°C for 10 minutes as described in Materials and Methods. Reactions were stopped with 0.1 mM PMSF, diluted in sample buffer and boiled. Samples were then separated by SDS-PAGE and probed for PDE8A, VDAC, and SOD (n=1).

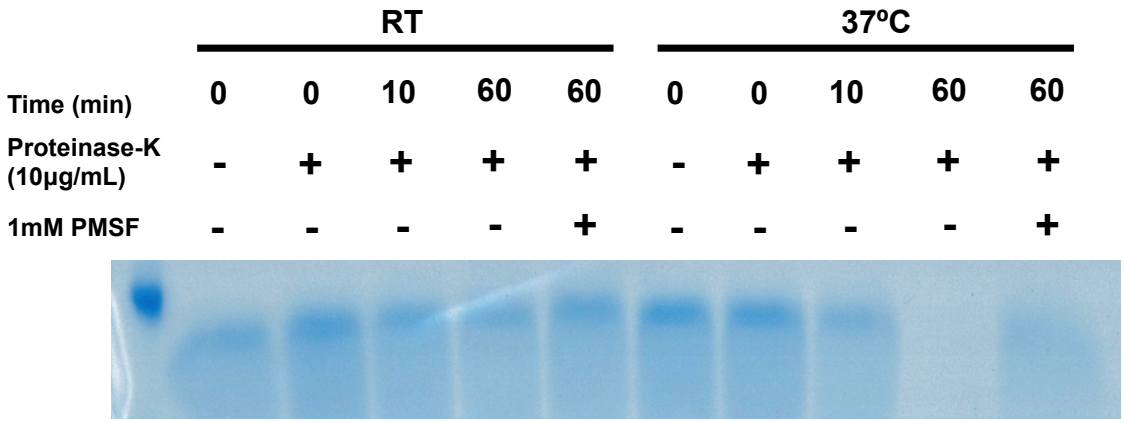

Figure 3.7. Proteinase-K activity assay using bovine hemoglobin as a substrate marker.
Bovine hemoglobin was digested by 10 µg proteinase K at either room temperature or at 37°C for 0, 10 or 60 min as described in Materials and Methods. Reactions were stopped with 1 mM PMSF, diluted in sample buffer and boiled. Samples were separated by SDS-PAGE and visualized in the gel with Coomassie blue stain (n=2).

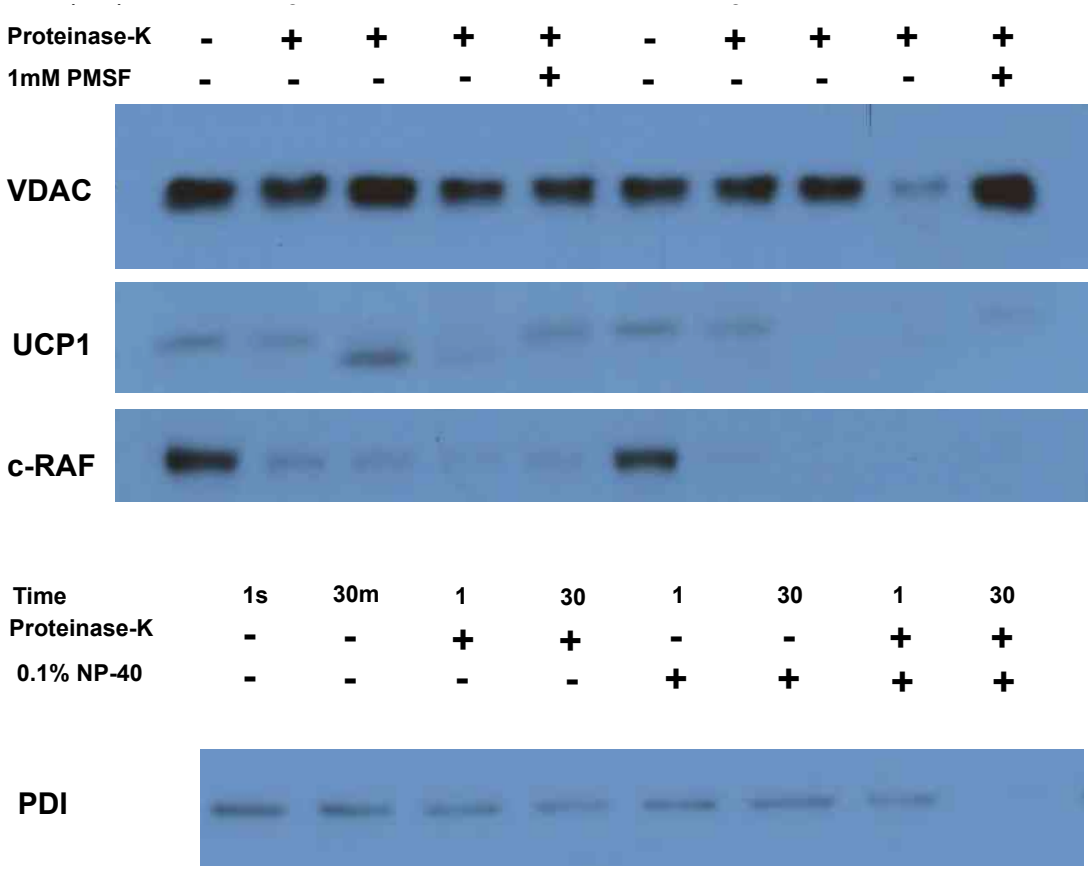

Figure 3.8. VDAC and PDI digestion by proteinase-K is dependent on detergent, while UCP1 and c-Raf digestion is not.
Crude mitochondria were isolated from mouse BAT, divided into equal aliquots, and exposed to 10 µg/mL proteinase-K (right) +/- 0.1% Triton X-100 or 0.1% NP-40 at 37°C for 0, 10, or 30 minutes as described in Materials and Methods. Reactions were stopped with 1 mM PMSF, diluted in sample buffer and boiled. Samples were then separated by SDS-PAGE and probed for VDAC, UCP1, c-Raf and PDI. Data are presented as a representative Western blot (n=1-2).

Chapter 4:
Summary and Future Implications

Brown adipose tissue is a highly metabolic organ that converts the energy stored in triglycerides and glucose into heat. It is this innate "energy wasting" function of the tissue that makes it so intriguing as a potential target for the design of future therapies in the treatment of obesity and its related diseases. As the notion that adult humans possess an appreciable quantity of brown fat has become more widely accepted, brown fat development and metabolism research over the past decade has come into a proverbial renaissance. However, despite significant advances into the characterization of brown fat development from its fibroblast-like precursors, such as its cell lineage (Wu et al., 2012), hormones like irisin that drive its production (Bostrom et al., 2012), and the identification of required transcription factor checkpoints (Seale et al., 2007), little has been done by way of finding a pharmacological tool to activate brown fat metabolism of existing brown adipose tissue. Even though the activating β_3-adrenergic receptor is expressed rather exclusively in the fat tissue in rodents, human fat tissue is essentially negative for this particular target. Because of this, agonists to this receptor that lead to weight loss in rodents, largely through BAT thermogenesis, are completely ineffective in humans. Therefore, alternative candidates in the pathways that lead to brown fat activation are in need of identification and characterization.

The goal of the investigations presented in this dissertation was to identify the phosphodiesterases that regulate the cAMP-dependent components of brown fat activity, both in its basal and stimulated states. I show in Chapter 2 that mouse BAT contains five different PDE subtypes that are capable of hydrolyzing cAMP: PDE1A,

PDE2A, PDE3B, PDE4B/D, and PDE8A. The predominant PDE enzyme activities found in brown adipocyte protein extracts were PDE3 and PDE4, though the other PDEs could also be detected. Yet, only inhibitors to PDE3 and PDE4 were effective in modulating virtually every process that was investigated, including cAMP, UCP1 mRNA expression, CREB phosphorylation, lipolysis and glucose uptake. Most importantly, it was revealed that BAT has an extremely high basal cAMP tone that is capable of facilitating a full activation of all of these important thermogenic processes, and that this "basal" production of cAMP is effectively neutralized by both PDE3B and at least one of the PDE4s together. Pharmacologically inhibiting either PDE alone had virtually no effect, but combining the inhibitors together resulted in a near-maximal, synergistic stimulation of BAT in the absence of any β-adrenergic agonists (Fig. 4.1A). However, when a β-adrenergic agonist, such as isoproterenol, is administered, there is a differential shift in the processes that PDE3B and PDE4 respectively regulate. More specifically, inhibiting PDE3B potentiated isoproterenol-stimulated UCP1 mRNA expression, but had no significant effect on lipolysis. Conversely, inhibiting PDE4 had no effect on isoproterenol-stimulated UCP1 mRNA expression, but did significantly potentiate lipolysis and global cAMP accumulation (Fig. 4.1B). These results indicate that PDE3 and PDE4 can govern the same basal compartment of cAMP production, but they govern different, possibly additional compartments when cAMP is produced in response to adrenergic stimuli.

Since BAT can take up glucose and fatty acids out of the circulation in a cAMP-dependent, insulin-independent fashion, I hypothesized that inhibiting one or more PDEs could stimulate glucose uptake by removing the PDE blockade of basal

cAMP production. I found that the same overall synergistic effect of combining PDE3 and PDE4 inhibitors could also be observed for glucose uptake in mouse BAT *in vivo*. Furthermore, when these inhibitors were combined in the PDE8A ablated mouse, there was an even greater potentiation of BAT glucose uptake than what was observed in the wild type (Fig. 4.1A). Though it is not definitive that the actions of these drugs and/or PDE8A ablation are working specifically at the brown fat, given what is presented here in the other models of brown fat, it is convincing that PDE inhibitors can remove a significant regulatory checkpoint in BAT activation both in cells and in the whole animal.

It is well understood that PDE3 isoforms localize to membranes and that PDE4 isoforms can differentially localize to cytosolic or membrane compartments through protein-protein interactions depending on certain signaling events. However, it is not well understood to what intracellular compartment PDE8A localizes. Since BAT is highly enriched in mitochondria, and since PDE8A is expressed in tissues that express a high amount of mitochondria (Soderling et al., 1998), I hypothesized that PDE8A localizes to the mitochondria. I show in Chapter 3 that PDE8A appears to localize with the crude and refined mitochondria fractions isolated from whole mouse BAT pads. Interestingly, PDE8A was digested when mitochondria were exposed to protease in the absence of detergent (Fig. 3.5, 3.6). These results were similar to what was observed for another protein that associates with the mitochondria exterior, c-Raf kinase, and suggest that PDE8A is somehow associated with the mitochondria exterior (Fig. 4.1A, 4.1B). Whether this interaction is through a protein-protein interaction (e.g. via the PAS-domain), or whether it is

directly associated with the mitochondria membrane remains to be seen. However, these results suggest a signaling domain in which PDE8A may reside, and they provide the basis for future studies into the effects of PDE8A on mitochondria function.

Despite the results presented here that demonstrate a synergistic effect of PDE3 and PDE4 inhibition on brown fat function, it remains unclear exactly how this particular relationship occurs. Notably, how do these PDEs interface with the source of the basal cAMP signal? For example, it is known that β-ARs can spontaneously switch into an active conformation in the absence of adrenergic agonists (Rasmussen et al., 2011), thereby providing a potential basal production of cAMP at the membrane. It is also known that PDE3B resides in membranes, particularly in adipocytes (Nilsson et al., 2006), and that in cardiomyocytes some PDE4D splice variants can interact with β_2-ARs in the basal state, while other PDE4D splice variants will interact with the receptor when agonist is bound (De Arcangelis et al., 2009). Even though the data presented in Chapter 2 identifies PDE4D in BAT, it has yet to be shown which splice variants of PDE4D are the ones expressed, let alone if they behave in a similar manner as in cardiomyocytes. It is also unclear if there is perhaps some other adenylyl cyclase that basally produces cAMP from a separate compartment governed by PDE4 that can possibly spill over into the compartment that stimulates UCP1, lipolysis, and glucose uptake once both PDE4 and PDE3 are inhibited at the same time (Fig. 4.1A).

It is possible that some, but not all, of the PDE4 subtypes are localized in the same relative vicinity to PDE3B, but that others are free to diffuse throughout the

cytosol. Such a differential localization to β-receptors could explain why an inhibitor to both PDEs will fully activate the tissue when β-AR agonists are absent, and why the inhibitors have differential effects when β-ARs are activated. For example, since PDE4 is important for regulating lipolysis, perhaps its cytosolic localization provides spatial control for the control of hormone sensitive lipase (HSL) phosphorylation by PKA, an event that stimulates the translocation of HSL from the cytosol to the lipid droplet. This may explain the reason why only a PDE4 inhibitor alone potentiated both global cAMP accumulation and lipolysis in response to isoproterenol, while a PDE3 inhibitor alone did not (Fig.4.1B). Future studies will be needed to illustrate how PDEs regulate the spatiotemporal relationship of cAMP signals in brown fat.

Additionally, it has yet to be shown whether PDE inhibitors alone can be used as an effective therapy for the treatment of obesity and its comorbidities. Do PDE inhibitors stimulate thermogenesis and weight loss in obese subjects? What is the level and duration of BAT activity that is necessary to get a large metabolic effect over time? Does inhibiting BAT PDEs stimulate blood glucose clearance in diabetic patients who no longer respond to insulin? These questions are in need of answers. So far, this has been problematic due to the lack of tools to test the basic hypothesis. This dissertation provides the basis for which a targeting strategy could be used to activate BAT without having to activate the β-adrenergic receptor. Most notable is the concept of synergy in combining PDE inhibitors. This is of particular importance regarding the avoidance of side effects. By definition, drug synergy may allow for lowering the dose of both drugs but still getting the same desired effect in the tissue of interest. PDE4 inhibitors are known to induce nausea, and PDE3

inhibitors are generally only used in situations of acute cardiac failure due to their propensity to decrease lifespan in such patients, though they are also approved for intermittent claudication. However, by administering low enough doses, a PDE3/PDE4 inhibitor combination, perhaps selective for the particular isoforms in BAT, could have a therapeutic result without the unwanted side effects. This type of strategy has immense therapeutic potential, but is often met with regulatory obstruction due to the difficult nature of testing multiple drugs. Still, this does not preclude the notion that a single molecule PDE3/PDE4 dual inhibitor could prove effective, and easier to pass regulatory standards. A few such drugs have entered clinical trials for the treatments of respiratory illness and have been fairly well tolerated (Banner and Press, 2009). However to our knowledge, their effects on glucose levels and BAT activity have not been explored.

In conclusion, selectively inhibiting PDE3, PDE4 and/or PDE8A may provide a potentially new clinical strategy for the activation of BAT. These enzymes play a critical role in the regulation of brown adipocyte physiology under a variety of contexts, and inhibiting these PDEs together results in the stimulation of the major cAMP-dependent processes that are known to be important for heat production.

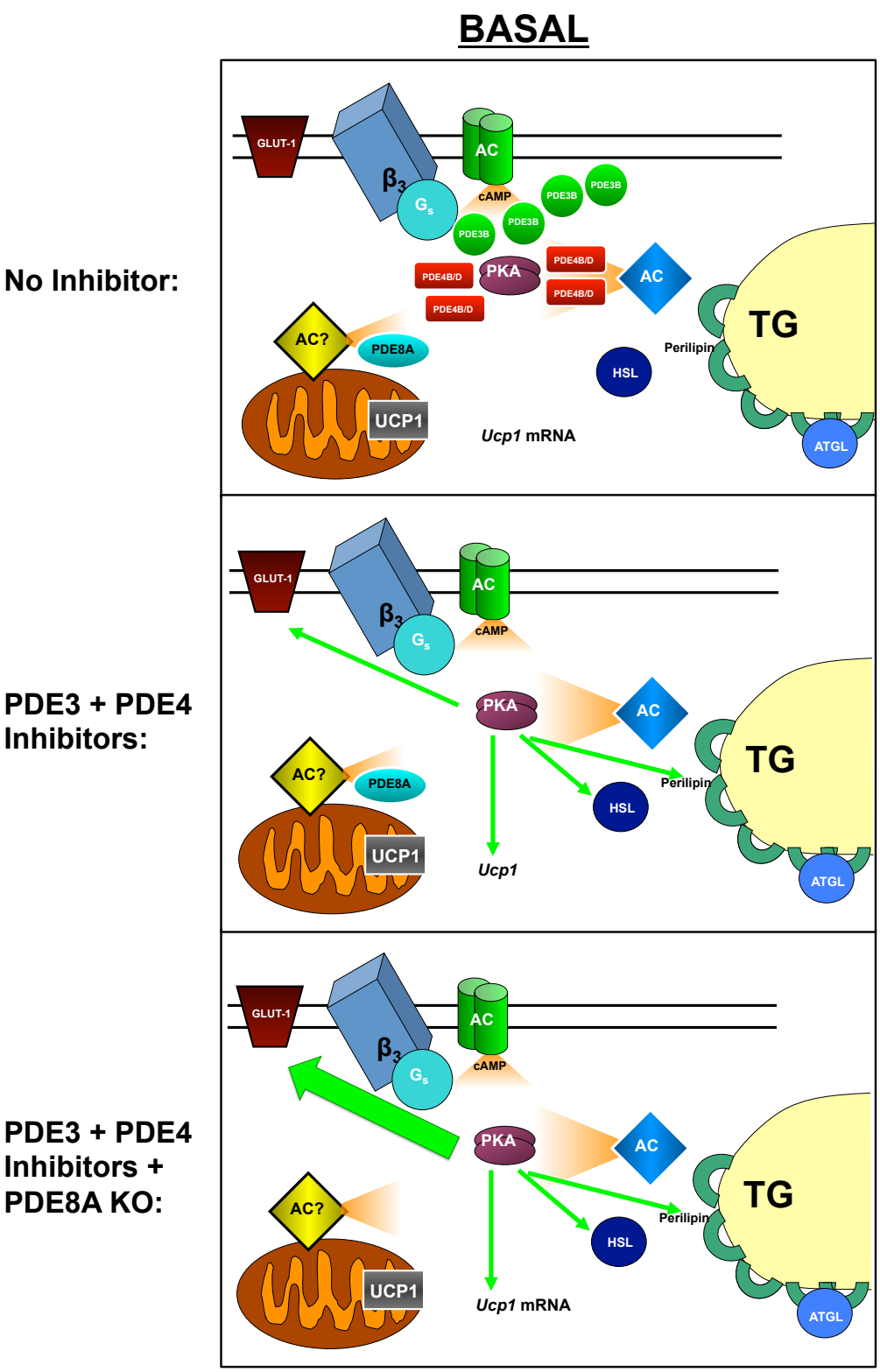

Figure 4.1A. Proposed Model for PDE Regulation of Basal Activity in BAT.

β-ADRENERGIC STIMULATION

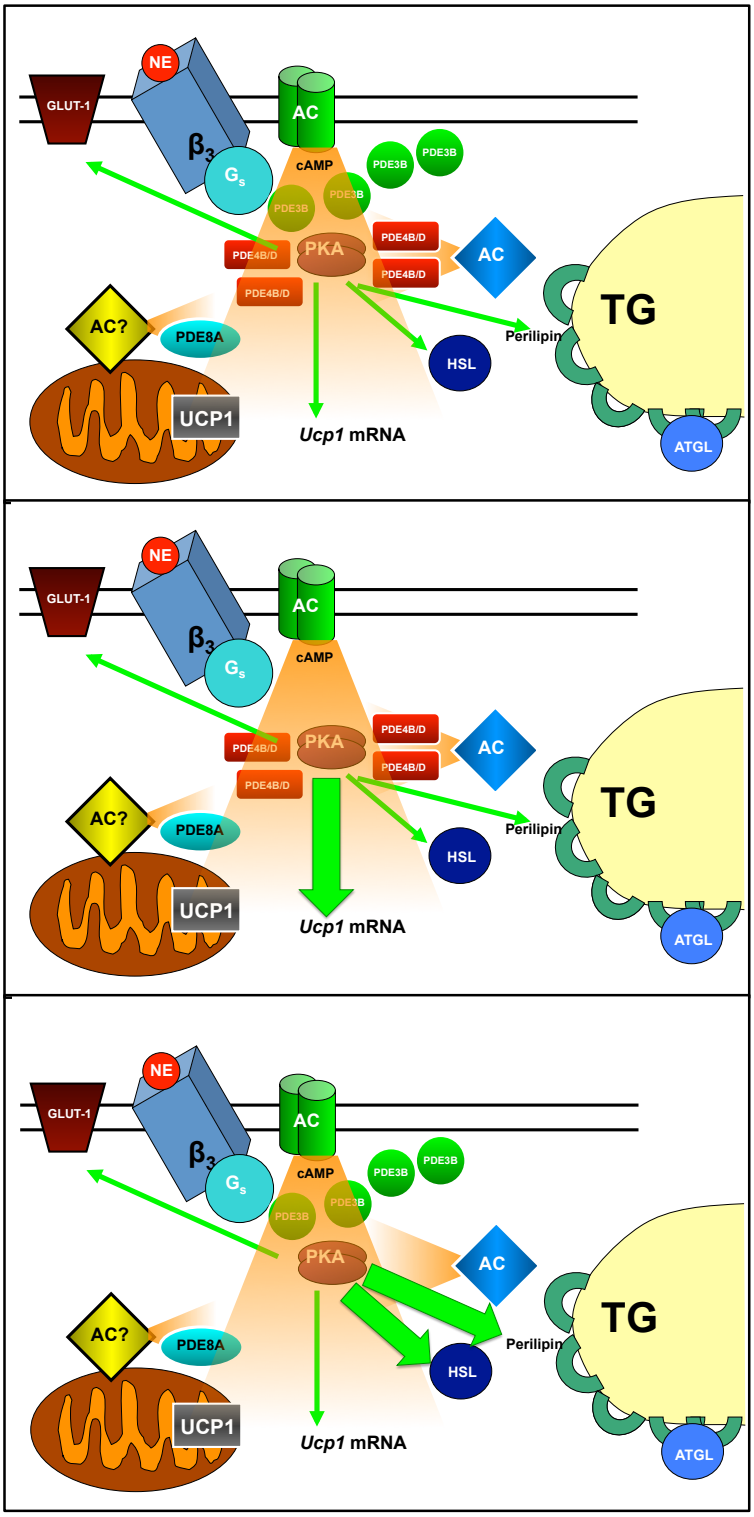

Figure 4.1B. Proposed Model for PDE Regulation of β-adrenergic Stimulated Activity in BAT.

Appendix A:
High Basal Lipolysis in Brown Adipocytes

Over the course of developing the isolated brown adipocyte model system for the study of lipolysis, several technical difficulties arose regarding the ability to measure an agonist-induced increase in lipolysis over the basal production of glycerol. I hypothesized that this could have been due to several possibilities. First, β_2-ARs are known to shift into an active conformation even in the absence of agonist (Rasmussen et al., 2007). However, little is known about the basal coupling properties of the β_3-AR. Furthermore, it is suspected that collagenase-based isolations may damage receptors on the surface of cells due to contaminating proteases, which could have implications in the degree to which adenosine is produced, thereby modulating lipolysis in a relatively unpredictable fashion (Dulloo et al., 1992). Similarly, some commercial collagenase types are specifically marketed for the isolation of adipocytes that leave the insulin receptors on the cell surface undamaged (C6885, Sigma). Since insulin is naturally anti-lipolytic, it is conceivable that damaging these receptors may result in an increased basal lipolysis. Finally, it is also known that brown adipocytes are densely innervated with sympathetic nerves. It has been shown that adipocytes isolated by collagenase digestion can still be covered by a "cob-webb" like mesh of sympathetic nerve endings depending on how long the digestion period was and how few washes the cells received after dissociation (Sbarbati et al., 1987). It was likely that several of these possibilities were true at the same time.

If endogenous norepinephrine (NE) was slowly being released from contaminating nerve stores, blocking the β-ARs should inhibit the basal production of

glycerol. In order to test this hypothesis, brown adipocytes were incubated with the nonselective β-AR antagonist propranolol (1 μM). Propranolol substantially inhibited the high rate of basal lipolysis in isolated brown adipocytes (Fig. A.A). Furthermore, this effect was mimicked by a selective competitive antagonist to the β_3-AR, SR-59230A (IC_{50} = 3.3 μM) (Tocris, Bristol, UK) (Fig. A.B, A.C). These results strongly indicated the presence of NE in the brown adipocyte incubations, but did not exclude the possibility that these drugs were acting as inverse agonists towards highly active β-ARs.

To more directly test whether or not contaminating nerve terminals were the source of the high basal lipolysis, brown adipocytes were subjected to a wash of Krebs Ringer buffer that contained 100 mM potassium chloride, 10-fold higher than the normally used concentration. This has been shown to depolarize the nerve endings in BAT and thereby deplete adrenergic stores, which can then be washed away (Barde et al., 1975). Indeed, a high-potassium wash substantially reduced the high basal rate of lipolysis in isolated mouse brown adipocytes and thereby restored the responsiveness to isoproterenol compared with cells that were washed normally (Fig. A.D).

As a result of these findings, I subsequently modified the brown adipocyte isolation protocol to include additional washes of the adipocytes, which in itself substantially improved the responsiveness of the adipocytes to adrenergic stimuli even with low-potassium concentrations (Fig. A.C). Additionally, propranolol was then used as a diagnostic agent in all subsequent lipolysis experiments to test for high amounts of adrenergic contamination, and also as a quantification method to assess the true basal rate of lipolysis that could be subtracted out from stimulated conditions.

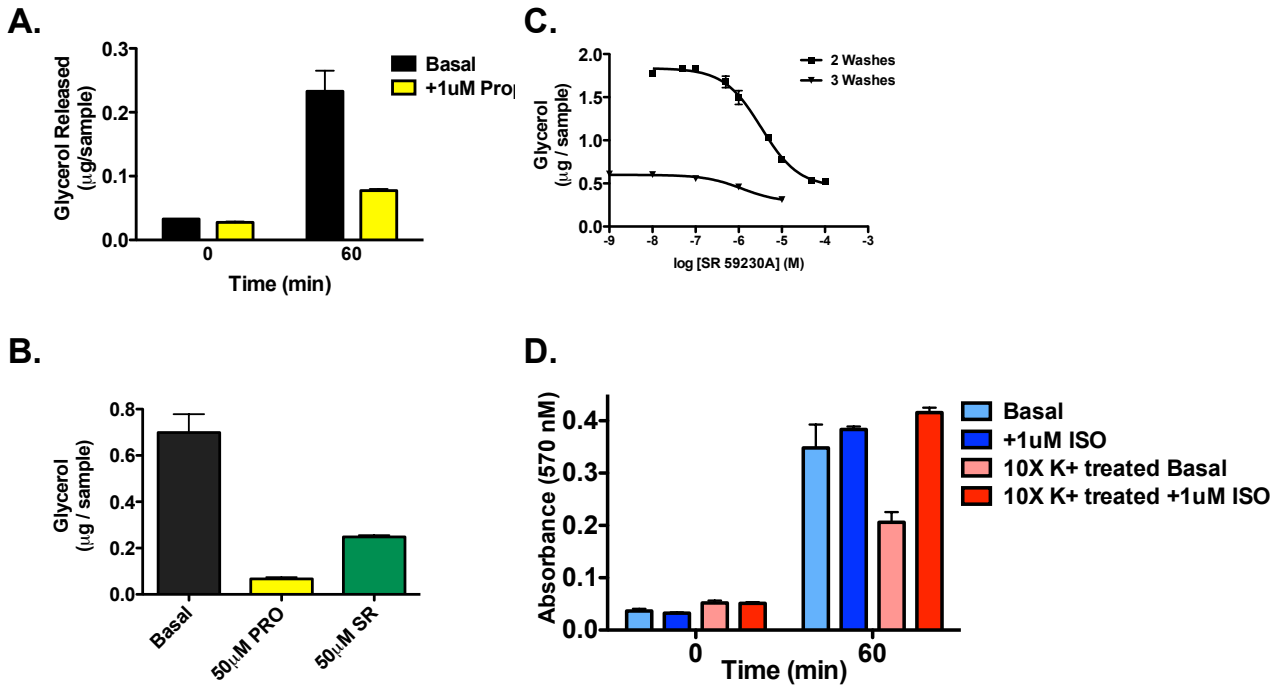

Figure A. Effects of adrenergic antagonists on basal lipolysis.
Freshly isolated brown adipocytes were incubated for 1 h in the presence or absence of [A] 1 µM propranolol (Prop), [B] 50 µM propranolol (PRO), a nonselective β-adrenergic receptor antagonist, 50 µM SR-59230A (SR), a selective β_3-adrenergic receptor antagonist, [C] increasing concentrations of SR-59230A in preparations that had received either two washes of Krebs Ringer buffer or three washes of Krebs Ringer buffer after collagenase digestion, or [D] 1 µM isoproterenol (ISO) after cells had received a normal washing with Krebs Ringer buffer containing 10 mM KCl or a Krebs Ringer buffer that contained 100 mM KCl (10X K+). Glycerol was measured and quantified as described in materials and methods, and data in [A-C] are presented as µg glycerol / sample, or by the absorbance of the free glycerol reagent in [D].

Appendix B:
PDE8A Knockout Brown Adipocytes Have Higher Maximal Lipolysis

Brown adipocytes were isolated from wild type (Taconic Farms, Inc., Hudson, NY) and PDE8A knockout mice by collagenase digestion in Krebs Ringer buffer according to the Materials and Methods section in Chapter 2 of this dissertation. The PDE8A KO mice were bred on a C57/Bl6 background from two PDE8A KO parents, and therefore were not littermates to the wild type mice used in these experiments. The brown adipocytes were incubated in 200 µL Krebs Ringer buffer with 4% fatty acid-free BSA at 37°C for 1 hour in the presence of increasing concentrations of isoproterenol or 50 µM propranolol to subtract out as background. The samples were frozen, thawed, and centrifuged at 14,000 rpm for 5 minutes. The samples were kept on ice, and 50 µL of the infranatant was pipetted into a 96-well plate in duplicate. Samples were diluted in the plate with 75 µL of the same Krebs Ringer solution with 4% fatty acid-free BSA. 125 µL of the Free Glycerol reagent (Sigma) made up at 2X was added to the wells, and incubated at room temperature for 20 min. The plate was then read at 570 nm, and glycerol released was expressed as µg per $1x10^6$ cells. The dose-response curves for wild type and PDE8A KO brown adipocytes indicated a 1.6 fold higher maximal level of lipolysis in PDE8A KO brown adipocytes than wild type brown adipocytes at 10 µM isoproterenol (V_{max}, *$p<0.05$) (Fig. B.A, B.B). However, the brown adipocytes from both genotypes did not differ in their response to isoproterenol potency (EC_{50}, n.s.) (Fig. B.B).

There are several possible explanations for an effect on V_{max} with little or no change in EC_{50}. The first, and probably most obvious, is that the PDE8A KO brown

adipocytes may have more β-adrenergic receptors expressed on the cell surface. This would provide more receptors and more lipolysis, however there would be no effect on agonist-receptor interaction. The second possibility is that there is more substrate available in the PDE8A KO condition. This would be somewhat unexpected, as one would anticipate the loss of a cAMP-selective PDE to result in a decrease in available triglyceride substrate if that PDE regulates lipolysis. A third possibility is that the PDE8A KO is affecting glycerol transport. It has been shown that cAMP-elevating agents can enhance aquaporin-7 expression in adipocytes (Kishida, JBC 2000). Aquaporin-7 acts as a channel for glycerol. It is conceivable that an increased amount of this channel, perhaps by chronic ablation of PDE8A, could result in an increased release of glycerol production with no overall effect on triglyceride breakdown or adrenergic agonist potency. Still, a final interpretation is that since these mice are not littermates, their histories are too different to compare the two genotypes.

Further experiments will need to be done to assess the true nature of this observation. First and foremost, it needs to be repeated using brown adipocytes from wild type and PDE8A KO littermates. If the effect is reproducible in these cells, then it is most certainly worth investigating the mechanism by which these effects occur, such as increased expression of adrenergic receptors or aquaporins.

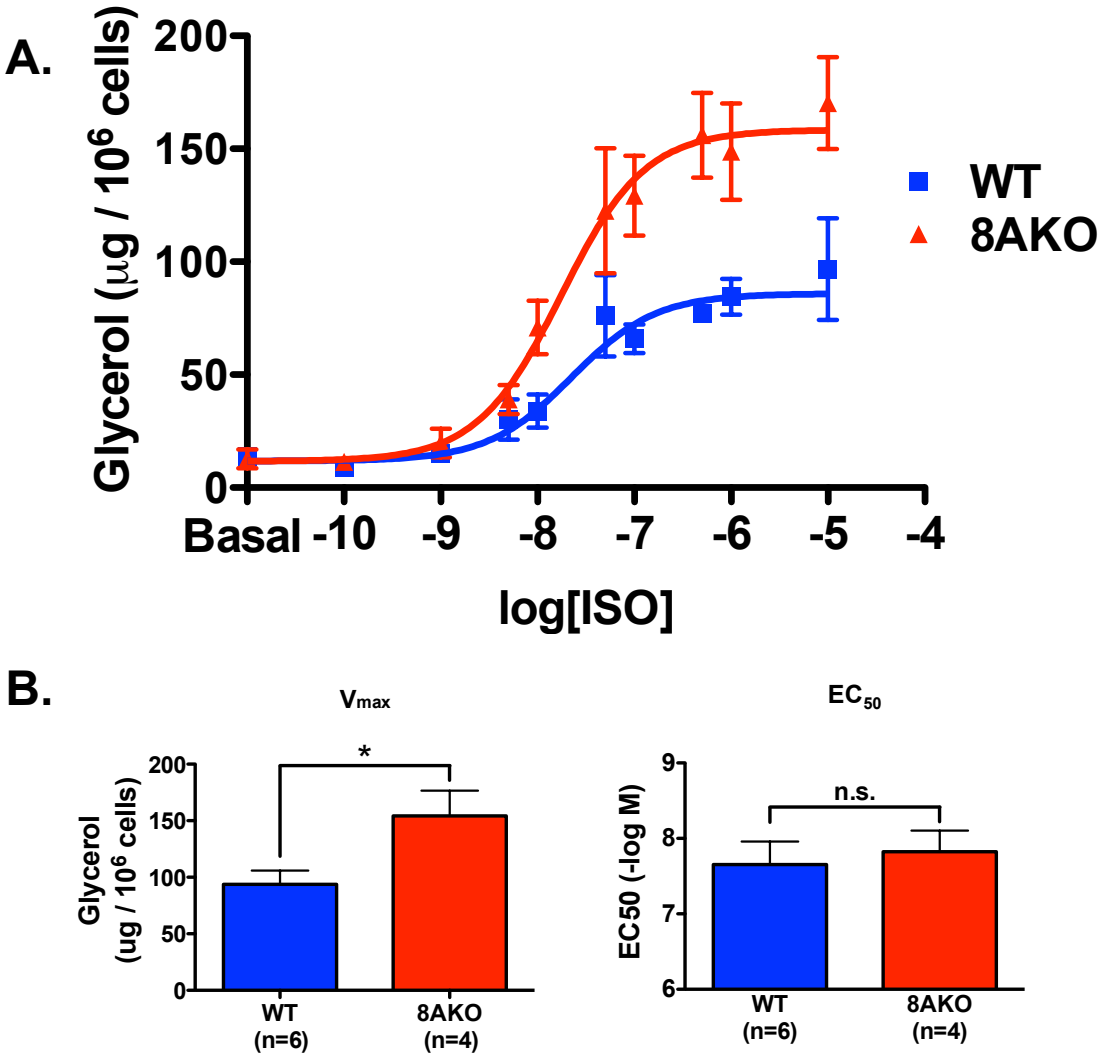

Figure B. PDE8A KO brown adipocytes have higher maximal lipolysis.
[A] Isolated mouse brown adipocytes from wild type (WT) and PDE8A knockout (8AKO) mice were incubated with increasing concentrations of isoproterenol. Data are presented as mean µg glycerol released per 10^6 cells (n=4-6). [B] The mean V_{max} and EC_{50} for each dose response curve was obtained using Prism software and plotted. V_{max} is presented as mean µg glycerol per 10^6 cells, and EC_{50} is plotted as the –log of the concentration of the molar concentration of isoproterenol, ± S.E.M (n=4-6). Statistical analyses were performed by Student's t-test: *, $p<0.05$; n.s., $p>0.05$ WT vs. 8AKO.

Appendix C:
Metabolic Characterization of PDE8A Knockout Mice

As described in the introduction of this dissertation, BAT mediates thermogenesis in response to a high fat diet that results in a slowed weight gain. Since PDE8A is highly expressed in brown adipose tissue, we hypothesized that the loss of PDE8A may impact weight gain in response to a high fat diet. We placed 6-week-old male wild type, PDE8A heterozygotes and PDE8A knockout mice on high fat diet (HFD) or a regular chow diet for 17 weeks and recorded body weight once per week. Animals fed the chow-fed diets appeared to gain the same amount of weight regardless of genotype, and mice on the HFD gained 20-40% more weight than their control-fed counterparts (Fig. C.1). However, despite PDE8A het and PDE8A KO mice gaining slightly less weight on average than the wild type controls while on the HFD, this difference was not statistically significant (Fig. C.1).

Additionally, we subjected both chow- and HFD-fed wild type and PDE8A knockout mice to metabolic phenotyping using the Seattle Mouse Metabolic Phenotyping Center. Transponders that recorded body temperature and locomotion were implanted into mice after transport to the facility, and mice were given approximately two weeks to recover from the surgery. Prior to calorimetry measurements, mice were scanned with magnetic resonance imaging (MRI) to assess the body fat and lean composition. Mice then were placed in metabolic cages for O_2 consumption, water and food intake, and locomotor activity measurements during a 12 h dark-12 h light-12 h dark cycle. In general, the mice exhibited virtually no significant differences between genotypes within a given diet type with the exception of body fat %. PDE8AKO mice fed a chow diet had 4.2 g

less body fat mass than their wild type littermates (*$p<0.05$), whereas lean mass remained the same and body weights were not different (Fig. C2A). Part of this may be explained by the fact that 8AKO mice seemed to be more active, though this difference was not statistically significant, and no other metabolic parameters were statistically different between the two genotypes (Table C.1). Interestingly, wild type mice consumed approximately 1.7 g less water and food on average than 8AKO mice, though this number also was not statistically significant (Table C.1). Wild type and PDE8A mice on a HFD also did not demonstrate any statistically different metabolic parameters, though the PDE8A knockout mice seemed to have less fat mass than their wild type counterparts and weigh slightly less as well (Table C.2, Fig. C2B, C2C).

Altogether, the basal metabolic characteristics of PDE8A knockout mice are not dissimilar from their wild type littermates. The minor differences between the two genotypes, such as fat body %, could simply be due to the small number of animals used in these experiments. Therefore, additional experiments will be needed to determine whether or not these results are truly indicative of a change due to the loss of PDE8A.

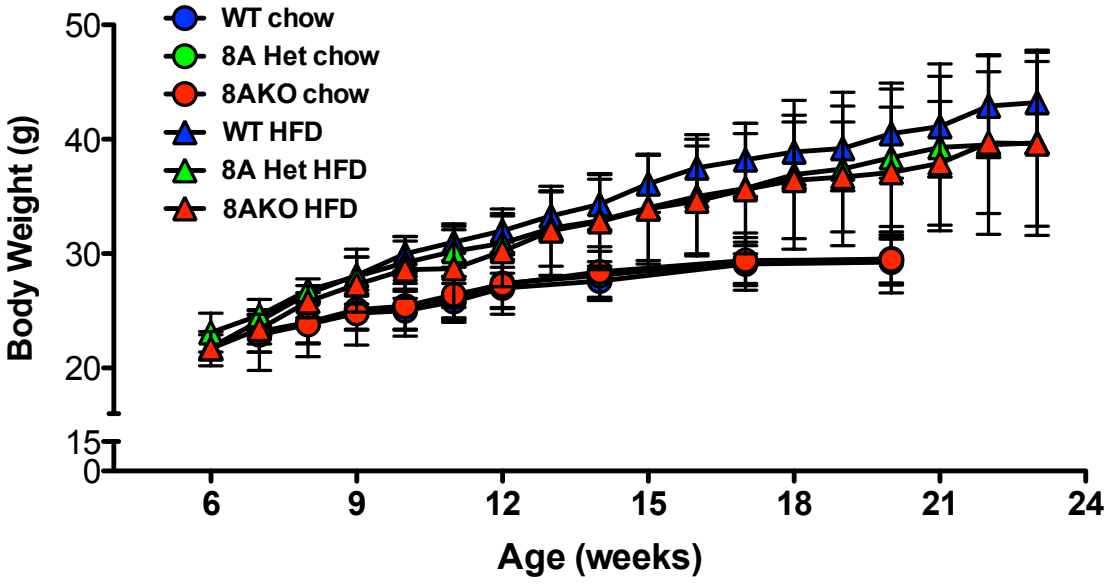

Figure C.1. WT and PDE8A KO mice weight gain on chow and high fat diet. Wild type (WT) and PDE8A KO male mice were monitored for 17 weeks while on a chow or high fat diet and their weights were recorded (n=7-17). Data are presented as mean weight in g ± S.D.

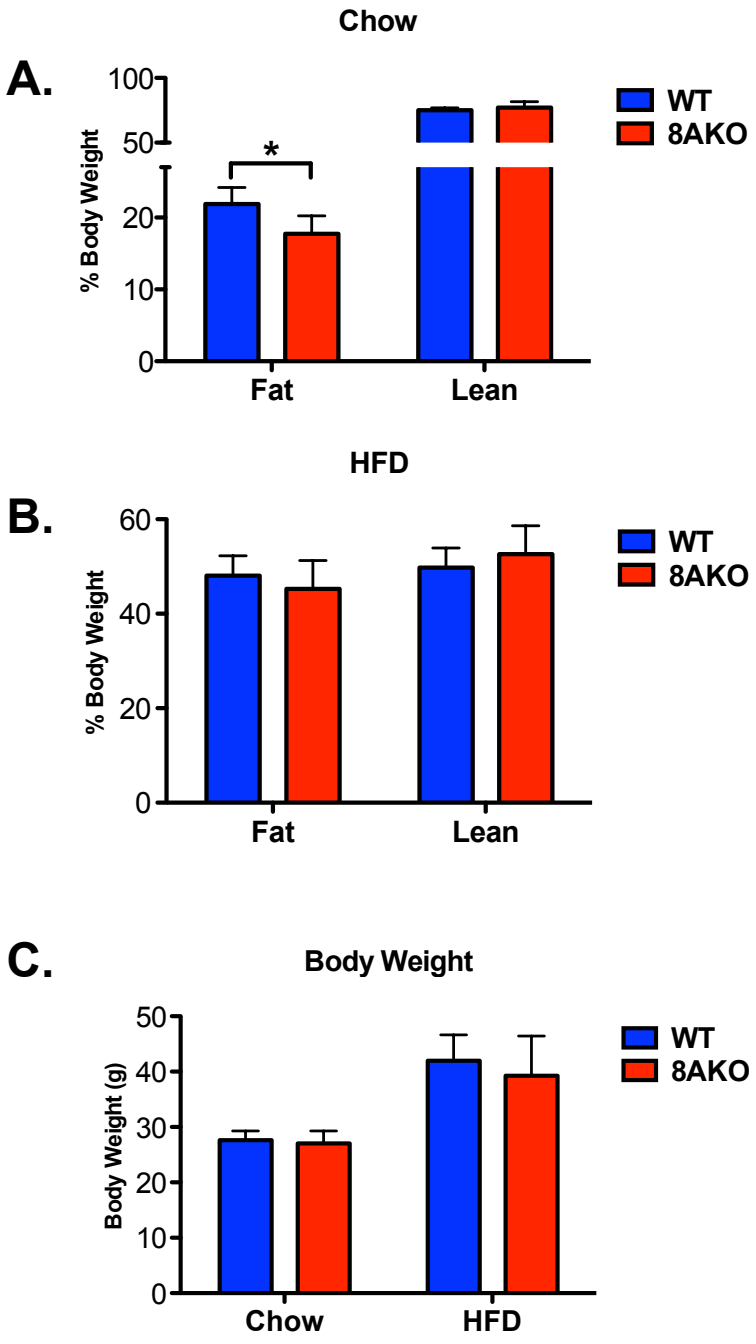

Figure C.2. Fat and lean mass comparison between WT and PDE8A KO mice fed a chow or high fat diet.
Fat and lean masses presented as mean % of body weight ± S.D as measured by MRI in wild type (WT) and PDE8A knockout (8AKO) mice fed a [A] chow (n=4) or [B] high fat diet (HFD) (n=7), and statistical analysis was performed by Student's t-test (*$p<0.05$). [C] Body weights of WT and 8AKO mice presented as mean g ± S.D.

SEX: MALE GENOTYPE: PDE8A (C57BL6) DIET: CHOW DOB: 6 month old												
ID		89	92	93	96		46	48	94	95		
GENOTYPE:		WT	WT	WT	WT	WT MEAN	KO	KO	KO	KO	KO MEAN	T-TEST
BODY COMPOSITION (measured before calorimetry)												
BODY WEIGHT (g)		26.7	26.8	30.1	26.9	**27.6**	25.3	27.8	29.9	25.2	**27.1**	0.689
FAT (g)		5.4	6.3	7.3	5.3	**6.1**	3.6	4.8	5.8	5.0	**4.8**	0.101
LEAN (g)		20.3	19.9	22.1	20.8	**20.8**	20.8	21.4	21.3	19.5	**20.8**	0.994
% FAT (%)		20.2	23.4	24.3	19.7	**21.9**	14.4	17.3	19.5	19.8	**17.8**	***0.049**
% LEAN (%)		75.8	74.1	73.4	77.4	**75.2**	82.5	77.0	71.3	77.4	**77.1**	0.489
VO2 (ml/Kg lean/hr)	D1	6740	6974	6631	6692	**6759**	6705	6907	6772	6749	**6783**	0.795
	L	5412	5661	5511	5422	**5502**	5501	5534	5630	5389	**5513**	0.883
	D2	6408	6758	6610	6397	**6543**	6804	6616	6746	6637	**6701**	0.173
ACC_O2 (l)	D1	1.64	1.66	1.75	1.67	**1.68**	1.68	1.77	1.73	1.58	**1.69**	0.870
	L	1.32	1.35	1.47	1.35	**1.37**	1.37	1.42	1.44	1.26	**1.37**	0.984
	D2	1.56	1.61	1.75	1.59	**1.63**	1.70	1.70	1.72	1.55	**1.67**	0.527
HEAT (Kcal/hr)	D1	0.69	0.69	0.74	0.71	**0.71**	0.71	0.75	0.74	0.67	**0.72**	0.720
	L	0.54	0.55	0.60	0.56	**0.56**	0.56	0.58	0.60	0.53	**0.57**	0.793
	D2	0.66	0.67	0.73	0.68	**0.69**	0.71	0.72	0.73	0.66	**0.70**	0.455
RQ (unitless)	D1	1.019	0.959	1.005	1.036	**1.005**	1.040	1.040	1.043	1.031	**1.039**	0.134
	L	0.926	0.842	0.890	0.929	**0.897**	0.889	0.898	0.946	0.982	**0.928**	0.329
	D2	1.013	0.972	0.981	1.045	**1.003**	0.998	1.020	1.025	1.028	**1.018**	0.452
TEMPERATURE (°C)	D1	36.4	36.7	36.5	36.4	**36.5**	36.74	36.27	36.71	38.41	**37.0**	0.352
	L	35.4	35.7	35.7	35.5	**35.6**	35.56	35.28	35.74	37.13	**35.9**	0.443
	D2	36.4	36.7	36.5	36.5	**36.5**	36.91	36.22	36.68	38.44	**37.1**	0.349
ACTIVITY (unitless)	D1	23142	19792	18866	23947	**21437**	34705	22232	34541	21697	**28294**	0.157
	L	5173	12440	3434	5349	**6599**	9923	13753	13238	6084	**10750**	0.171
	D2	15258	25930	17026	13590	**17951**	31199	22348	28898	11545	**23498**	0.334
FOOD (g)	D1	2.60	1.83	2.53	3.01	**2.49**	3.33	2.96	2.88	3.06	**3.06**	0.100
	L	0.87	0.69	1.12	1.05	**0.93**	0.75	0.74	1.23	0.99	**0.93**	0.975
	D2	2.67	2.70	2.48	3.07	**2.73**	2.74	2.88	3.53	2.87	**3.01**	0.256
WATER (ml)	D1	2.14	1.68	1.86	2.28	**1.99**	3.30	2.40	2.22	2.22	**2.54**	0.127
	L	0.32	0.40	0.48	0.26	**0.37**	0.48	0.34	0.52	0.40	**0.44**	0.307
	D2	1.78	1.96	1.60	2.18	**1.88**	2.64	2.08	1.96	1.84	**2.13**	0.296

Table **C.1. Metabolic characteristics of WT and PDE8A KO mice fed a chow diet.**
VO2 refers to the volume of oxygen consumed. D1 is dark period 1, L the light period, and D2 is the second dark period. RQ refers to Respiratory Quotient, which is a metabolic parameter that relates CO_2 elimination to O_2 consumption (n=4).

SEX: MALE GENOTYPE: PDE8A (C57BL6) DIET: HIGH-FAT DOB: 6 month old																		
ID		414	424	434	448	451	415	418		412	413	423	435	453	454	416		
GENOTYPE:		WT	WT	WT	WT	WT	WT	WT	WT MEAN	KO	KO	KO	KO	KO	KO	KO	KO MEAN	T-TEST
BODY COMPOSITION (measured before calorimetry)																		
BODY WEIGHT (g)		38.7	33.5	44.5	44.6	43.0	47.9	41.5	**41.9**	39.9	31.9	32.5	39.0	49.2	48.3	33.9	**39.2**	0.421
FAT (g)		17.0	13.7	22.9	21.6	21.2	24.7	21.2	**20.3**	17.9	12.2	12.9	18.9	26.3	24.8	13.7	**18.1**	0.409
LEAN (g)		20.9	19.2	20.7	21.8	20.6	22.4	19.6	**20.7**	21.4	19.1	18.8	19.1	22.1	22.3	19.3	**20.3**	0.566
% FAT (%)		43.8	40.8	51.5	48.4	49.3	51.6	51.1	**48.1**	45.0	38.3	39.6	48.6	53.4	51.4	40.4	**45.2**	0.332
% LEAN (%)		53.9	57.3	46.4	48.9	47.8	46.8	47.2	**49.8**	53.5	60.0	57.7	49.0	45.0	46.1	57.1	**52.6**	0.321
VO2 (ml/Kg lean/hr)	D1	6832	7774	7048	7841	9207	6618	7848	**7374**	7947	7931	7432	7899	7924	8274	6880	**7901**	0.128
	L	6317	6724	6229	6873	7250	6201	6600	**6599**	6890	6567	6496	7251	7065	7520	6418	**6887**	0.094
	D2	6792	7511	7051	7741	8003	6692	7498	**7273**	7625	7337	7672	8115	7941	8516	6756	**7868**	0.071
ACC_O2 (l)	D1	1.71	1.78	1.74	2.04	2.26	1.77	1.84	**1.82**	2.04	1.81	1.67	1.81	2.09	2.21	1.59	**1.94**	0.330
	L	1.59	1.55	1.56	1.80	1.79	1.68	1.56	**1.63**	1.77	1.51	1.48	1.67	1.88	2.01	1.49	**1.72**	0.389
	D2	1.70	1.73	1.75	2.02	1.97	1.79	1.75	**1.80**	1.96	1.68	1.72	1.86	2.10	2.27	1.56	**1.93**	0.290
HEAT (Kcal/hr)	D1	0.68	0.72	0.69	0.81	0.89	0.70	0.72	**0.72**	0.81	0.72	0.66	0.72	0.83	0.87	0.63	**0.77**	0.376
	L	0.63	0.66	0.61	0.71	0.70	0.65	0.60	**0.65**	0.70	0.59	0.58	0.66	0.74	0.79	0.58	**0.68**	0.563
	D2	0.68	0.74	0.69	0.81	0.78	0.71	0.69	**0.73**	0.78	0.67	0.68	0.74	0.83	0.90	0.61	**0.77**	0.436
RQ (unitless)	D1	0.775	0.752	0.733	0.761	0.723	0.714	0.684	**0.755**	0.773	0.739	0.719	0.757	0.744	0.754	0.733	**0.748**	0.521
	L	0.763	0.736	0.727	0.767	0.723	0.727	0.687	**0.748**	0.761	0.743	0.736	0.769	0.750	0.733	0.726	**0.748**	0.976
	D2	0.777	0.742	0.737	0.779	0.731	0.733	0.703	**0.759**	0.777	0.760	0.739	0.752	0.748	0.747	0.715	**0.754**	0.707
TEMPERATURE (°C)	D1	ND*	36.6	36.4	36.5	37.1	35.8	37.6	**36.5**	36.2	36.5	36.8	35.0	36.6	36.4	36.0	**36.2**	0.398
	L	ND	35.6	35.7	35.7	35.9	35.4	37.4	**35.7**	35.4	35.8	35.9	35.0	35.5	35.8	35.3	**35.6**	0.504
	D2	ND	36.5	36.3	36.5	36.2	35.8	37.8	**36.4**	36.4	36.6	36.7	35.4	36.1	36.6	35.5	**36.3**	0.547
ACTIVITY (unitless)	D1	15645	14806	6003	20576	9260	4943	3916	**14258**	16519	15998	30534	9818	25217	12840	8343	**18488**	0.367
	L	4997	2923	1315	7704	2356	1566	2124	**4235**	7043	2438	8074	2720	3531	6505	2070	**5052**	0.648
	D2	12497	12238	4976	16458	6714	5303	4398	**11542**	14248	9617	19386	11405	12050	16032	4635	**13790**	0.457
WATER (ml)	D1	1.00	1.06	0.16	0.4	0.2	0.18	0.02	**0.66**	1.58	3.06	0.36	1.52	0.54	0.28	0.04	**1.22**	0.283
	L	0.52	0.18	0.58	0.48	0.26	0.42	0.44	**0.44**	0.42	0.88	0.72	0.66	0.54	0.28	0.34	**0.58**	0.288
	D2	1.50	0.98	1.28	1.12	0.26	0.16	0.10	**1.22**	1.38	1.38	1.14	1.06	1.36	1.68	0.02	**1.33**	0.455

Table **C.2. Metabolic characteristics of WT and PDE8A KO mice fed a high fat diet.**
VO2 refers to the volume of oxygen consumed. D1 is dark period 1, L the light period, and D2 is the second dark period. RQ refers to Respiratory Quotient, which is a metabolic parameter that relates CO_2 elimination to O_2 consumption (n=7).

Appendix D:
PF-04957325 Stimulates Hormone Sensitive Lipase Phosphorylation in BAT

Since the BAT PDE8A knockout mice took up more glucose in response to PDE3 and PDE4 inhibitors, I hypothesized that the PDE8 inhibitor PF-04957325 (PF) would mimic the same effect when injected into wild type mice along with cilostamide and rolipram, a PDE3 and PDE4 inhibitor, respectively. At 0.3 mg/kg, PF did not further potentiate glucose uptake when combined with 3 mg/kg cilostamide and 3 mg/kg rolipram beyond what these drugs stimulate when injected together in wild type mice (Fig D.1). To test drug availability, I injected 0.3 mg/kg PF compound into mice that were fasted overnight and warmed to 37°C for at least 30 minutes prior to injection. 10 mg/kg isoproterenol was injected as a positive control. After 10 minutes, mice were sacrificed via cervical dislocation, and their BAT quickly dissected out and flash-frozen between two aluminum blocks that had been sitting in liquid nitrogen. The tissue was homogenized as described in Chapter 2 Materials and Methods, and protein was analyzed via Western blot. The PF compound stimulated the phosphorylation of hormone sensitive lipase (HSL) at its putative PKA site, serine-660 (Fig. D.2). Given the lack of effect of PDE8A inhibition on lipolysis in primary brown adipocytes (Fig. 2.11), this result was surprising. However, PF-04957325 can inhibit PDE4 at a dose that exceeds 1 μM. Since there is no known report for the pharmacokinetic properties of this compound, it is impossible to accurately estimate the plasma concentration of a 0.3 mg/kg dose 10 minutes after injection. Therefore, this drug could be acting nonselectively at this dose, or could be acting upstream of BAT. Still, even if it were inhibiting PDE4 at this dose, this would suggest the dose is certainly high enough to inhibit PDE8A. Since a PDE4

inhibitor is also injected, this fact is therefore moot. Regardless of mechanism or selectivity, this is the first potential biomarker discovered for the injection of PF-04957325 into a mouse.

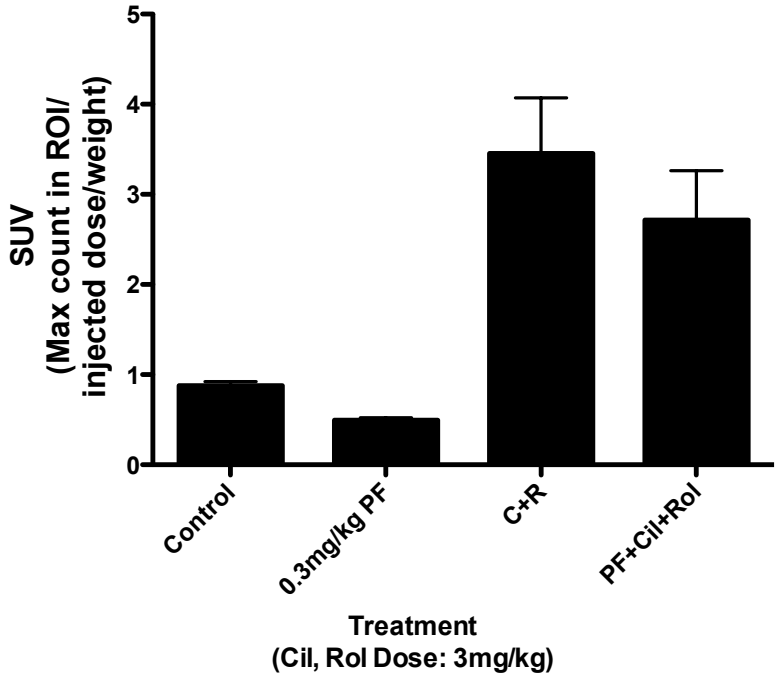

Figure D.1. PF-04957325 does not potentiate glucose uptake stimulated by cilostamide and rolipram.
Wild type mice were injected with vehicle control (n=3), 3 mg/kg cilostamide and 3 mg/kg rolipram (n=4), 0.3 mg/kg PF-04957325 (n=2) or both (n=3), and imaged by PET scanning as described in Chapter 2 Materials and Methods.

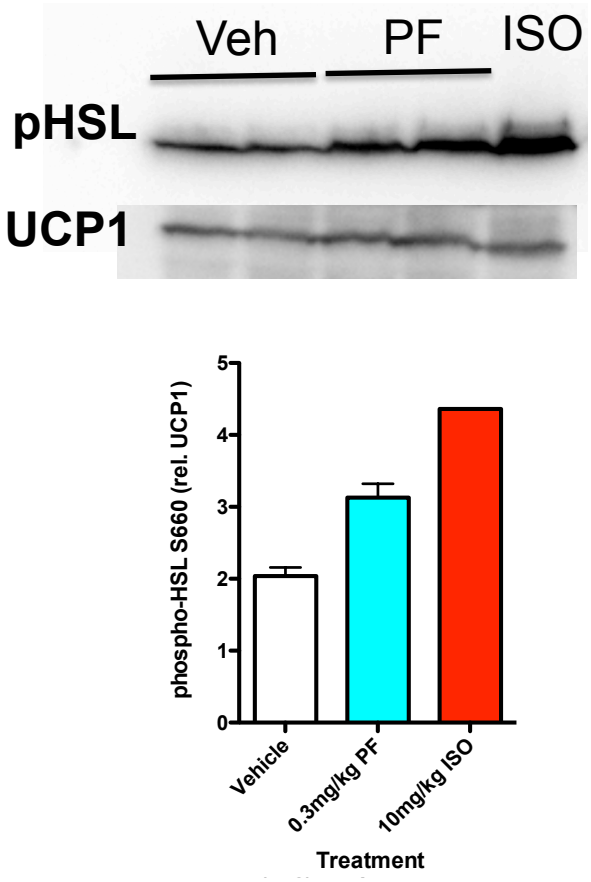

Figure D.2. Hormone sensitive lipase phosphorylation was stimulated by PF-04957325.
Wild type mice were fasted overnight and then warmed with a heating pad 30 min prior to injection of 0.3 mg/kg PF-04957325 (n=2), 10 mg/kg isoproterenol (n=1) or vehicle (n=2). 10 µg BAT protein extract was separated by 10% SDS-PAGE and analyzed by Western blot as described in Chapter 2 Materials and Methods. Antibodies used were HSL p-S660 (Cell Signaling) [1:1000 (vol/vol)], and second with goat anti-rabbit conjugated to horseradish peroxidase [1:5000 (vol/vol)]. Band intensity was quantified using ImageJ. Error bars correspond to the range of duplicate animals in this particular experiment.

Bibliography

Acin-Perez R, Russwurm M, Gunnewig K, Gertz M, Zoidl G, Ramos L, Buck J, Levin LR, Rassow J, Manfredi G and Steegborn C (2011) A phosphodiesterase 2A isoform localized to mitochondria regulates respiration. *J Biol Chem* **286**(35): 30423-30432.

Acin-Perez R, Salazar E, Brosel S, Yang H, Schon EA and Manfredi G (2009a) Modulation of mitochondrial protein phosphorylation by soluble adenylyl cyclase ameliorates cytochrome oxidase defects. *EMBO Mol Med* **1**(8-9): 392-406.

Acin-Perez R, Salazar E, Kamenetsky M, Buck J, Levin LR and Manfredi G (2009b) Cyclic AMP produced inside mitochondria regulates oxidative phosphorylation. *Cell metabolism* **9**(3): 265-276.

Arch JR, Ainsworth AT, Cawthorne MA, Piercy V, Sennitt MV, Thody VE, Wilson C and Wilson S (1984) Atypical beta-adrenoceptor on brown adipocytes as target for anti-obesity drugs. *Nature* **309**(5964): 163-165.

Asirvatham AL, Galligan SG, Schillace RV, Davey MP, Vasta V, Beavo JA and Carr DW (2004) A-kinase anchoring proteins interact with phosphodiesterases in T lymphocyte cell lines. *J Immunol* **173**(8): 4806-4814.

Atgie C, D'Allaire F and Bukowiecki LJ (1997) Role of beta1- and beta3-adrenoceptors in the regulation of lipolysis and thermogenesis in rat brown adipocytes. *Am J Physiol* **273**(4 Pt 1): C1136-1142.

Bachman ES, Dhillon H, Zhang CY, Cinti S, Bianco AC, Kobilka BK and Lowell BB (2002) betaAR signaling required for diet-induced thermogenesis and obesity resistance. *Science* **297**(5582): 843-845.

Baker JL, Olsen LW and Sorensen TI (2007) Childhood body-mass index and the risk of coronary heart disease in adulthood. *N Engl J Med* **357**(23): 2329-2337.

Banner KH and Press NJ (2009) Dual PDE3/4 inhibitors as therapeutic agents for chronic obstructive pulmonary disease. *Br J Pharmacol* **157**(6): 892-906.

Barbe P, Millet L, Galitzky J, Lafontan M and Berlan M (1996) In situ assessment of the role of the beta 1-, beta 2- and beta 3-adrenoceptors in the control of lipolysis and nutritive blood flow in human subcutaneous adipose tissue. *Br J Pharmacol* **117**(5): 907-913.

Barde YA, Chinet A and Girardier L (1975) Potassium-induced increase in oxygen consumption of brown adipose tissue from the rat. *J Physiol* **252**(2): 523-536.

Barnes K, Ingram JC, Porras OH, Barros LF, Hudson ER, Fryer LG, Foufelle F, Carling D, Hardie DG and Baldwin SA (2002) Activation of GLUT1 by metabolic and osmotic stress: potential involvement of AMP-activated protein kinase (AMPK). *J Cell Sci* **115**(Pt 11): 2433-2442.

Bartelt A, Bruns OT, Reimer R, Hohenberg H, Ittrich H, Peldschus K, Kaul MG, Tromsdorf UI, Weller H, Waurisch C, Eychmuller A, Gordts PL, Rinninger F, Bruegelmann K, Freund B, Nielsen P, Merkel M and Heeren J (2011) Brown adipose tissue activity controls triglyceride clearance. *Nature medicine* **17**(2): 200-205.

Beavo J, Francis SH and Houslay MD (2007) *Cyclic nucleotide phosphodiesterases in health and disease*. CRC Press/Taylor & Francis, Boca Raton.

Beavo JA, Hansen RS, Harrison SA, Hurwitz RL, Martins TJ and Mumby MC (1982) Identification and properties of cyclic nucleotide phosphodiesterases. *Mol Cell Endocrinol* **28**(3): 387-410.

Beavo JA, Hardman JG and Sutherland EW (1970a) Hydrolysis of cyclic guanosine and adenosine 3',5'-monophosphates by rat and bovine tissues. *J Biol Chem* **245**(21): 5649-5655.

Beavo JA, Rogers NL, Crofford OB, Hardman JG, Sutherland EW and Newman EV (1970b) Effects of xanthine derivatives on lipolysis and on adenosine 3',5'-monophosphate phosphodiesterase activity. *Molecular pharmacology* **6**(6): 597-603.

Belenguer P and Pellegrini L (2013) The dynamin GTPase OPA1: more than mitochondria? *Biochim Biophys Acta* **1833**(1): 176-183.

Bender AT and Beavo JA (2006) Cyclic nucleotide phosphodiesterases: molecular regulation to clinical use. *Pharmacol Rev* **58**(3): 488-520.

Bertin R and Portet R (1975) 3':5'-Cyclic-AMP phosphodiesterase activities in white and brown adipose tissues of cold-acclimated rats. *Can J Biochem* **53**(12): 1301-1308.

Beviz A, Lundholm L and Mohme-Lundholm E (1968) Cyclic AMP as a mediator of hormonal metabolic effects in brown adipose tissue. *Br J Pharmacol* **34**(1): 198P-199P.

Bickel PE, Tansey JT and Welte MA (2009) PAT proteins, an ancient family of lipid droplet proteins that regulate cellular lipid stores. *Biochim Biophys Acta* **1791**(6): 419-440.

Bostrom P, Wu J, Jedrychowski MP, Korde A, Ye L, Lo JC, Rasbach KA, Bostrom EA, Choi JH, Long JZ, Kajimura S, Zingaretti MC, Vind BF, Tu H, Cinti S, Hojlund K, Gygi SP and Spiegelman BM (2012) A PGC1-alpha-dependent myokine that drives brown-fat-like development of white fat and thermogenesis. *Nature* **481**(7382): 463-468.

Brasaemle DL, Levin DM, Adler-Wailes DC and Londos C (2000) The lipolytic stimulation of 3T3-L1 adipocytes promotes the translocation of hormone-sensitive lipase to the surfaces of lipid storage droplets. *Biochim Biophys Acta* **1483**(2): 251-262.

Bronnikov G, Bengtsson T, Kramarova L, Golozoubova V, Cannon B and Nedergaard J (1999a) beta1 to beta3 switch in control of cyclic adenosine monophosphate during brown adipocyte development explains distinct beta-adrenoceptor subtype mediation of proliferation and differentiation. *Endocrinology* **140**(9): 4185-4197.

Bronnikov G, Houstek J and Nedergaard J (1992) Beta-adrenergic, cAMP-mediated stimulation of proliferation of brown fat cells in primary culture. Mediation via beta 1 but not via beta 3 adrenoceptors. *J Biol Chem* **267**(3): 2006-2013.

Bronnikov GE, Zhang SJ, Cannon B and Nedergaard J (1999b) A dual component analysis explains the distinctive kinetics of cAMP accumulation in brown adipocytes. *J Biol Chem* **274**(53): 37770-37780.

Brooker G, Thomas LJ, Jr. and Appleman MM (1968) The assay of adenosine 3',5'-cyclic monophosphate and guanosine 3',5'-cyclic monophosphate in biological materials by enzymatic radioisotopic displacement. *Biochemistry* **7**(12): 4177-4181.

Brooks SL, Rothwell NJ, Stock MJ, Goodbody AE and Trayhurn P (1980) Increased proton conductance pathway in brown adipose tissue mitochondria of rats exhibiting diet-induced thermogenesis. *Nature* **286**(5770): 274-276.

Brown KM, Day JP, Huston E, Zimmermann B, Hampel K, Christian F, Romano D, Terhzaz S, Lee LC, Willis MJ, Morton DB, Beavo JA, Shimizu-Albergine M, Davies SA, Kolch W, Houslay MD and Baillie GS (2013) Phosphodiesterase-8A binds to and regulates Raf-1 kinase. *Proc Natl Acad Sci U S A* **110**(16): E1533-1542.

Brownell KD (2010) The humbling experience of treating obesity: Should we persist or desist? *Behav Res Ther* **48**(8): 717-719.

Bukowiecki L, Follea N, Vallieres J and Leblanc J (1978) Beta-Adrenergic receptors in brown-adipose tissue. Characterization and alterations during acclimation of rats to cold. *European journal of biochemistry / FEBS* **92**(1): 189-196.

Calle EE, Rodriguez C, Walker-Thurmond K and Thun MJ (2003) Overweight, obesity, and mortality from cancer in a prospectively studied cohort of U.S. adults. *N Engl J Med* **348**(17): 1625-1638.

Cannon B and Nedergaard J (2001) Respiratory and thermogenic capacities of cells and mitochondria from brown and white adipose tissue. *Methods Mol Biol* **155**: 295-303.

Cannon B and Nedergaard J (2004) Brown adipose tissue: function and physiological significance. *Physiol Rev* **84**(1): 277-359.

Cannon B and Nedergaard J (2009) Thermogenesis challenges the adipostat hypothesis for body-weight control. *Proc Nutr Soc* **68**(4): 401-407.

Cao W, Daniel KW, Robidoux J, Puigserver P, Medvedev AV, Bai X, Floering LM, Spiegelman BM and Collins S (2004) p38 mitogen-activated protein kinase is the central regulator of cyclic AMP-dependent transcription of the brown fat uncoupling protein 1 gene. *Mol Cell Biol* **24**(7): 3057-3067.

Carlucci A, Lignitto L and Feliciello A (2008) Control of mitochondria dynamics and oxidative metabolism by cAMP, AKAPs and the proteasome. *Trends Cell Biol* **18**(12): 604-613.

Chandra D, Choy G, Deng X, Bhatia B, Daniel P and Tang DG (2004) Association of active caspase 8 with the mitochondrial membrane during apoptosis: potential roles in cleaving BAP31 and caspase 3 and mediating mitochondrion-endoplasmic reticulum cross talk in etoposide-induced cell death. *Mol Cell Biol* **24**(15): 6592-6607.

Chang CR and Blackstone C (2007) Cyclic AMP-dependent protein kinase phosphorylation of Drp1 regulates its GTPase activity and mitochondrial morphology. *J Biol Chem* **282**(30): 21583-21587.

Chanoit G, Zhou J, Lee S, McIntosh R, Shen X, Zvara DA and Xu Z (2011) Inhibition of phosphodiesterases leads to prevention of the mitochondrial permeability transition pore opening and reperfusion injury in cardiac H9c2 cells. *Cardiovasc Drugs Ther* **25**(4): 299-306.

Chaudhry A, MacKenzie RG, Georgic LM and Granneman JG (1994) Differential interaction of beta 1- and beta 3-adrenergic receptors with Gi in rat adipocytes. *Cell Signal* **6**(4): 457-465.

Chernogubova E, Cannon B and Bengtsson T (2004) Norepinephrine increases glucose transport in brown adipocytes via beta3-adrenoceptors through a cAMP, PKA, and PI3-kinase-dependent pathway stimulating conventional and novel PKCs. *Endocrinology* **145**(1): 269-280.

Choi YH, Park S, Hockman S, Zmuda-Trzebiatowska E, Svennelid F, Haluzik M, Gavrilova O, Ahmad F, Pepin L, Napolitano M, Taira M, Sundler F, Stenson Holst L, Degerman E and Manganiello VC (2006) Alterations in regulation of energy homeostasis in cyclic nucleotide phosphodiesterase 3B-null mice. *The Journal of clinical investigation* **116**(12): 3240-3251.

Cohade C, Mourtzikos KA and Wahl RL (2003) "USA-Fat": prevalence is related to ambient outdoor temperature-evaluation with 18F-FDG PET/CT. *Journal of nuclear medicine : official publication, Society of Nuclear Medicine* **44**(8): 1267-1270.

Commins SP, Watson PM, Levin N, Beiler RJ and Gettys TW (2000) Central leptin regulates the UCP1 and ob genes in brown and white adipose tissue via different beta-adrenoceptor subtypes. *J Biol Chem* **275**(42): 33059-33067.

Connolly E, Nanberg E and Nedergaard J (1986) Norepinephrine-induced Na+ influx in brown adipocytes is cyclic AMP-mediated. *J Biol Chem* **261**(31): 14377-14385.

Cooney GJ, Caterson ID and Newsholme EA (1985) The effect of insulin and noradrenaline on the uptake of 2-[1-14C]deoxyglucose in vivo by brown adipose tissue and other glucose-utilising tissues of the mouse. *FEBS Lett* **188**(2): 257-261.

Coudray C, Charon C, Komas N, Mory G, Diot-Dupuy F, Manganiello V, Ferre P and Bazin R (1999) Evidence for the presence of several phosphodiesterase isoforms in brown adipose tissue of Zucker rats: modulation of PDE2 by the fa gene expression. *FEBS Lett* **456**(1): 207-210.

Cribbs JT and Strack S (2007) Reversible phosphorylation of Drp1 by cyclic AMP-dependent protein kinase and calcineurin regulates mitochondrial fission and cell death. *EMBO Rep* **8**(10): 939-944.

Cypess AM, Lehman S, Williams G, Tal I, Rodman D, Goldfine AB, Kuo FC, Palmer EL, Tseng YH, Doria A, Kolodny GM and Kahn CR (2009) Identification and importance of brown adipose tissue in adult humans. *N Engl J Med* **360**(15): 1509-1517.

D'Allaire F, Atgie C, Mauriege P, Simard PM and Bukowiecki LJ (1995) Characterization of beta 1- and beta 3-adrenoceptors in intact brown adipocytes of the rat. *Br J Pharmacol* **114**(2): 275-282.

Dallner OS, Chernogubova E, Brolinson KA and Bengtsson T (2006) Beta3-adrenergic receptors stimulate glucose uptake in brown adipocytes by two mechanisms independently of glucose transporter 4 translocation. *Endocrinology* **147**(12): 5730-5739.

Dawkins MJ and Hull D (1964) Brown Adipose Tissue and the Response of New-Born Rabbits to Cold. *J Physiol* **172**: 216-238.

De Arcangelis V, Liu R, Soto D and Xiang Y (2009) Differential association of phosphodiesterase 4D isoforms with beta2-adrenoceptor in cardiac myocytes. *J Biol Chem* **284**(49): 33824-33832.

Degerman E, Smith CJ, Tornqvist H, Vasta V, Belfrage P and Manganiello VC (1990) Evidence that insulin and isoprenaline activate the cGMP-inhibited low-Km cAMP phosphodiesterase in rat fat cells by phosphorylation. *Proc Natl Acad Sci U S A* **87**(2): 533-537.

Deng C, Paoloni-Giacobino A, Kuehne F, Boss O, Revelli JP, Moinat M, Cawthorne MA, Muzzin P and Giacobino JP (1996) Respective degree of expression of beta 1-, beta 2- and beta 3-adrenoceptors in human brown and white adipose tissues. *Br J Pharmacol* **118**(4): 929-934.

Depocas F and Behrens WA (1978) Levels of noradrenaline in plasma during thermogenesis induced by cold-exposure or by noradrenaline infusion in warm- and in cold-acclimated rats. *Experientia Suppl* **32**: 135-146.

Dolgacheva LP, Abzhalelov BB, Zhang SJ, Zinchenko VP and Bronnikov GE (2003) Norepinephrine induces slow calcium signalling in murine brown preadipocytes through the beta-adrenoceptor/cAMP/protein kinase A pathway. *Cell Signal* **15**(2): 209-216.

Ducharme NA and Bickel PE (2008) Lipid droplets in lipogenesis and lipolysis. *Endocrinology* **149**(3): 942-949.

Dulloo AG, Seydoux J and Girardier L (1991) Peripheral mechanisms of thermogenesis induced by ephedrine and caffeine in brown adipose tissue. *International journal of obesity* **15**(5): 317-326.

Dulloo AG, Seydoux J and Girardier L (1992) Potentiation of the thermogenic antiobesity effects of ephedrine by dietary methylxanthines: adenosine antagonism or phosphodiesterase inhibition? *Metabolism* **41**(11): 1233-1241.

Dunkern TR and Hatzelmann A (2007) Characterization of inhibitors of phosphodiesterase 1C on a human cellular system. *Febs J* **274**(18): 4812-4824.

Ebner S, Burnol AF, Ferre P, de Saintaurin MA and Girard J (1987) Effects of insulin and norepinephrine on glucose transport and metabolism in rat brown adipocytes. Potentiation by insulin of norepinephrine-induced glucose oxidation. *Eur J Biochem* **170**(1-2): 469-474.

Fedorenko A, Lishko PV and Kirichok Y (2012) Mechanism of Fatty-Acid-Dependent UCP1 Uncoupling in Brown Fat Mitochondria. *Cell* **151**(2): 400-413.

Feldmann HM, Golozoubova V, Cannon B and Nedergaard J (2009) UCP1 ablation induces obesity and abolishes diet-induced thermogenesis in mice exempt from thermal stress by living at thermoneutrality. *Cell Metab* **9**(2): 203-209.

Finkelstein EA, Trogdon JG, Cohen JW and Dietz W (2009) Annual medical spending attributable to obesity: payer-and service-specific estimates. *Health Aff (Millwood)* **28**(5): w822-831.

Fisher DA, Smith JF, Pillar JS, St Denis SH and Cheng JB (1998) Isolation and characterization of PDE8A, a novel human cAMP-specific phosphodiesterase. *Biochem Biophys Res Commun* **246**(3): 570-577.

Flegal KM, Carroll MD, Ogden CL and Curtin LR (2010) Prevalence and trends in obesity among US adults, 1999-2008. *Jama* **303**(3): 235-241.

Flegal KM, Graubard BI, Williamson DF and Gail MH (2007) Cause-specific excess deaths associated with underweight, overweight, and obesity. *Jama* **298**(17): 2028-2037.

Frank S, Gaume B, Bergmann-Leitner ES, Leitner WW, Robert EG, Catez F, Smith CL and Youle RJ (2001) The role of dynamin-related protein 1, a mediator of mitochondrial fission, in apoptosis. *Dev Cell* **1**(4): 515-525.

Frederich RC, Hamann A, Anderson S, Lollmann B, Lowell BB and Flier JS (1995) Leptin levels reflect body lipid content in mice: evidence for diet-induced resistance to leptin action. *Nature medicine* **1**(12): 1311-1314.

Fredriksson JM and Nedergaard J (2002) Norepinephrine specifically stimulates ribonucleotide reductase subunit R2 gene expression in proliferating brown adipocytes: mediation via a cAMP/PKA pathway involving Src and Erk1/2 kinases. *Exp Cell Res* **274**(2): 207-215.

Fueger BJ, Czernin J, Hildebrandt I, Tran C, Halpern BS, Stout D, Phelps ME and Weber WA (2006) Impact of animal handling on the results of 18F-FDG PET studies in mice. *J Nucl Med* **47**(6): 999-1006.

Fumeron F, Durack-Bown I, Betoulle D, Cassard-Doulcier AM, Tuzet S, Bouillaud F, Melchior JC, Ricquier D and Apfelbaum M (1996) Polymorphisms of uncoupling protein (UCP) and beta 3 adrenoreceptor genes in obese people submitted to a low calorie diet. *Int J Obes Relat Metab Disord* **20**(12): 1051-1054.

Gagnon J, Lago F, Chagnon YC, Perusse L, Naslund I, Lissner L, Sjostrom L and Bouchard C (1998) DNA polymorphism in the uncoupling protein 1 (UCP1) gene has no effect on obesity related phenotypes in the Swedish Obese Subjects cohorts. *Int J Obes Relat Metab Disord* **22**(6): 500-505.

Gamanuma M, Yuasa K, Sasaki T, Sakurai N, Kotera J and Omori K (2003) Comparison of enzymatic characterization and gene organization of cyclic nucleotide phosphodiesterase 8 family in humans. *Cell Signal* **15**(6): 565-574.

Garcia CA, Van Nostrand D, Atkins F, Acio E, Butler C, Esposito G, Kulkarni K and Majd M (2006) Reduction of brown fat 2-deoxy-2-[F-18]fluoro-D-glucose uptake by controlling environmental temperature prior to positron emission tomography scan. *Mol Imaging Biol* **8**(1): 24-29.

Gesta S, Tseng YH and Kahn CR (2007) Developmental origin of fat: tracking obesity to its source. *Cell* **131**(2): 242-256.

Glick Z, Wickler SJ, Stern JS and Horwitz BA (1984) Blood flow into brown fat of rats is greater after a high carbohydrate than after a high fat test meal. *J Nutr* **114**(10): 1934-1939.

Gomes LC, Di Benedetto G and Scorrano L (2011) During autophagy mitochondria elongate, are spared from degradation and sustain cell viability. *Nat Cell Biol* **13**(5): 589-598.

Granneman JG (1992) Effects of agonist exposure on the coupling of beta 1 and beta 3 adrenergic receptors to adenylyl cyclase in isolated adipocytes. *J Pharmacol Exp Ther* **261**(2): 638-642.

Granneman JG and MacKenzie RG (1988) Neural modulation of the stimulatory regulatory protein of adenylate cyclase in rat brown adipose tissue. *J Pharmacol Exp Ther* **245**(3): 1068-1074.

Guyenet SJ and Schwartz MW (2012) Clinical review: Regulation of food intake, energy balance, and body fat mass: implications for the pathogenesis and treatment of obesity. *The Journal of clinical endocrinology and metabolism* **97**(3): 745-755.

Hamann A, Tafel J, Busing B, Munzberg H, Hinney A, Mayer H, Siegfried W, Ricquier D, Greten H, Hebebrand J and Matthaei S (1998) Analysis of the uncoupling protein-1 (UCP1) gene in obese and lean subjects: identification of four amino acid variants. *Int J Obes Relat Metab Disord* **22**(9): 939-941.

Hansen RS and Beavo JA (1982) Purification of two calcium/calmodulin-dependent forms of cyclic nucleotide phosphodiesterase by using conformation-specific monoclonal antibody chromatography. *Proc Natl Acad Sci U S A* **79**(9): 2788-2792.

Heilbronn LK, Kind KL, Pancewicz E, Morris AM, Noakes M and Clifton PM (2000) Association of -3826 G variant in uncoupling protein-1 with increased BMI in overweight Australian women. *Diabetologia* **43**(2): 242-244.

Heim T and Hull D (1966) The effect of propranalol on the calorigenic response in brown adipose tissue of new-born rabbits to catecholamines, glucagon, corticotrophin and cold exposure. *J Physiol* **187**(2): 271-283.

Hidaka H and Kobayashi R (1992) Pharmacology of protein kinase inhibitors. *Annu Rev Pharmacol Toxicol* **32**: 377-397.

Hoffmann C, Leitz MR, Oberdorf-Maass S, Lohse MJ and Klotz KN (2004) Comparative pharmacology of human beta-adrenergic receptor subtypes--characterization of stably transfected receptors in CHO cells. *Naunyn Schmiedebergs Arch Pharmacol* **369**(2): 151-159.

Houstek J, Andersson U, Tvrdik P, Nedergaard J and Cannon B (1995) The expression of subunit c correlates with and thus may limit the biosynthesis of the mitochondrial F0F1-ATPase in brown adipose tissue. *J Biol Chem* **270**(13): 7689-7694.

Iyer RB, Guo CC and Perrier N (2009) Adrenal pheochromocytoma with surrounding brown fat stimulation. *AJR Am J Roentgenol* **192**(1): 300-301.

Janssens K, Boussemaere M, Wagner S, Kopka K and Denef C (2008) Beta1-adrenoceptors in rat anterior pituitary may be constitutively active. Inverse agonism of CGP 20712A on basal 3',5'-cyclic adenosine 5'-monophosphate levels. *Endocrinology* **149**(5): 2391-2402.

Jensen CD, Aylward BS and Steele RG (2012) Predictors of attendance in a practical clinical trial of two pediatric weight management interventions. *Obesity (Silver Spring)* **20**(11): 2250-2256.

Jensen J (2007) More PKA independent beta-adrenergic signalling via cAMP: is Rap1-mediated glucose uptake in vascular smooth cells physiologically important? *Br J Pharmacol* **151**(4): 423-425.

Jespersen NZ, Larsen TJ, Peijs L, Daugaard S, Homoe P, Loft A, de Jong J, Mathur N, Cannon B, Nedergaard J, Pedersen BK, Moller K and Scheele C (2013) A classical brown adipose tissue mRNA signature partly overlaps with brite in the supraclavicular region of adult humans. *Cell metabolism* **17**(5): 798-805.

Jung RT, Shetty PS, James WP, Barrand MA and Callingham BA (1979) Reduced thermogenesis in obesity. *Nature* **279**(5711): 322-323.

Kajimura S, Seale P, Kubota K, Lunsford E, Frangioni JV, Gygi SP and Spiegelman BM (2009) Initiation of myoblast to brown fat switch by a PRDM16-C/EBP-beta transcriptional complex. *Nature* **460**(7259): 1154-1158.

Kajimura S, Seale P and Spiegelman BM (2010) Transcriptional control of brown fat development. *Cell metabolism* **11**(4): 257-262.

Karamitri A, Shore AM, Docherty K, Speakman JR and Lomax MA (2009) Combinatorial transcription factor regulation of the cyclic AMP-response element on the Pgc-1alpha promoter in white 3T3-L1 and brown HIB-1B preadipocytes. *J Biol Chem* **284**(31): 20738-20752.

Kim H, Scimia MC, Wilkinson D, Trelles RD, Wood MR, Bowtell D, Dillin A, Mercola M and Ronai ZA (2011) Fine-tuning of Drp1/Fis1 availability by AKAP121/Siah2 regulates mitochondrial adaptation to hypoxia. *Mol Cell* **44**(4): 532-544.

Kleiber M (1932) Body Size and Metabolism. *Journal of Agricultural Science* **6**(11): 315-353.

Kozak LP (2010) Brown fat and the myth of diet-induced thermogenesis. *Cell metabolism* **11**(4): 263-267.

Kraynik SM, Miyaoka RS and Beavo JA (2013) PDE3 and PDE4 isozyme selective inhibitors are both required for synergistic activation of brown adipose tissue. *Molecular pharmacology*.

Larsen TM, Toubro S, van Baak MA, Gottesdiener KM, Larson P, Saris WH and Astrup A (2002) Effect of a 28-d treatment with L-796568, a novel beta(3)-adrenergic receptor agonist, on energy expenditure and body composition in obese men. *Am J Clin Nutr* **76**(4): 780-788.

Le Mellay V, Troppmair J, Benz R and Rapp UR (2002) Negative regulation of mitochondrial VDAC channels by C-Raf kinase. *BMC Cell Biol* **3**: 14.

Lee P, Greenfield JR, Ho KK and Fulham MJ (2010) A critical appraisal of the prevalence and metabolic significance of brown adipose tissue in adult humans. *Am J Physiol Endocrinol Metab* **299**(4): E601-606.

Lee TF, Wang LC and Russell JC (1987) Enhancement of cold-stimulated thermogenesis in the corpulent rat (LA/N cp) by aminophylline. *Am J Physiol* **252**(4 Pt 2): R737-742.

Li HT, Jiao M, Chen J and Liang Y (2010) Roles of zinc and copper in modulating the oxidative refolding of bovine copper, zinc superoxide dismutase. *Acta Biochim Biophys Sin (Shanghai)* **42**(3): 183-194.

Liu X, Perusse F and Bukowiecki LJ (1998) Mechanisms of the antidiabetic effects of the beta 3-adrenergic agonist CL-316243 in obese Zucker-ZDF rats. *Am J Physiol* **274**(5 Pt 2): R1212-1219.

Loten EG and Sneyd JG (1970) An effect of insulin on adipose-tissue adenosine 3':5'-cyclic monophosphate phosphodiesterase. *Biochem J* **120**(1): 187-193.

MacFarland RT, Zelus BD and Beavo JA (1991) High concentrations of a cGMP-stimulated phosphodiesterase mediate ANP-induced decreases in cAMP and steroidogenesis in adrenal glomerulosa cells. *J Biol Chem* **266**(1): 136-142.

Marette A and Bukowiecki LJ (1989) Stimulation of glucose transport by insulin and norepinephrine in isolated rat brown adipocytes. *Am J Physiol* **257**(4 Pt 1): C714-721.

Marette A and Bukowiecki LJ (1991) Noradrenaline stimulates glucose transport in rat brown adipocytes by activating thermogenesis. Evidence that fatty acid activation of mitochondrial respiration enhances glucose transport. *Biochem J* **277 (Pt 1)**: 119-124.

Matthias A, Ohlson KB, Fredriksson JM, Jacobsson A, Nedergaard J and Cannon B (2000) Thermogenic responses in brown fat cells are fully UCP1-dependent. UCP2 or UCP3 do not substitute for UCP1 in adrenergically or fatty scid-induced thermogenesis. *J Biol Chem* **275**(33): 25073-25081.

Moon EY and Lerner A (2003) PDE4 inhibitors activate a mitochondrial apoptotic pathway in chronic lymphocytic leukemia cells that is regulated by protein phosphatase 2A. *Blood* **101**(10): 4122-4130.

Murphy GJ, Kirkham DM, Cawthorne MA and Young P (1993) Correlation of beta 3-adrenoceptor-induced activation of cyclic AMP-dependent protein kinase with activation of lipolysis in rat white adipocytes. *Biochem Pharmacol* **46**(4): 575-581.

Nagaoka T, Shirakawa T, Balon TW, Russell JC and Fujita-Yamaguchi Y (1998) Cyclic nucleotide phosphodiesterase 3 expression in vivo: evidence for tissue-specific expression of phosphodiesterase 3A or 3B mRNA and activity in the aorta and adipose tissue of atherosclerosis-prone insulin-resistant rats. *Diabetes* **47**(7): 1135-1144.

Nedergaard J, Becker W and Cannon B (1983) Effects of dietary essential fatty acids on active thermogenin content in rat brown adipose tissue. *J Nutr* **113**(9): 1717-1724.

Nilsson R, Ahmad F, Sward K, Andersson U, Weston M, Manganiello V and Degerman E (2006) Plasma membrane cyclic nucleotide phosphodiesterase 3B (PDE3B) is associated with caveolae in primary adipocytes. *Cell Signal* **18**(10): 1713-1721.

Nolan MA, Sikorski MA and McKnight GS (2004) The role of uncoupling protein 1 in the metabolism and adiposity of RII beta-protein kinase A-deficient mice. *Mol Endocrinol* **18**(9): 2302-2311.

Omar B, Zmuda-Trzebiatowska E, Manganiello V, Goransson O and Degerman E (2009) Regulation of AMP-activated protein kinase by cAMP in adipocytes: roles for phosphodiesterases, protein kinase B, protein kinase A, Epac and lipolysis. *Cell Signal* **21**(5): 760-766.

Omatsu-Kanbe M and Kitasato H (1992) Insulin and noradrenaline independently stimulate the translocation of glucose transporters from intracellular stores to the plasma membrane in mouse brown adipocytes. *FEBS Lett* **314**(3): 246-250.

Oppert JM, Vohl MC, Chagnon M, Dionne FT, Cassard-Doulcier AM, Ricquier D, Perusse L and Bouchard C (1994) DNA polymorphism in the uncoupling protein (UCP) gene and human body fat. *Int J Obes Relat Metab Disord* **18**(8): 526-531.

Ouellet V, Labbe SM, Blondin DP, Phoenix S, Guerin B, Haman F, Turcotte EE, Richard D and Carpentier AC (2012) Brown adipose tissue oxidative metabolism contributes to energy expenditure during acute cold exposure in humans. *The Journal of clinical investigation* **122**(2): 545-552.

Palmer D, Tsoi K and Maurice DH (1998) Synergistic inhibition of vascular smooth muscle cell migration by phosphodiesterase 3 and phosphodiesterase 4 inhibitors. *Circ Res* **82**(8): 852-861.

Papa S, Sardanelli AM, Scacco S and Technikova-Dobrova Z (1999) cAMP-dependent protein kinase and phosphoproteins in mammalian mitochondria. An extension of the cAMP-mediated intracellular signal transduction. *FEBS Lett* **444**(2-3): 245-249.

Petersen RK, Madsen L, Pedersen LM, Hallenborg P, Hagland H, Viste K, Doskeland SO and Kristiansen K (2008) Cyclic AMP (cAMP)-mediated stimulation of adipocyte differentiation requires the synergistic action of Epac- and cAMP-dependent protein kinase-dependent processes. *Mol Cell Biol* **28**(11): 3804-3816.

Pidoux G, Witczak O, Jarnaess E, Myrvold L, Urlaub H, Stokka AJ, Kuntziger T and Tasken K (2011) Optic atrophy 1 is an A-kinase anchoring protein on lipid droplets that mediates adrenergic control of lipolysis. *The EMBO journal* **30**(21): 4371-4386.

Puigserver P, Wu Z, Park CW, Graves R, Wright M and Spiegelman BM (1998) A cold-inducible coactivator of nuclear receptors linked to adaptive thermogenesis. *Cell* **92**(6): 829-839.

Rasmussen SG, Choi HJ, Rosenbaum DM, Kobilka TS, Thian FS, Edwards PC, Burghammer M, Ratnala VR, Sanishvili R, Fischetti RF, Schertler GF, Weis WI and Kobilka BK (2007) Crystal structure of the human beta2 adrenergic G-protein-coupled receptor. *Nature* **450**(7168): 383-387.

Rasmussen SG, DeVree BT, Zou Y, Kruse AC, Chung KY, Kobilka TS, Thian FS, Chae PS, Pardon E, Calinski D, Mathiesen JM, Shah ST, Lyons JA, Caffrey M, Gellman SH, Steyaert J, Skiniotis G, Weis WI, Sunahara RK and Kobilka BK (2011) Crystal structure of the beta2 adrenergic receptor-Gs protein complex. *Nature* **477**(7366): 549-555.

Raymond DR, Carter RL, Ward CA and Maurice DH (2009) Distinct phosphodiesterase-4D variants integrate into protein kinase A-based signaling complexes in cardiac and vascular myocytes. *Am J Physiol Heart Circ Physiol* **296**(2): H263-271.

Rehnmark S, Antonson P, Xanthopoulos KG and Jacobsson A (1993) Differential adrenergic regulation of C/EBP alpha and C/EBP beta in brown adipose tissue. *FEBS Lett* **318**(3): 235-241.

Reinhardt RR, Chin E, Zhou J, Taira M, Murata T, Manganiello VC and Bondy CA (1995) Distinctive anatomical patterns of gene expression for cGMP-inhibited cyclic nucleotide phosphodiesterases. *The Journal of clinical investigation* **95**(4): 1528-1538.

Rizzuto R, De Stefani D, Raffaello A and Mammucari C (2012) Mitochondria as sensors and regulators of calcium signalling. *Nat Rev Mol Cell Biol* **13**(9): 566-578.

Rodbell M (1964) Metabolism of Isolated Fat Cells. I. Effects of Hormones on Glucose Metabolism and Lipolysis. *J Biol Chem* **239**: 375-380.

Rodriguez AM, Monjo M, Roca P and Palou A (2002) Opposite actions of testosterone and progesterone on UCP1 mRNA expression in cultured brown adipocytes. *Cell Mol Life Sci* **59**(10): 1714-1723.

Rothwell NJ and Stock MJ (1979) A role for brown adipose tissue in diet-induced thermogenesis. *Nature* **281**(5726): 31-35.

Rothwell NJ and Stock MJ (1983) Luxuskonsumption, diet-induced thermogenesis and brown fat: the case in favour. *Clinical science* **64**(1): 19-23.

Rouru J, Cusin I, Zakrzewska KE, Jeanrenaud B and Rohner-Jeanrenaud F (1999) Effects of intravenously infused leptin on insulin sensitivity and on the expression of uncoupling proteins in brown adipose tissue. *Endocrinology* **140**(8): 3688-3692.

Rousseau C, Bourbouloux E, Campion L, Fleury N, Bridji B, Chatal JF, Resche I and Campone M (2006) Brown fat in breast cancer patients: analysis of serial (18)F-FDG PET/CT scans. *European journal of nuclear medicine and molecular imaging* **33**(7): 785-791.

Sadurskis A, Dicker A, Cannon B and Nedergaard J (1995) Polyunsaturated fatty acids recruit brown adipose tissue: increased UCP content and NST capacity. *Am J Physiol* **269**(2 Pt 1): E351-360.

Saito M, Okamatsu-Ogura Y, Matsushita M, Watanabe K, Yoneshiro T, Nio-Kobayashi J, Iwanaga T, Miyagawa M, Kameya T, Nakada K, Kawai Y and Tsujisaki M (2009) High incidence of metabolically active brown adipose tissue in healthy adult humans: effects of cold exposure and adiposity. *Diabetes* **58**(7): 1526-1531.

Salinas T, Duchene AM, Delage L, Nilsson S, Glaser E, Zaepfel M and Marechal-Drouard L (2006) The voltage-dependent anion channel, a major component of the tRNA import machinery in plant mitochondria. *Proc Natl Acad Sci U S A* **103**(48): 18362-18367.

Sbarbati A, Zancanaro C, Cigolini M and Cinti S (1987) Brown adipose tissue: a scanning electron microscopic study of tissue and cultured adipocytes. *Acta Anat (Basel)* **128**(1): 84-88.

Seale P, Bjork B, Yang W, Kajimura S, Chin S, Kuang S, Scime A, Devarakonda S, Conroe HM, Erdjument-Bromage H, Tempst P, Rudnicki MA, Beier DR and Spiegelman BM (2008) PRDM16 controls a brown fat/skeletal muscle switch. *Nature* **454**(7207): 961-967.

Seale P, Kajimura S, Yang W, Chin S, Rohas LM, Uldry M, Tavernier G, Langin D and Spiegelman BM (2007) Transcriptional control of brown fat determination by PRDM16. *Cell metabolism* **6**(1): 38-54.

Sell H, Berger JP, Samson P, Castriota G, Lalonde J, Deshaies Y and Richard D (2004) Peroxisome proliferator-activated receptor gamma agonism increases the capacity for sympathetically mediated thermogenesis in lean and ob/ob mice. *Endocrinology* **145**(8): 3925-3934.

Shakur Y, Takeda K, Kenan Y, Yu ZX, Rena G, Brandt D, Houslay MD, Degerman E, Ferrans VJ and Manganiello VC (2000) Membrane localization of cyclic nucleotide phosphodiesterase 3 (PDE3). Two N-terminal domains are required for the efficient targeting to, and association of, PDE3 with endoplasmic reticulum. *J Biol Chem* **275**(49): 38749-38761.

Shetty M, Ismail-Beigi N, Loeb JN and Ismail-Beigi F (1993) Induction of GLUT1 mRNA in response to inhibition of oxidative phosphorylation. *Am J Physiol* **265**(5 Pt 1): C1224-1229.

Shibata H, Perusse F, Vallerand A and Bukowiecki LJ (1989) Cold exposure reverses inhibitory effects of fasting on peripheral glucose uptake in rats. *Am J Physiol* **257**(1 Pt 2): R96-101.

Shimizu Y, Kielar D, Masuno H, Minokoshi Y and Shimazu T (1994) Dexamethasone induces the GLUT4 glucose transporter, and responses of glucose transport to norepinephrine and insulin in primary cultures of brown adipocytes. *J Biochem* **115**(6): 1069-1074.

Shimizu Y, Nikami H, Tsukazaki K, Machado UF, Yano H, Seino Y and Saito M (1993) Increased expression of glucose transporter GLUT-4 in brown adipose tissue of fasted rats after cold exposure. *Am J Physiol* **264**(6 Pt 1): E890-895.

Shimizu Y, Satoh S, Yano H, Minokoshi Y, Cushman SW and Shimazu T (1998) Effects of noradrenaline on the cell-surface glucose transporters in cultured brown adipocytes: novel mechanism for selective activation of GLUT1 glucose transporters. *Biochem J* **330 (Pt 1)**: 397-403.

Shimizu-Albergine M, Tsai LC, Patrucco E and Beavo JA (2012) cAMP-specific phosphodiesterases 8A and 8B, essential regulators of Leydig cell steroidogenesis. *Molecular pharmacology* **81**(4): 556-566.

Smith RE and Hock RJ (1963) Brown fat: thermogenic effector of arousal in hibernators. *Science* **140**(3563): 199-200.

Snyder PB, Esselstyn JM, Loughney K, Wolda SL and Florio VA (2005) The role of cyclic nucleotide phosphodiesterases in the regulation of adipocyte lipolysis. *J Lipid Res* **46**(3): 494-503.

Soderling SH, Bayuga SJ and Beavo JA (1998) Cloning and characterization of a cAMP-specific cyclic nucleotide phosphodiesterase. *Proc Natl Acad Sci U S A* **95**(15): 8991-8996.

Soeder KJ, Snedden SK, Cao W, Della Rocca GJ, Daniel KW, Luttrell LM and Collins S (1999) The beta3-adrenergic receptor activates mitogen-activated protein kinase in adipocytes through a Gi-dependent mechanism. *J Biol Chem* **274**(17): 12017-12022.

Sordahl LA and Schwartz A (1967) Effects of dipyridamole on heart muscle mitochondria. *Molecular pharmacology* **3**(6): 509-515.

Stanford KI, Middelbeek RJ, Townsend KL, An D, Nygaard EB, Hitchcox KM, Markan KR, Nakano K, Hirshman MF, Tseng YH and Goodyear LJ (2013) Brown adipose tissue regulates glucose homeostasis and insulin sensitivity. *The Journal of clinical investigation* **123**(1): 215-223.

Stocco DM (2001) StAR protein and the regulation of steroid hormone biosynthesis. *Annu Rev Physiol* **63**: 193-213.

Sundin U and Nechad M (1983) Trophic response of rat brown fat by glucose feeding: involvement of sympathetic nervous system. *Am J Physiol* **244**(3): C142-149.

Susulic VS, Frederich RC, Lawitts J, Tozzo E, Kahn BB, Harper ME, Himms-Hagen J, Flier JS and Lowell BB (1995) Targeted disruption of the beta 3-adrenergic receptor gene. *J Biol Chem* **270**(49): 29483-29492.

Sutherland EW and Rall TW (1958) Fractionation and characterization of a cyclic adenine ribonucleotide formed by tissue particles. *J Biol Chem* **232**(2): 1077-1091.

Svoboda P, Unelius L, Dicker A, Cannon B, Milligan G and Nedergaard J (1996) Cold-induced reduction in Gi alpha proteins in brown adipose tissue. Effects on the cellular hypersensitization to noradrenaline caused by pertussis-toxin treatment. *Biochem J* **314 (Pt 3)**: 761-768.

Tam CS, Lecoultre V and Ravussin E (2012) Brown adipose tissue: mechanisms and potential therapeutic targets. *Circulation* **125**(22): 2782-2791.

Tatsumi M, Engles JM, Ishimori T, Nicely O, Cohade C and Wahl RL (2004) Intense (18)F-FDG uptake in brown fat can be reduced pharmacologically. *Journal of nuclear medicine : official publication, Society of Nuclear Medicine* **45**(7): 1189-1193.

Taylor WM, Mak ML and Halperin ML (1976) Effect of 3':5'-cyclic AMP on glucose transport in rat adipocytes. *Proc Natl Acad Sci U S A* **73**(12): 4359-4363.

Tchernof A and Despres JP (2013) Pathophysiology of human visceral obesity: an update. *Physiological reviews* **93**(1): 359-404.

Thonberg H, Lindgren EM, Nedergaard J and Cannon B (2001) As the proliferation promoter noradrenaline induces expression of ICER (induced cAMP early repressor) in proliferative brown adipocytes, ICER may not be a universal tumour suppressor. *Biochem J* **354**(Pt 1): 169-177.

Uldry M, Yang W, St-Pierre J, Lin J, Seale P and Spiegelman BM (2006) Complementary action of the PGC-1 coactivators in mitochondrial biogenesis and brown fat differentiation. *Cell metabolism* **3**(5): 333-341.

Urhammer SA, Hansen T, Borch-Johnsen K and Pedersen O (2000) Studies of the synergistic effect of the Trp/Arg64 polymorphism of the beta3-adrenergic receptor gene and the -3826 A-->G variant of the uncoupling protein-1 gene on features of obesity and insulin resistance in a population-based sample of 379 young Danish subjects. *The Journal of clinical endocrinology and metabolism* **85**(9): 3151-3154.

Ursino MG, Vasina V, Raschi E, Crema F and De Ponti F (2009) The beta3-adrenoceptor as a therapeutic target: current perspectives. *Pharmacol Res* **59**(4): 221-234.

Vague J (1956) The degree of masculine differentiation of obesities: a factor determining predisposition to diabetes, atherosclerosis, gout, and uric calculous disease. *Am J Clin Nutr* **4**(1): 20-34.

Van Harmelen V, Reynisdottir S, Cianflone K, Degerman E, Hoffstedt J, Nilsell K, Sniderman A and Arner P (1999) Mechanisms involved in the regulation of free fatty acid release from isolated human fat cells by acylation-stimulating protein and insulin. *J Biol Chem* **274**(26): 18243-18251.

van Marken Lichtenbelt WD and Schrauwen P (2011) Implications of nonshivering thermogenesis for energy balance regulation in humans. *American journal of physiology Regulatory, integrative and comparative physiology* **301**(2): R285-296.

van Marken Lichtenbelt WD, Vanhommerig JW, Smulders NM, Drossaerts JM, Kemerink GJ, Bouvy ND, Schrauwen P and Teule GJ (2009) Cold-activated brown adipose tissue in healthy men. *N Engl J Med* **360**(15): 1500-1508.

Vang AG, Ben-Sasson SZ, Dong H, Kream B, DeNinno MP, Claffey MM, Housley W, Clark RB, Epstein PM and Brocke S (2010) PDE8 regulates rapid Teff cell adhesion and proliferation independent of ICER. *PLoS One* **5**(8): e12011.

Vasta V, Shimizu-Albergine M and Beavo JA (2006) Modulation of Leydig cell function by cyclic nucleotide phosphodiesterase 8A. *Proc Natl Acad Sci U S A* **103**(52): 19925-19930.

Vemulapalli S, Watkins RW, Chintala M, Davis H, Ahn HS, Fawzi A, Tulshian D, Chiu P, Chatterjee M, Lin CC and Sybertz EJ (1996) Antiplatelet and antiproliferative effects of SCH 51866, a novel type 1 and type 5 phosphodiesterase inhibitor. *J Cardiovasc Pharmacol* **28**(6): 862-869.

Virtanen KA, Lidell ME, Orava J, Heglind M, Westergren R, Niemi T, Taittonen M, Laine J, Savisto NJ, Enerback S and Nuutila P (2009) Functional brown adipose tissue in healthy adults. *N Engl J Med* **360**(15): 1518-1525.

Wang LC and Anholt EC (1982) Elicitation of supramaximal thermogenesis by aminophylline in the rat. *J Appl Physiol* **53**(1): 16-20.

Wang LC, Jourdan ML and Lee TF (1989) Mechanisms underlying the supra-maximal thermogenesis elicited by aminophylline in rats. *Life sciences* **44**(14): 927-934.

Weyer C, Gautier JF and Danforth E, Jr. (1999) Development of beta 3-adrenoceptor agonists for the treatment of obesity and diabetes--an update. *Diabetes Metab* **25**(1): 11-21.

Wijkander J, Landstrom TR, Manganiello V, Belfrage P and Degerman E (1998) Insulin-induced phosphorylation and activation of phosphodiesterase 3B in rat adipocytes: possible role for protein kinase B but not mitogen-activated protein kinase or p70 S6 kinase. *Endocrinology* **139**(1): 219-227.

Williams LM (2012) Hypothalamic dysfunction in obesity. *Proc Nutr Soc* **71**(4): 521-533.

Wu J, Bostrom P, Sparks LM, Ye L, Choi JH, Giang AH, Khandekar M, Virtanen KA, Nuutila P, Schaart G, Huang K, Tu H, van Marken Lichtenbelt WD, Hoeks J, Enerback S, Schrauwen P and Spiegelman BM (2012) Beige adipocytes are a distinct type of thermogenic fat cell in mouse and human. *Cell* **150**(2): 366-376.

Yao XJ, Velez Ruiz G, Whorton MR, Rasmussen SG, DeVree BT, Deupi X, Sunahara RK and Kobilka B (2009) The effect of ligand efficacy on the formation and stability of a GPCR-G protein complex. *Proc Natl Acad Sci U S A* **106**(23): 9501-9506.

Yoneshiro T, Aita S, Matsushita M, Kameya T, Nakada K, Kawai Y and Saito M (2011a) Brown adipose tissue, whole-body energy expenditure, and thermogenesis in healthy adult men. *Obesity (Silver Spring)* **19**(1): 13-16.

Yoneshiro T, Aita S, Matsushita M, Okamatsu-Ogura Y, Kameya T, Kawai Y, Miyagawa M, Tsujisaki M and Saito M (2011b) Age-related decrease in cold-activated brown adipose tissue and accumulation of body fat in healthy humans. *Obesity (Silver Spring)* **19**(9): 1755-1760.

Yoshida T, Sakane N, Wakabayashi Y, Umekawa T and Kondo M (1994) Anti-obesity and anti-diabetic effects of CL 316,243, a highly specific beta 3-adrenoceptor agonist, in yellow KK mice. *Life Sci* **54**(7): 491-498.

Young JB and Walgren MC (1994) Differential effects of dietary fats on sympathetic nervous system activity in the rat. *Metabolism* **43**(1): 51-60.

Zhao J, Cannon B and Nedergaard J (1997) alpha1-Adrenergic stimulation potentiates the thermogenic action of beta3-adrenoreceptor-generated cAMP in brown fat cells. *J Biol Chem* **272**(52): 32847-32856.

Zingaretti MC, Crosta F, Vitali A, Guerrieri M, Frontini A, Cannon B, Nedergaard J and Cinti S (2009) The presence of UCP1 demonstrates that metabolically active adipose tissue in the neck of adult humans truly represents brown adipose tissue. *Faseb J* **23**(9): 3113-3120.

Zmuda-Trzebiatowska E, Oknianska A, Manganiello V and Degerman E (2006) Role of PDE3B in insulin-induced glucose uptake, GLUT-4 translocation and lipogenesis in primary rat adipocytes. *Cell Signal* **18**(3): 382-390.

Curriculum Vitae

Stephen Michael Kraynik

kraynik1@u.washington.edu
Phone – (614) 327-4528

EDUCATION:

University of Washington, Seattle, WA — **Graduation:** June 7th, 2013
Ph.D. Pharmacology

The Ohio State University, Columbus, OH — **Graduation:** June, 2005
B.S. Biochemistry, English Minor — **Cum Laude with Honors**

RESEARCH EXPERIENCE:

The University of Washington Department of Pharmacology
Predoctoral Trainee (June, 2006 to Present) – Dr. Joseph Beavo
Project Aim: *Exploring the roles of Phosphodiesterases in Brown Adipose Tissue*

- Investigated the effects of combining selective PDE inhibitors on brown adipocyte physiology.
- Implemented and optimized protocols for isolation and culture of mature mouse brown adipocytes from interscapular BAT pads, as well as differentiation of brown adipocyte precursors (immortalized by Dr. Bruce Spiegelman's laboratory, Harvard, MA).
- Utilized multiple biochemical and molecular biology techniques to measure glycerol and cAMP production, gene expression by RT-PCR, and protein phosphorylation by Western blot in multiple brown adipocyte models.
- Established collaborations to study physiological changes in BAT *in vivo* using positron emission tomography (PET) in response to injected pharmacological agents.
- Designed high fat diet induced obesity studies on genetic knockout mice, which involved monitoring metabolic parameters, including energy expenditure, with implanted transponders, metabolic chambers and MRI.
- Explored the mitochondrial localization of PDE enzymes using organelle isolation techniques coupled with radioactive substrate-based enzymatic activity assay.

The University of Washington Department of Pharmacology
First Year Rotation Student (April 2006 to June, 2006) – Dr. Edith Wang
Project Aim: *Illustrate the structure-function relationship of zinc-finger DNA binding domains in the transcription factor CHCR in skeletal muscle differentiation*

- Used molecular biology cloning techniques – including PCR, ligation, and transformation – to generate multiple truncation length DNA constructs.
- Employed retroviral-packaging technology to deliver constructs to muscle precursor cell line.
- Isolated and cultured GFP(+)/infected cells via FACS.

The University of Washington Department of Pharmacology
First Year Rotation Student (January, 2006 to April, 2006) – Dr. Joseph Beavo
Project Aim: *Characterize the regulatory domain function of Trypanosoma brucei PDE2B using a new, fluorescence-based PDE assay.*

- Established a PDE enzyme assay that employs fluorescence-labeled cyclic nucleotide substrates.
- Extensively troubleshot the purification of reaction substrates by using affinity chromatography and establishing new ways to enzymatically alter reaction products for more sensitive measurement.

The University of Washington Department of Pharmacology
First Year Rotation Student (September, 2005 to December, 2005) – Dr. Ning Zheng
Project Aim: *Determine the X-Ray crystal structure of the Phosphodiesterase Type 5A tandem GAF domains.*

- Cloned multiple GST-tagged expression constructs for *E. coli* transformation and over-expression.
- Extensively trained in protein purification techniques – including glutathione resin, enzymatic cleavage, FPLC purification using size exclusion and UV absorbance, protein quantification assays and quality assessment using SDS-PAGE.
- Obtained experience in the design and implementation of protein crystallization screens

The Ohio State University Pharmacy School – Pharmaceutics Division
Undergraduate Research Assistant (June 14, 2004 to September 17, 2004) - Dr. Jim Dalton
Project Aim: *Characterize mouse stem cell differentiation stimulated by a novel Steroidal Androgen Receptor Modulator (SARM)*

- Designed and implemented pharmacological dose-response studies to test the efficacy and potency of previously uncharacterized small molecules.
- Developed assays using RT-PCR and immunocytochemistry techniques to screen for changes in stem cell fate after drug administration.

The Ohio State University Biochemistry Department Summer Undergraduate Research Program
Undergraduate Research Assistant (June 16, 2003 to September 3, 2003) - Dr. Mark Foster
Project Aim: Determine the NMR structure of RNase-P protein subunit

PUBLICATIONS:

Peer Reviewed:

1. **Kraynik, Stephen M.**, Miyaoka, Robert S., Beavo, Joseph A. "PDE3 and PDE4 isozyme selective inhibitors are required for synergistic activation of brown adipose tissue." ***Molecular Pharmacology.*** *Accepted Mar. 14, 2013, [Epub ahead of print].*
2. Patrucco, Enrico. **Kraynik, Stephen**. Beavo, Joseph. "Phosphodiesterase 8A, cAMP specific." *UCSD- Molecule Pages* (2011).

Abstracts:

1. **Stephen M. Kraynik**, Thomas R. Hinds, and Joseph A. Beavo. "Differential Regulation of Brown Adipose Tissue Activation by PDE3 and PDE4." FASEB J March 29, 2012 26:666.7
2. **Stephen Kraynik**, Enrico Patrucco, Masami Shimizu, and Joseph Beavo. "Phosphodiesterase 8A Modulates Lipolysis in Primary Brown Adipocytes." FASEB J April 22, 2009 23:582.5

SCIENTIFIC PRESENTATIONS:

Posters:
American Society of Pharmacology and Experimental Therapeutics, Experimental Biology Meeting, San Diego, CA (2012)

American Society of Pharmacology and Experimental Therapeutics, Experimental Biology Meeting, New Orleans, LA (2009)

Oral Presentations:
Department of Pharmacology Retreat, University of Washington, Seattle, WA (2012)

Stroum Fellowship Lecture, Diabetes Research Center – Nutrition Obesity Research Center Annual Retreat, Seattle, WA (2011)

Department of Pharmacology Retreat, University of Washington, Seattle, WA (2009)

TEACHING EXPERIENCE:

Rotation Student Mentor:
Project Aim: Characterize the mitochondrial localization of PDE8A (April, 2008 to June, 2008).
Project Aim: Determine the pharmacological selectivity of a novel PDE8 inhibitor across multiple PDE subtypes. (January, 2010 to March, 2010).

Undergraduate Student Mentor:
Project Aim: Effect of PDE3/PDE4 combined inhibition on AMPK phosphorylation (January, 2011 to March, 2011).

Teaching Assistant:
University of Washington PHCOL 401 – General Pharmacology I, Autumn Quarter 2005
University of Washington PHCOL 402 – General Pharmacology II, Winter Quarter 2006

HONORS AND FUNDING AWARDS:

Graduate:

University of Washington Diabetes and Endocrinology Research Center: Samuel and Althea Stroum Endowed Graduate Fellowship (July 2011-July 2012)
– 1-year $20,000 stipend

ASPET Graduate Student Travel Award – Experimental Biology (2012)
– $600

ASPET Graduate Student Travel Award – Experimental Biology (2009)
– $600

Pharmacological Sciences Training Grant Recipient (June 2008- June 2011)
– Full 3-year stipend, plus $1000/year research expenses

Undergraduate:

The Ohio State Honors Program Maximus Scholarship Competition: Medalist Scholar Finalist
– 4 Years Full Undergraduate In-State Tuition (2001-2005)

OSU Biochemistry Program: Summer Undergraduate Research Program Fellowship (2003)
– $2000 Stipend

Automatic Data Processing National Merit Scholarship
– $ 500 / year

Walter H. Kidd Dean's Engineering Scholarship
– $300 / year

PROFESSIONAL SOCIETIES:

American Society of Pharmacology and Experimental Therapeutics (ASPET)
– Graduate Student Member (2008-present)

GRADUATE ACTIVITIES:

Pharmacology Student Association – Graduate Student-Faculty Liaison (2006-2007)

VOLUNTEER WORK:

St. Catherine Parish - 8th Grade Volleyball Coach (Spring 2011)

St. Xavier High School (Cincinnati, OH) Science Fair/Exploravision – Student Group Mentor (2009)